

MATERNAL DETERMINANTS OF OOCYTE AND EMBRYO QUALITY

A Dissertation
Submitted to
the Temple University Graduate Board

in Partial Fulfillment
of the Requirements for the Degree of
DOCTOR OF PHILOSOPHY

By
Young S. Lee
May, 2011

Examining Committee Members:

Keith Latham, Advisory Chair, Molecular Biology & Genetics
Carmen Sapienza, Pathology
Scott Shore, Molecular Biology & Genetics
Judith Litvin, Anatomy & Cell Biology
Ana Gamero, External examiner, Biochemistry

©
Copyright
2011

by

Young S. Lee
All Rights Reserved

ABSTRACT

Maternal Determinants of Oocyte and Embryo Quality
Young S. Lee
Doctor of Philosophy
Temple University, 2011
Doctoral Advisory Committee Chair: Keith E. Latham, Ph. D.

Oocyte quality plays a critical role in establishment of pregnancies, embryo development, implantation and the health of offspring. The oocyte provides maternal factors necessary for the initial development of its embryo during the period of transcriptional silence. Despite the consistent increase in number of couples seeking assisted reproductive treatments, oocyte quality still remains as an obstacle in successful fertility treatments and the mechanisms governing the quality of oocyte are poorly understood. Among various factors that may potentially affect the quality of oocyte, the acquisition of oocyte developmental competence seems to mainly occur during the final stage of oocyte maturation. The correct temporal regulation of series of molecular events and the proper exchange of signals with surrounding follicular environment during this critical period will ensure the developmental competence of oocyte and its subsequent embryo. In order to identify molecular factors affecting oocyte quality, I have compared oocytes and cumulus cells of different qualities at a molecular level. I present in this thesis the pathways and molecules that may determine the developmental competence of oocyte as well as candidate molecular markers of oocyte and embryo quality.

A cDNA microarray analysis was performed, comparing the transcriptomes of rhesus monkey MII oocytes of different qualities, high quality VVM oocytes and poor quality IVM oocytes. A small set of 59 mRNAs was identified as differentially expressed between the two types of oocytes. These mRNAs are involved in steroid metabolism, cell-cell interactions, cellular homeostasis, cell adhesion, mRNA stability and translation.

In addition, the overexpression of several imprinted genes in IVM oocytes were detected, indicating a possible loss of correct epigenetic programming during IVM. These results indicate that normal oocyte-somatic cell interactions may be disrupted during IVM and the interruptions of these interactions during the final phase of oocyte maturation may be the prime cause of reduced developmental competence of IVM oocytes.

To elucidate oocyte quality factors linked to the cumulus cell phenotype, the transcriptomes of two types of rhesus monkey cumulus cells, IVM and VVM, were compared using a cDNA microarray analysis. In contrast to a relatively small difference between IVM and VVM oocytes, a large number of genes were differentially expressed between IVM and VVM rhesus cumulus cells. Moreover, a much larger number of differential mRNA expressions were observed comparing the transitions from pre-maturation cumulus cells to the IVM and VVM cumulus cells. The results from these array comparisons indicated that the cumulus cells may fail to achieve successfully normal gene regulation during IVM and thus make a remarkable amount of changes in gene expression to compensate for the loss. Numerous genes involved in lipid metabolism are incorrectly regulated during IVM, and the synthesis of sex hormones appears not suppressed during IVM. In addition, a panel of 24 cumulus cell markers of oocyte quality was identified.

Genetic effects on oocyte quality were explored by comparing transcriptomes of oocytes obtained from two different inbred mouse strains, B6 and D2, and F1 hybrid. A clustering analysis and statistical tests showed that the transcriptome of F1 oocytes is more similar to the B6 transcriptome than to the D2 at both GV and MII stages. Also, comparison analyses of GV stage oocyte transcriptomes with MII oocyte transcriptomes from three different mouse strains indicated that the number of overdominance genes at the MII stage is bigger than the number of overdominance genes at the GV stage. In

order to investigate how the genes gain the overdominance during the GV to MII transition, overdominance genes were categorized according to their mRNA expression patterns at GV and MII stages. The results showed that more than 80% of overdominance genes belong to one of the four major transition groups. The further evaluation of changes in array intensities from GV to MII stage transition revealed that F1 oocytes and inbred strain oocytes differentially regulate the mRNA abundance during oocyte maturation and that the differential regulation of mRNA abundance by the F1 genotype is responsible for the increase of the number of overdominance genes during maturation from GV stage to MII stage. A mRNA sequence analysis indicated that the gain of overdominant low in F1 mRNA expression pattern during maturation may be regulated by 3'UTR motif elements.

The number of dominance genes also increase during GV to MII transition. At both GV and MII stages, there are more genes with B6 dominant mRNA expression pattern than those with D2 dominance pattern. Lipid metabolism, small molecule biochemistry and cell death are biofunctions overrepresented in both dominance and overdominance genes. In addition, 'blebbing' was identified as a biofunction significantly downregulated in the F1 and B6 MII eggs, indicating that the cellular function may be involved in oocyte maturation.

ACKNOWLEDGEMENTS

I am deeply indebted to my thesis advisor, Dr. Keith Latham, for all the support and encouragement he has provided me during the course of my Ph.D. research. He has been my motivation and inspiration to study science and become an independent research scientist. I would like to give special thanks to my committee members, Dr. Carmen Sapienza, Dr. Scott Shore and Dr. Judith Litvin, for their insightful suggestions and advice. I would also like to thank my external thesis reviewer, Dr. Ana Gamero, for taking her time to review my doctoral thesis.

I would like to give a special recognition to my collaborator, Dr. Catherine VandeVoort, who provided me precious samples for my rhesus monkey microarray studies. Without her help, it would not have been possible for me to conduct my research. My thanks also go to the current and former members of the Latham lab as well as to the students, faculty members and administrative staffs of the Fels Institute.

Last, but not least, I would like to thank my family members. My husband, John, and my son, Samuel, receive my deepest gratitude for their understanding and support during the past six years. I would also like to express my gratitude to my parents who have given me unconditional love and many years of support. My thesis would not have been possible without their support and encouragement.

TABLE OF CONTENTS

	Page
ABSTRACT.....	iii
ACKNOWLEDGMENTS.....	vi
LIST OF TABLES.....	xii
LIST OF FIGURES.....	xvi
LIST OF SUPPLEMENTAL TABLES	xix
LIST OF ABBREVIATIONS.....	xxi

CHAPTER

1. INTRODUCTION.....	1
1.1 Background	2
1.1.1 Overview of Folliculogenesis and Oogenesis.....	2
1.1.2 Nuclear Maturation of Oocyte	5
1.1.2.1 Large-Scale Chromatin Changes And Global Transcriptional Silencing In Oocytes	5
1.1.2.2 Germinal Vesicle Break Down (GVBD)	7
1.1.3 Cytoplasmic Maturation of Oocyte	10
1.1.3.1 Post-transcriptional / Translational Controls	11
1.1.3.2 Post-translational Controls	12

1.1.4	Oocyte-Follicle Interactions	13
1.2	Scientific and Clinical Significance of Oocyte Quality	16
1.2.1	Assisted Reproductive Technologies	16
1.2.2	In Vitro Maturation	17
1.2.3	Oocyte Quality Screening Markers.....	19
1.3	Hypothesis and Specific Aims	20
2.	MATERIALS AND METHODS.....	21
2.1	Collection of Rhesus Oocytes and Cumulus Cells	21
2.2	Collection of Mouse Oocytes and Eggs	24
2.3	RNA Purification, Amplification and Array Hybridization	24
2.4	Microarray Data Analysis	27
2.4.1	Rhesus Monkey MII Oocyte Arrays	27
2.4.2	Rhesus Monkey Cumulus Cells Arrays	27
2.4.3	Mouse GV and MII Oocytes Arrays	29
2.5	Quantitative mRNA Expression Analysis	30
2.5.1	Rhesus Monkey IVM and VVM MII oocytes	30
2.5.2	Rhesus Monkey IVM and VVM Cumulus Cells	31
2.5.3	Mouse GV and MII stage Oocytes	32
2.6	Transcription Factor Binding Motif Analysis	36
2.7	3' UTR Analysis	36
2.7.1	3' UTR Analysis of mRNAs Over-expressed in Rhesus Monkey IVM Oocytes	36

2.7.2	3' UTR Analysis of mRNAs Overdominant Low in Mouse MII stage Oocytes	37
3.	EFFECTS OF IN VITRO MATURATION ON GENE EXPRESSION IN RHESUS MONKEY OOCYTES	40
3.1	Identification of Genes Differentially Expressed Between IVM and VVM Oocytes	40
3.2	Quantitative mRNA Expression Analysis	47
3.3	Biological Functions of Differentially Expressed Genes in Rhesus Monkey MII Oocytes.....	49
3.4	Transcription Factor Binding Motif Analysis	56
3.5	3' UTR Analysis.....	56
3.6	Expression of Imprinted Genes	59
3.7	Discussion	62
4.	EXTENSIVE EFFECTS OF IN VITRO OOCYTE MATURATION ON RHESUS MONKEY CUMULUS CELL TRANSCRIPTOME	67
4.1	Overview of the Array Analysis	67
4.2	Identification of Differentially Regulated Gene Sets	72
4.2.1	Identification of Genes Incorrectly Regulated During IVM	73
4.2.2	Identification of Correctly Regulated Genes.....	74
4.2.3	Direct comparison of IVM and VVM cumulus cells & Identification of more incorrectly regulated genes	77

4.3	Biofunctional Analysis of Differentially Expressed Gene Sets	81
4.3.1	Functional Characteristics of Correctly Regulated Genes.....	81
4.3.2	Functional Characteristics of Incorrectly Regulated Genes.....	83
4.4	Identification of Oocyte Quality Markers by qRT-PCR and Statistical Analysis	96
4.5	Discussion	100
5.	EFFECTS OF HYBRID GENOTYPE ON GENE EXPRESSION IN MOUSE OOCYTES AND EGGS	107
5.1	Overview of the Array Analysis	107
5.2	Overdominance Effects in Gene Expression	113
5.2.1	Identification of Overdominance Genes	113
5.2.2	Biofunctional Analysis for Overdominance Genes	125
5.2.3	3'UTR Analysis for MII-Stage Overdominance Genes.....	141
5.3	Dominance Effects in Gene Expression	145
5.3.1	Identification of Dominance Genes	145
5.3.2	Biofunctional Analysis for Dominance Genes	145
5.3.2.1	Biofunctional Analysis for the GV-stage Dominance Genes	146
5.3.2.2	Biofunctional Analysis for the B6 Dominance Genes at the MII- stage.....	151
5.3.2.3	Biofunctional Analysis for the D2 Dominance Genes at the MII- stage	151

5.4 Discussion	156
6. DISCUSSION	162
REFERENCES CITED.....	168

LIST OF TABLES

Table	Page
2.1 Primers used to obtain cDNA probes for QADB.....	33
2.2 Primer and Probe Sequences of the Custom-designed TaqMan assays used in qRT-PCR.....	34
2.3 Published CPE motifs employed in analysis.....	39
3.1 Quality control parameters for array hybridization (Rhesus monkey IVM and VVM MII eggs)	42
3.2 Genes expressed higher in VVM oocytes than in IVM oocytes	44
3.3 Genes expressed higher in IVM oocytes than in VVM oocytes	45
3.4 EASE analysis output for genes over-expressed in IVM oocytes	50
3.5 Transcription factor binding sites.....	57
3.6 Characteristics of published 3'UTRs for human homologs of mRNAs over-expressed in IVM oocytes	58
3.7 Expression of maternally imprinted genes in IVM and VVM oocytes	60
3.8 Expression of paternally imprinted genes in IVM and VVM oocytes	61
4.1 Quality control parameters for array hybridization (Rhesus monkey IVM and VVM MII cumulus cells).....	68
4.2 Probe sets significantly up- or down-regulated in rhesus monkey cumulus cells during VVM or IVM	71

4.3	Probe sets differentially expressed between IVM and VVM cumulus cells.....	79
4.4	Molecular and cellular functions over-represented among genes differentially regulated between IVM and VVM cumulus cells.....	80
4.5	Top ten molecular and cellular functions over-represented in genes correctly regulated during IVM (Fold change of difference ≥ 2).....	82
4.6	Molecular and cellular functions enriched in VVM-unique and IVM-unique genes (Fold change of difference ≥ 2).....	85
4.7	Number of genes over-represented in cell cycle, cell death, and cellular growth and proliferation	87
4.8	Comparison of G1/S cell cycle regulation genes over-represented during VVM and IVM.....	88
4.9	Genes involved in cell death	89
4.10	Genes involved in cellular growth and proliferation.....	90
4.11	Molecular and cellular functions over-represented among genes up- or down-regulated during VVM with the fold change of difference greater than 10	93
4.12	Molecules in an IPA network constructed from genes down-regulated only during VVM (Figure 4.6).....	95
4.13	Univariate GEE analysis of gene expression data related to oocyte quality	98

4.14	Multiple variable GEE analysis of gene expression data related to oocyte quality	99
5.1	Quality control parameters for array hybridization (Mouse GV and MII oocytes).....	109
5.2	Number of differentially expressed genes among oocytes/eggs of three genotypes identified by Significance Analysis of Microarray (SAM).....	112
5.3	Identification of Overdominance and Dominance Genes	114
5.4	Number of Overdominance and Dominance Genes	115
5.5	Genes that showed the overdominant mRNA expression pattern in both GV and MII stages	116
5.6	Theoretically possible types of transitions in gene expressions	118
5.7	Comparison of gene expression changes in oocytes from F1 and parental strains during the GV-to-MII stage transition.....	123
5.8	Genes that showed the biggest difference in the mRNA expression changes among 3 strains during the GV-to-MII transition.....	124
5.9	Molecular and Cellular Functions over-represented in GV-ODH genes [Threshold = Fisher's exact test p-value <0.01 & #Molecules ≥5]	126
5.10	Molecular and Cellular Functions over-represented in GV-ODL genes [Threshold = Fisher's exact test p-value <0.01 & # Molecules ≥5]	130
5.11	Molecular and Cellular Functions over-represented in MII-ODH genes [Threshold = Fisher's exact test p-value <0.01 & #Molecules ≥5]	134

5.12	Molecular and Cellular Functions over-represented among genes in “from GV-Equal to MII-ODL” transition (T23)	137
5.13	Molecular and cellular functions over-represented among genes in “from GV-Equal to MII-ODH” transition (T24)	139
5.14	45 motifs that were only detected in 3’UTR sequences of MII-ODL genes	143
5.15	Molecular and cellular functions over-represented in GV-B6-dominance genes (GV-FBL & GV-FBH).....	147
5.16	Molecular and cellular functions over-represented in GV-D2-dominance genes (GV-FDL & GV-FDH)	149
5.17	Molecular and Cellular Functions over-represented in MII-D2-dominance genes (MII-FDL & MII-FDH).....	154
6.1	Genes that showed significant differential expressions in all three array studies	166
6.2	Genes that showed significant differential expressions in two of the three array studies.....	167

LIST OF FIGURES

Figure	Page
1.1 Schematic diagram of follicle maturation in the ovary.....	4
1.2 Nuclear and cytoplasmic maturations of oocyte	8
1.3 Inhibition of CDK1 during prophase I arrest and CDK1 activation during resumption of meiosis.....	9
1.4 Bidirectional communication between the oocyte and cumulus cells.....	15
2.1 Summary of procedures employed to obtain oocytes for array analysis.....	23
2.2 Schematic summary of experimental design	26
3.1 Hierarchical clustering (HCL) of in vitro (IVM) and in vivo (VVM) matured oocytes	43
3.2 Comparison of differences in mRNA expression revealed by microarray analysis and independent measurements using the QADB (striped) or qRT-PCR assays	48
3.3 Ingenuity pathway analysis gene interaction network 1	53
3.4 Ingenuity pathway analysis gene interaction network 2	55
4.1 Hierarchical Clustering Analysis (rhesus monkey PM, IVM, VVM-CC)	69
4.2 Principal Component Analysis (rhesus monkey PM, IVM, VVM-CC)	70

4.3	Venn diagram to identify differential patterns of mRNA regulations in cumulus cells during IVM and VVM.....	75
4.4	Venn diagrams to identify genes regulated in the opposite directions during IVM and VVM.....	76
4.5	Comparison biofunctional analysis of VVM-unique vs IVM-unique genes (F.C. ≥ 2) using Ingenuity Pathway Analysis (IPA)	86
4.6	IPA network for genes down-regulated only during VVM.....	94
4.7	Quantitative analysis of selected mRNAs by quantitative RT-PCR	97
4.8	Misregulation of Genes Involved in Steroidogenesis during IVM	106
5.1	Hierarchical Clustering Analysis (Mouse GV and MII oocytes).....	110
5.2	Principal Component Analysis (Mouse GV and MII oocytes).....	111
5.3	K-means clustering analysis for the genes which mRNA expressions are equal in GV stage but are low in F1-overdominant in MII stage. (T23)	119
5.4	K-means clustering analysis for the genes which mRNA expressions are equal in GV stage but are high in F1-overdominant in MII stage. (T24)	120
5.5	Molecular and Cellular Functions over-represented in GV-ODH genes [Threshold = Fisher's exact test p-value <0.01 & #Molecules ≥ 5]	127
5.6	Molecular and Cellular Functions over-represented in GV-ODL genes [Threshold = Fisher's exact test p-value <0.01 & #Molecules ≥ 5]	131
5.7	IPA network for GV-ODL genes	132

5.8	Molecular and Cellular Functions over-represented in MII-ODL genes [Threshold = Fisher's exact test p-value <0.01 & #Molecules ≥5]	133
5.9	Molecular and Cellular Functions over-represented in MII-ODH genes [Threshold = Fisher's exact test p-value <0.01 & #Molecules ≥5].....	135
5.10	Molecular and Cellular Functions over-represented among genes in “from GV-Equal to MII-ODL” transition (T23).....	138
5.11	Molecular and Cellular Functions over-represented among genes in “from GV-Equal to MII-ODH” transition (T24)	140
5.12	Hierarchical clustering of motifs enriched in MII-ODL 3'UTR sequences	144
5.13	Molecular and Cellular Functions over-represented in GV-B6-dominance genes (GV-FBL & GV-FBH)	148
5.14	Molecular and Cellular Functions over-represented in GV-D2-dominance genes (GV-FDL & GV-FDH)	150
5.15	Molecular and Cellular Functions over-represented in MII-B6-dominance genes (MII-FBL & MIIV-FBH)	153
5.16	Molecular and Cellular Functions over-represented in MII-D2-dominance genes (MII-FDL & MIIV-FDH)	155

LIST OF SUPPLEMENTAL TABLES

- S1a. Probe sets for which mRNA expression was significantly down-regulated only during IVM.
- S1b. Probe sets for which mRNA expression was significantly up-regulated only during IVM.
- S2a. Probe sets for which mRNA expression was significantly down-regulated only during VVM.
- S2b. Probe sets for which mRNA expression was significantly up-regulated only during VVM.
- S3a. Genes upregulated during IVM but down-regulated during VVM
- S3b. Genes down-regulated during IVM but up-regulated during VVM
- S4a. Genes up-regulated during IVM and VVM
- S4b. Genes down-regulated during IVM and VVM
- S5a. Additional genes up-regulated during IVM but down-regulated during VVM
- S5b. Additional genes down-regulated during IVM but up-regulated during VVM
- S6a. Genes up-regulated during IVM (F.C. ≥ 10)
- S6b. Genes down-regulated during IVM (F.C. ≥ 10)
- S7a. Genes up-regulated during VVM (F.C. ≥ 10)
- S7b. Genes down-regulated during VVM (F.C. ≥ 10)
- S8. Gene homologies across species for the 24 oocyte quality markers

- S9a. Low in F1 overdominance genes at GV stage [GV-ODL]
- S9b. High in F1 overdominance genes at GV stage [GV-ODH]
- S10a. Low in F1 overdominance genes at MII stage [MII-ODL]
- S10b. High in F1 overdominance genes at MII stage [MII-ODH]
- S11. Changes in mRNA abundance of genes in T23 group (from GV-equal to MII-ODL)
- S12. Changes in mRNA abundance of genes in T24 group (from GV-equal to MII-ODH)
- S13. The analysis of motif coverage in MII-ODL 3'UTR sequences
- S14. Molecular and cellular functions over-represented in MII-ODL genes
- S15a. High in D2-B6 dominance genes at GV stage [GV-FBL]
- S15b. Low in D2-B6 dominance genes at GV stage [GV-FBH]
- S16a. High in B6-D2 dominance genes at GV stage [GV-FDL]
- S16b. Low in B6-D2 dominance genes at GV stage [GV-FDH]
- S17a. High in D2-B6 dominance genes at MII stage [MII-FBL]
- S17b. Low in D2-B6 dominance genes at MII stage [MII-FBH]
- S18a. High in B6-D2 dominance genes at MII stage [MII-FDL]
- S18b. Low in B6-D2 dominance genes at MII stage [MII-FDH]
- S19. Molecular and cellular functions over-represented in MII-B6-dominance genes
- S20. Subcategories of biological functions for B6-dominance genes in MII stage
- S21. Subcategories of biological functions for D2-dominance genes in MII stage

LIST OF ABBREVIATIONS

B6	C57BL/6 strain of mice
BH	Benjamini-Hochberg
bp	base pair
cAMP	Cyclic adenosine monophosphate
CC	Cumulus Cells
cGMP	Cyclic guanosine monophosphate
CNPRC	California National Primate Research Center
COC	Cumulus Oocyte Complex
CPE	Cytoplasmic Polyadenylation Element
CPEB	Cytoplasmic Polyadenylation Element Binding protein
cRNA	complementary Ribonucleic Acid
CT	Cycle Threshold
D2	DBA/2 strain of mice
EASE	Expression Analysis Systematic Explorer
eCG	Equine Chorionic Gonadotropin
EGA	Embryonic Genome Activation
EGF	Epidermal Growth Factor
F1	B6D2F1 (C57BL/6 Female X DBA/2 Male)
FBH	B6 dominant expression Low in D2
FBL	B6 dominant expression High in D2
FDH	D2 dominant expression Low in B6
FDL	D2 dominant expression High in B6
FDR	False Discovery Rate
FSH	Follicle Stimulating Hormone

GC	Granulosa Cells
GEE	Generalized Estimating Equations
GEO	Gene Expression Omnibus
GO	Gene Ontology
GV	Germinal Vesicle
GVBD	Germinal Vesicle Break Down
GV-FBH	B6 dominant expression Low in D2 at the GV stage
GV-FBL	B6 dominant expression High in D2 at the GV stage
GV-FDH	D2 dominant expression Low in B6 at the GV stage
GV-FDL	D2 dominant expression High in B6 at the GV stage
HCL	Hierarchical Clustering
HEPES	4-(2-hydroxyethyl)-1-piperazineethanesulfonic acid
IBMX	3-isobutyl-1-methoxyxanthine
IM	Intramuscular injection
IPA	Ingenuity Pathway Analysis
IVM	In Vitro Maturation
IVM-DOWN	Down-regulated during VVM (from PM to IVM)
IVM-UP	Up-regulated during IVM (from PM to IVM)
LH	Luteinizing Hormone
MAS5	Microarray Suite 5
mg	Microgram
MI	Metaphase I
MII	Metaphase II
MII-FBH	B6 dominant expression Low in D2 at the MII stage
MII-FBL	B6 dominant expression High in D2 at the MII stage
MII-FDH	D2 dominant expression Low in B6 at the MII stage

MII-FDL	D2 dominant expression High in B6 at the MII stage
MPF	Maturation Promoting Factor
NCBI	National Center for Biotechnology Information
ng	Nanogram
ODH	Overdominant expression High in F1
ODL	Overdominant expression Low in F1
PB	Polar Body
PCA	Principal Component Analysis
PKA	Protein Kinase A
PM	Pre-Matuation
PREGER	Primate Embryo Gene Expression Resource
PVA	Polyvinyl Alcohol
QADB	Quantitative Amplification and Dot Blotting
qRT-PCR	Quantitative Real Time RT-PCR
REST	Relative Expression Software Tool
r-hCG	Recombinant Human Chorionic Gonadotropin
r-hFSH	Recombinant human Follicle Stimulating Hormone
r-hLH	Recombinant Human Luteinizing Hormone
RISC	RNA induced silencing complex
RMA	Robust Multichip Analysis
RNP	Ribonucleoprotein Particle
SAM	Significance Analysis of Microarrays
SCMC	Subcortical Maternal Complex
SCRD	Subcortical Ribonucleoprotein Particle Domain
TFBS	Transcription Factor Binding Sites
TL	Tyrode Lactate

TZP	Transzonal Process
UTR	Untranslated Region
VVM	In Vivo Maturation
VVM-DOWN	Down-regulated during VVM (from PM to VVM)
VVM-UP	Up-regulated during VVM (from PM to VVM)

CHAPTER 1

INTRODUCTION

“Omne vivum ex ovo: every living thing comes from an egg.” As implied in William Harvey’s famous statement, the developmental fate of embryo gets determined well before fertilization. The initial phase of embryo development takes place during the period of transcriptional silence until embryonic genome activation (EGA) and thus entirely depends upon the maternal reservoir of macromolecules that are accumulated in the oocyte during oogenesis (Latham, 1999; Latham & Schultz, 2001). Consequently, oocyte quality is a critical determining factor for the establishment and maintenance of pregnancy.

Oocyte quality is defined as the ability of an oocyte to accumulate necessary maternal factors, to complete the maturation process, to undergo fertilization and support the embryo development to term. Oocyte quality thus holds great significance in the field of the Assisted Reproductive Technologies (ARTs). Poor oocyte quality is considered as the prime cause of infertility in a significant number of populations (Garrido *et al.*, 2000; Garrido *et al.*, 2003; Krey & Grifo, 2001; Navot *et al.*, 1991; Sauer, 1998). Couples with infertility are seeking therapies using ARTs (National action plan for the prevention, detection and management of infertility, available online at <http://www.cdc.gov/art.htm>) in increasing numbers, and the number of babies born through ART procedures accounts for more than 1% of all U.S.-born infants (Reynolds *et al.*, 2003). Identification of maternal factors that determine oocyte quality will aid in the development of improved ARTs. Furthermore, it will elucidate important control mechanisms involved in early stage embryonic development.

1.1 Background

1.1.1 Overview of Folliculogenesis and Oogenesis

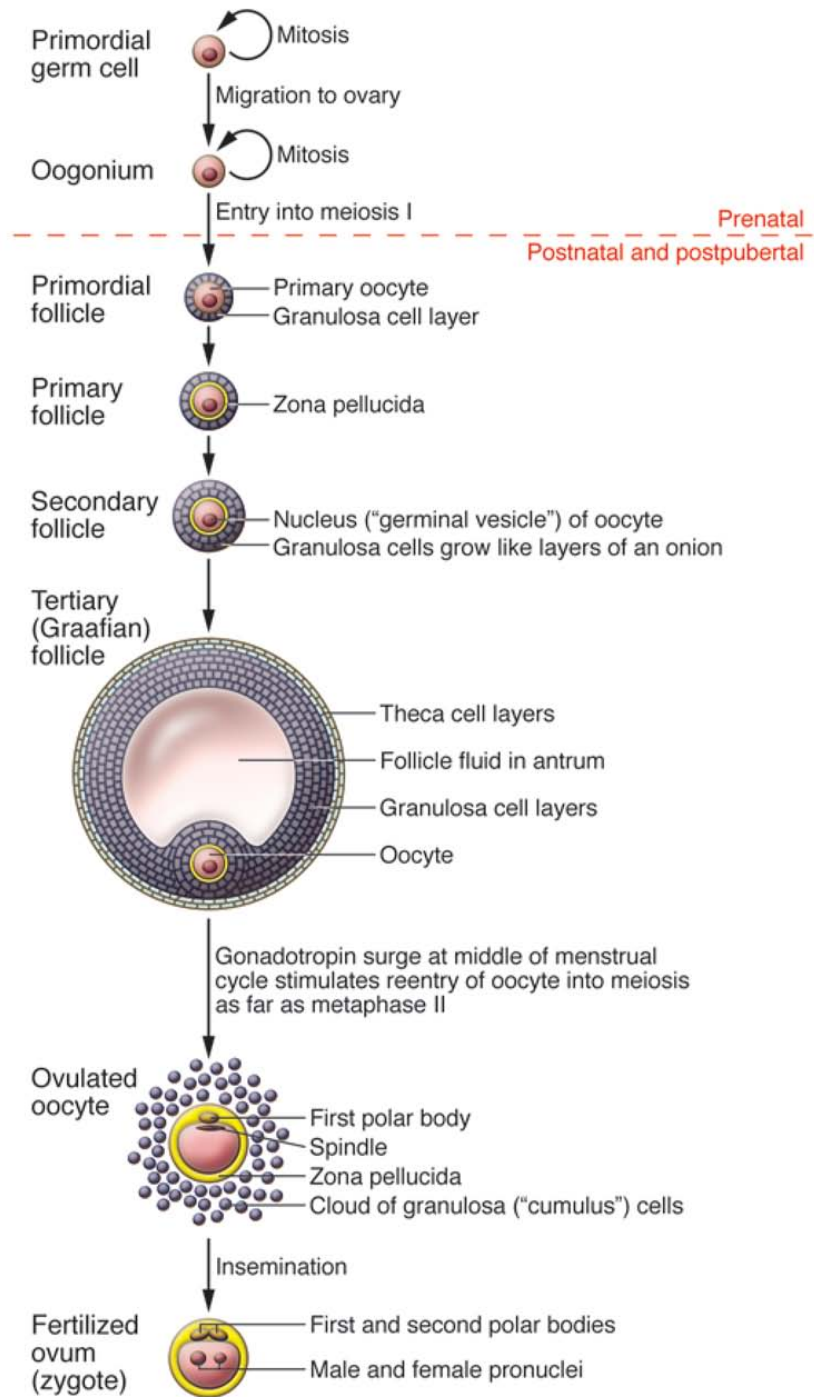
At birth, thousands of oocytes are stored in the ovaries of mammalian females. Oocytes at this stage are relatively small in size and must increase their volume in order to store materials that support the development of their subsequent embryos (Eppig & O'Brien, 1996). Each oocyte resides in a confined space surrounded by specialized somatic cells; this unit of an oocyte and companion somatic cells is called a 'follicle.' In this stage, the oocyte is arrested at prophase I of the first meiotic division and surrounded by a single layer of flattened somatic cells (Amleh & Dean, 2002). The prophase I arrested oocytes and the follicles containing the oocytes are referred to 'primordial oocytes' and 'primordial follicles', respectively (Figure 1.1).

At puberty, oocytes enter the growth phase and somatic cells surrounding the oocytes become cuboidal and divide. Also, an extensive network of gap junctions becomes established between the oocyte and its companion granulosa cells as well as among granulosa cells themselves at the onset of the follicle growth (Albertini & Anderson, 1974; Juneja *et al.*, 1999; A. M. Simon *et al.*, 1997). As the oocyte grows, it accumulates mRNAs and proteins, and reorganizes its chromatin configuration. During this process, the oocyte acquires the competency to undergo both cytoplasmic and nuclear maturation, and consequently give rise to an embryo when fertilized (Eppig *et al.*, 1994; Sorensen & Wassarman, 1976). In parallel, small cavities form between granulosa cells, and later get merge into a larger cavity called the 'antrum.' The follicle at this stage is called an 'antral follicle' and houses a fully grown oocyte that is still arrested at prophase I of meiosis. Somatic cells in the antral follicle are divided into two groups. Cells that are directly surrounding the oocyte are cumulus cells (CC) and those that are lining the follicle wall are called mural granulosa cells (GC). The surge of

luteinizing hormone (LH) triggers fully grown oocytes to resume meiosis and undergo germinal vesicle break down (GVBD). Following GVBD, the oocyte completes meiosis I and immediately enters meiosis II. The mammalian mature secondary oocyte remains arrested at metaphase II until fertilization.

During the growth period, oocytes acquire the meiotic competence (oocyte's ability to resume meiosis) and only the fully grown oocyte can resume meiosis. The acquisition of full meiotic competence ensures the oocyte not only to resume meiosis but also to undergo two meiotic divisions in correct temporal sequence and successfully complete the maturation. Oocyte maturation consists of two interdependent processes, nuclear and cytoplasmic maturation, which are interlinked and must be tightly regulated throughout the entire maturation process. Nuclear maturation involves the re-entry to the cell cycle to complete meiosis I and the subsequent progression to meiosis II, whereas Cytoplasmic maturation encompasses general processes that prepare the oocyte for fertilization and embryogenesis, such as changes in the distribution of cortical granules (Ducibella *et al.*, 1988), reorganization of endoplasmic reticulum (Mehlmann *et al.*, 1995), changes in transcriptional (Paynton & Bachvarova, 1994), translational, and posttranslational activities (Richter & McGaughey, 1981; Schultz & Wassarman, 1977).

Figure 1.1: Schematic diagram of follicle maturation in the ovary.



(Gosden & Lee, 2010)

1.1.2 Nuclear Maturation of Oocyte

Nuclear maturation encompasses chromatin changes during oocyte maturation from germinal vesicle breakdown (GVBD) throughout meiosis I (MI) to meiosis II (MII). In vertebrates, oocytes are arrested at prophase of the first meiotic division around the time of birth. Only fully grown oocytes can resume meiosis in response to hormonal stimulation and complete nuclear maturation leads to the formation of an oocyte arrested in metaphase II. Oocytes are arrested at metaphase of the second meiotic division until fertilization (Figure 1.2). Large-Scale Chromatin Changes and Global Transcriptional Silencing In Oocytes

During the growth phase, oocyte synthesizes and accumulates mRNAs and proteins in order to prepare for the upcoming oocyte maturation and embryo development processes. Among those accumulated in the oocyte are cell cycle proteins such as cyclin B, p34^{cdc2} (Mitra and Schultz, 1996) and cell cycle kinases (de Vantery *et al.*, 1997; Mitra and Schultz, 1996), all of which are subunits of maturation (or metaphase) promoting factor (MPF). MPF is composed of a kinase subunit, CDK1 (cyclin-dependent kinase 1; initially called p34^{cdc2} as a product of *Cdc2* gene for “cell division control 2” identified in yeasts) associated with a regulatory subunit - cyclin B (Gautier *et al.*, 1988; Lohka *et al.*, 1988). Meiotic resumption depends on the activation of MPF complex which is triggered by the dephosphorylation of the inactive CDK1 by Cdc25B phosphatase (Figure 1.3). In immature oocytes, MPF is in an inactive form with phosphorylated CDK1 (Dunphy & Newport, 1989). Cyclic AMP (cAMP) activates protein kinase A (PKA), which inhibits CDC25B from dephosphorylating and activating CDK1. Therefore, high cAMP level maintains meiotic arrest (Conti *et al.*, 2002). The level of cAMP in the oocyte is maintained through a pathway involving G protein Gs, G-protein-coupled receptor GPR3 or GPR12 (Horner *et al.*, 2003; Kalinowski *et al.*, 2004;

Mehlmann *et al.*, 2002). The G-protein-coupled receptors activate the G protein Gs that in turn induces adenylyl cyclase to upregulate cAMP level. LH increases the expression of epidermal growth factor (EGF)-like factors in granulosa cells leading to reduced cGMP transfer from cumulus cells to oocyte via gap junctions (Norris *et al.*, 2009; J. Y. Park *et al.*, 2004). The role of cGMP is to inhibit the hydrolysis of cAMP by phosphodiesterase 3A (PDE3A): a decline in cGMP thus results in increased PDE3A activity and reduced cAMP level in the oocyte (Norris, *et al.*, 2009; Vaccari *et al.*, 2009). Following the decline in cAMP level in the oocyte, dephosphorylations of WEE2 and CDC25B occur, which results in the activation of CDK1 and meiotic resumption.

The growing oocytes also undergo dynamic changes in their chromatin configurations. During the germinal vesicle (GV) stage, oocyte chromatin changes its configuration to a more condensed form from a diffuse one (Debey *et al.*, 1993; Mattson and Albertini, 1990; Wickramasinghe *et al.*, 1991; Zuccotti *et al.*, 1995). Also, this transition is accompanied by global repression of transcription (BouniolBaly *et al.*, 1999). The mechanisms involved in modulating changes in large-scale chromatin structure and global transcriptional silencing in mammalian oocytes are not well-understood. However, it is well known that the global transcription silencing and the timely storage of maternal transcripts prior to the meiotic resumption are critical for the full developmental potentials of an oocyte (De La Fuente & Eppig, 2001).

1.1.2.2 Germinal Vesicle Break Down (GVBD)

A fully grown oocyte has a nucleus with an intact nuclear envelope, called a germinal vesicle (GV), and remains arrested in prophase I until the LH surge induces ovulation and the first meiotic division (MI). Activation of MPF induces the breakdown of the oocyte nuclear envelope a process termed as germinal vesicle breakdown (GVBD). The activation of MPF also triggers the oocyte to re-enter the cell cycle. The condensation of chromosomes occurs and the spindle assembles around the bivalent chromosomes and the homologous chromosomes get separated (metaphase I), half of which get eventually extruded in a polar body. The remaining chromosomes are aligned in the metaphase II spindle and the egg remains arrested in this stage until fertilization.

Nuclear maturation is complete when the oocyte successfully undergoes GVBD and becomes arrested in the metaphase II. The maintenance of high MPF activity keeps eggs arrested at the metaphase II. At fertilization, a sperm Ca^{2+} signal stimulates APC/C activity leading to the degradation of cyclin B. The degradation of cyclin B results in MPF loss and the exit from MII (Madgwick & Jones, 2007).

Figure 1.2: Nuclear and cytoplasmic maturations of mouse oocyte

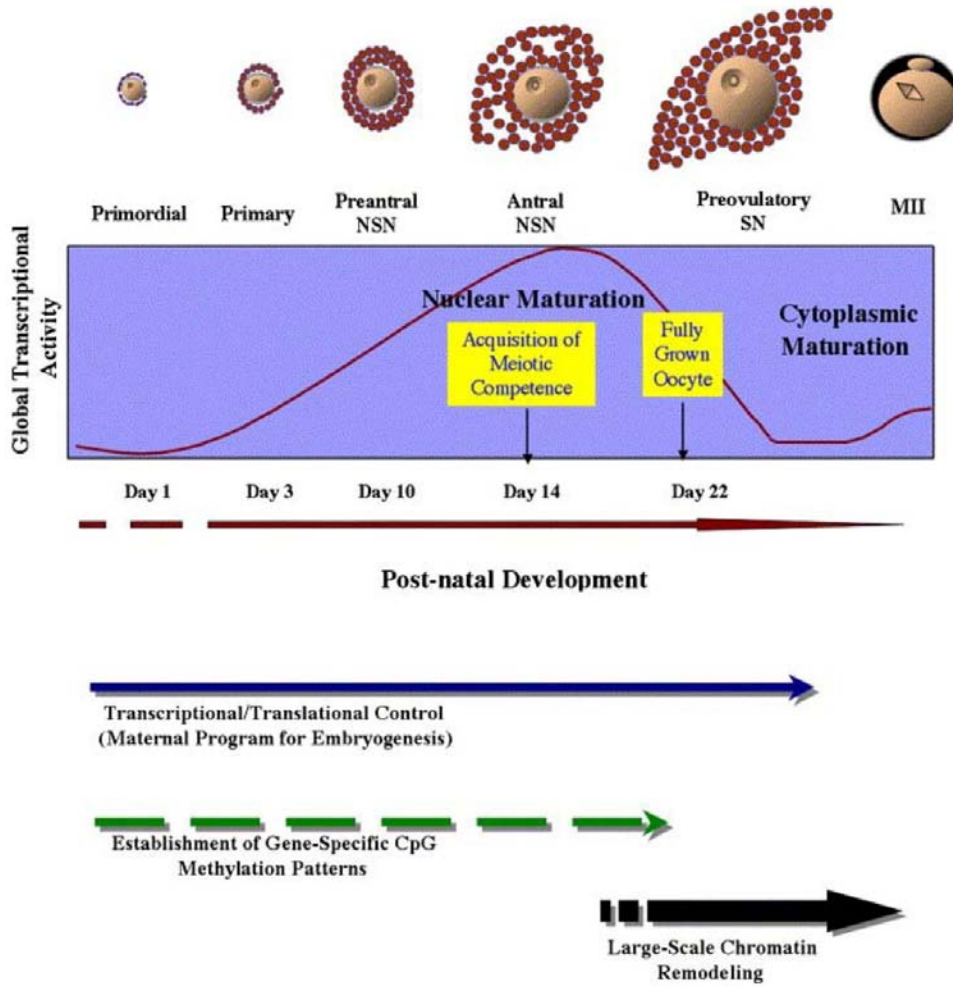
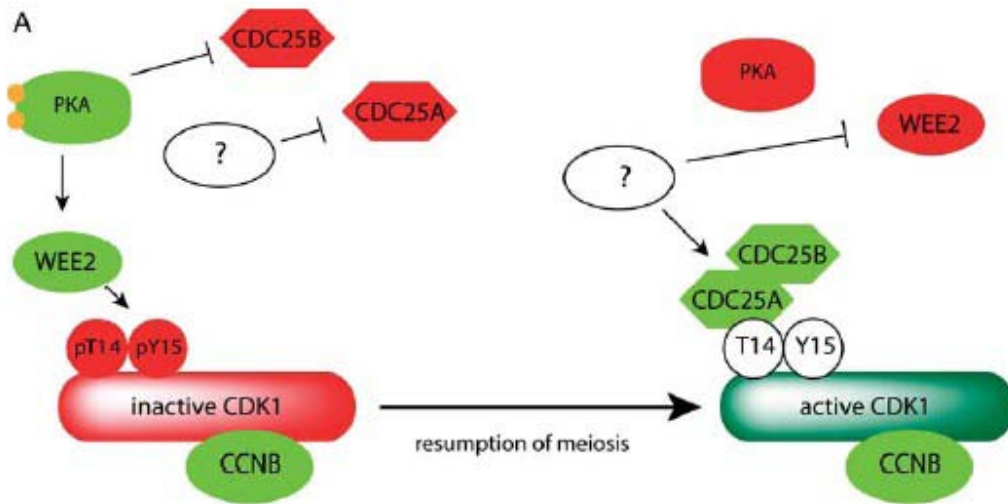


Figure 1.3: Inhibition of CDK1 during prophase I arrest and CDK1 activation during resumption of meiosis.



(Solc *et al.*, 2010)

1.1.3 Cytoplasmic Maturation of Oocyte

In addition to the nuclear maturation, cytoplasmic maturation is also vital for establishing oocyte competence (Eppig, 1996). Fully grown oocytes with only partial cytoplasmic maturation may have incomplete nuclear maturation (Chesnel *et al.*, 1994; Eppig, *et al.*, 1994). Cytoplasmic maturation includes changes that are necessary for egg activation, fertilization and preimplantation embryo development, such as the synthesis of maternal mRNAs and proteins (De Leon *et al.*, 1983; Schultz, 1993), post-transcriptional (Bettegowda & Smith, 2007), translational (Richter, 1991; Schultz & Wassarman, 1977) and post-translational modification (de Vantery *et al.*, 1997; Levesque & Sirard, 1995; Viveiros *et al.*, 2003) as well as cytoskeletal changes (Brevini *et al.*, 2007; Schatten & Schatten, 1987) and the organelle redistribution (Ducibella, *et al.*, 1988; Sun *et al.*, 2001).

During oocyte growth, there is an active production and accumulation of maternal mRNAs (Bachvarova & De Leon, 1980; Piko & Clegg, 1982). The transcription of maternal mRNAs ceases before the oocyte reaches its full size and does not resume until EGA. In mice, a growing oocyte contains about 0.20 ng of RNA and the RNA content increases to 0.57 ng per a fully-grown oocyte (Sternlicht & Schultz, 1981). The poly(A) mRNA content in a fully grown oocyte was reported to be 1.5 - 1.9 pg (Levey *et al.*, 1978; Sternlicht & Schultz, 1981). During oocyte maturation, massive degradation of maternal mRNAs occurs and it continues after fertilization. The mRNAs recruited for translation during maturation become degraded or deadenylated and thus the total poly(A) content decreases in the oocyte (Bachvarova *et al.*, 1985). The poly(A) content increases again after fertilization (Clegg & Piko, 1983; Piko & Clegg, 1982) as maternal mRNAs become recruited for translation in embryo. Most maternal mRNAs become degraded by the mid two-cell stage in mouse embryo (Schultz, 1993).

1.1.3.1 Post-transcriptional / Translational Controls

Transcriptional silencing occurs at the start of nuclear maturation of the oocyte until the EGA. Therefore, mRNAs and proteins necessary for the maturation, fertilization and early embryonic development must be stored in the oocyte in their inactive forms until needed. The activation of mRNA for translation is controlled by polyadenylation and cytoplasmic polyadenylation is mostly regulated by the cytoplasmic polyadenylation element (CPE) in 3'UTR region of mRNA sequence. Different sequences of 3' CPEs are recognized by different RNA binding proteins, and thus the mRNA polyadenylation and translation can be controlled temporally and spatially.

Cytoplasmic polyadenylation seems to be a critical event for the oocyte developmental competence because it can regulate the translation of important maternal factors such as *c-mos*, *cyclins*, *Cdk2*, etc. In *xenopus* oocytes, cytoplasmic polyadenylation element binding protein (CPEB) binds the CPEs of *G10*, *c-mos*, *cdk2*, *cyclins A1*, *B1* and *B2* mRNAs and induces polyadenylation of these RNAs (Stebbins-Boaz *et al.*, 1996). CPE also plays an important role in translational regulation of mouse maternal mRNAs, such as *c-mos* (Gebauer *et al.*, 1994), *cyclin B1* (Tay *et al.*, 2000) and tissue-type plasminogen activator (*tPA*) (Huarte *et al.*, 1987; Vassalli *et al.*, 1989). CPEB has dual roles in translational regulation: it can both activate and repress translation (de Moor & Richter, 1999; Minshall *et al.*, 1999). In *xenopus* oocytes, CPEB interacts with maskin protein, which binds to elongation factor eukaryotic initiation factor 4E (eIF4E) blocking an interaction of eIF4E with eIF4G (Stebbins-Boaz *et al.*, 1999). The inhibition of this interaction between eIF4E and eIF4G by maskin suppresses translation.

However, the translational repression mechanism involving maskin has been recently challenged (Kozak, 2008; Standart & Minshall, 2008). It was reported that

maskin protein is not produced until late in oogenesis (Meijer *et al.*, 2007) implicating there should be another mechanism to repress *cyclin B1* translation in earlier stages of oogenesis. The proposed interaction between maskin and eIF4E was based on the yeast two hybrid assay (Stebbins-Boaz, *et al.*, 1999) and other assays would be needed to present a stronger evidence for the interaction (Kozak, 2008). Additionally, maskin's weak eIF4E-binding site is absent from mammalian maskin proteins (Kozak, 2008), TACC3 (transforming, acidic coiled-coil containing protein 3) (de Moor *et al.*, 2005; Meijer, *et al.*, 2007). A recent identification of a CPEB-binding partner protein, KHDC1B, specifically expressed in mouse oocytes and early embryo, indicated a possibility of a maskin-independent mechanism of translational repression in oocytes (C. Cai *et al.*, 2010).

1.1.3.2 Post-translational Controls

Factors stored in the oocyte may be regulated at the post-translational level, for instance, via phosphorylation or ubiquitination. Unlike protein synthesis that's irreversible in nature, phosphorylation provides a rapid reversible regulation of maternal proteins. As discussed in the previous section, cell cycle proteins critical for meiosis are controlled by phosphorylation and dephosphorylation. In addition to phosphorylation, ubiquitination is also an important mechanism to control the level of maternal proteins. The degradation of maternal proteins is necessary in order to achieve a successful transition from maternal to embryonic control of development and an essential part of normal development (DeRenzo & Seydoux, 2004; Verlhac *et al.*, 2010; Wang *et al.*, 2010). Proteins involved in the ubiquitination pathway are highly abundant in the oocyte and preimplantation embryo and considered major contributors to the degradation of maternal proteins (Knowles *et al.*, 2003). The differential mRNA regulation between oocytes of different qualities for proteins involved in the ubiquitination pathway suggests

that the ubiquitination pathway may play a role in oocyte quality (Mtango & Latham, 2007).

1.1.4 Oocyte-Follicle Interactions

Throughout growth, maturation and fertilization, the oocyte and its surrounding somatic granulosa cells are closely associated with each other. This interaction between the oocyte and the granulosa cells is bi-directional and crucial for the growth and maturation of both the oocyte and granulosa cells (Figure 1.4). During folliculogenesis, follicular cells become differentiated into two types of highly specialized cells, cumulus and mural granulosa cells. Cumulus cells establish direct physical contact with the oocyte via transzonal processes (TZPs) forming cumulus-oocyte complex (COC) (Albertini *et al.*, 2001). Mural granulosa cells are separated from COC by a space called 'antrum' and line the inner wall of the follicle.

Small molecules such as ions, metabolites and amino acids are exchanged between cumulus cells and the oocyte via gap junction channels located at the end of the TZPs while larger molecules get transported by the receptor-mediated endocytosis (Albertini, *et al.*, 2001; Grant & Hirsh, 1999; Herman & Albertini, 1982; Schneider, 2009). In addition to the direct exchange of molecules, the oocyte and cumulus cells also communicate via paracrine hormone signaling. This bidirectional dialog between the oocyte and its surrounding cumulus cells is essential for development and fertility (Matzuk *et al.*, 2002; Yeo *et al.*, 2009).

Oocyte-secreted factors direct the growth, expansion and differentiation of cumulus and granulosa cells (Vanderhyden *et al.*, 1990). The oocyte secretes factors that promote the proliferation of granulosa cells (Vanderhyden *et al.*, 1992), modulate the synthesis of steroid hormones (Coskun *et al.*, 1995) and suppress the luteinization of cumulus granulosa cells by inhibiting LHR mRNA expression (Elvin *et al.*, 2000). The

best-studied oocyte-secreted factors are GDF9 and BMP15, both of which are members of TGF β 1 superfamily. Other members of TGF β 1 superfamily such as TGF β 1, TGF β 2 and activins are also paracrine factors secreted by the oocyte (Gilchrist *et al.*, 2003).

The communication between cumulus cells and the oocyte is essential for the proper maturation of the oocyte following the gonadotropin stimulation (Carabatsos *et al.*, 2000). It was demonstrated that this communication is required for the maintenance of meiotic arrest: mammalian oocytes removed from the follicle spontaneously resume meiosis (Pincus & Enzmann, 1935). During the LH surge, cumulus cells relay the maturation signal from the extra-follicular environment to the oocyte and initiates meiotic resumption in the oocyte. Also, cumulus cells provide essential nutrients and macromolecules to the oocyte throughout maturation, ovulation and fertilization processes.

Figure 1.4: Bidirectional communication between the oocyte and cumulus cells

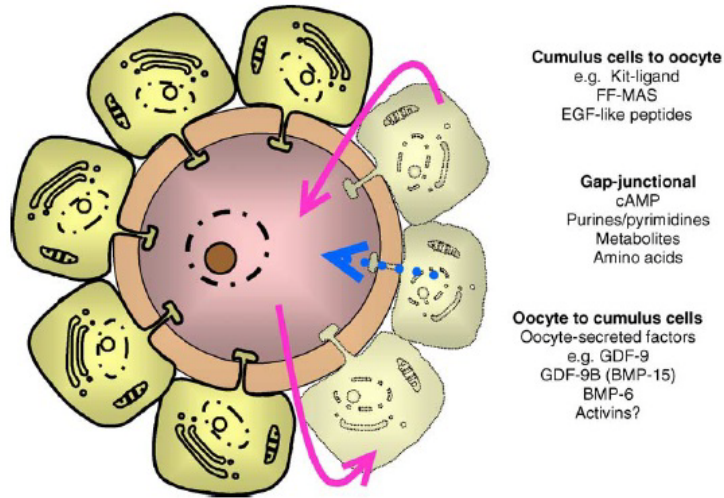


Fig. 1. Oocyte-granulosa cell communication is essential for normal growth and development of both the oocyte and the follicle. Communication occurs via paracrine signaling (curved arrows) and gap-junctional exchange of small regulatory molecules (straight arrow). This is a bi-directional communication axis. (Modified from Sutton et al., 2003a by permission of Oxford University Press).

1.2 Significance

1.2.1 Assisted Reproductive Technologies

The use of ARTs has continuously increased over the past decade and by 2006 over 3 million children had been born worldwide following ARTs (Horsey, 2006; Wright *et al.*, 2006). According to U.S. Centers for Diseases Control and Prevention's latest report, 61,426 infants were born from 148,055 ART cycles in the United States during the year 2008 alone, accounting for more than 1% of all infants born in the U.S. each year. With a constant increase in the number of ART treatments performed worldwide, the demand for the methods giving a higher efficiency and predictability of pregnancy and birth is also growing. There has been an increased awareness of potential long-term health consequences of ARTs. Several studies indicated an increased risk of imprinting disorders like Angelman syndrome and Beckwith-Wiedemann syndrome (Cox *et al.*, 2002; DeBaun *et al.*, 2003; Gicquel *et al.*, 2003; T. Li *et al.*, 2005; Sutcliffe *et al.*, 2006). Moreover, children conceived by ART have a higher rate of major birth defects as compared with babies conceived naturally (Hansen *et al.*, 2002). Birth defects identified among ART children include musculoskeletal and cardiovascular defects, chromosomal abnormalities, congenital malformations like gastroschisis or hypospadias, and low birthweight (D'Souza *et al.*, 1997; Koudstaal *et al.*, 2000; Schieve *et al.*, 2002). Also, the increased rate of multiple pregnancies from ART treatment may further raise the frequencies of preterm deliveries, low birthweight infants, and other complications associated with multiple births (MMWR, 2000; Reynolds, *et al.*, 2003).

It is anticipated that the optimization of ART efficiency may result in a declined rate of multiple pregnancy and minimize potential risks to the offsprings. The ability of an embryo to undergo pre-implantation development, to implant, and to give a rise to an offspring depends on the quality of the oocyte. Therefore, understanding the molecular

characteristics of a high oocyte developmental competence will aid us develop methods to screen and select high quality oocytes for assisted reproduction.

1.2.2 In Vitro Maturation

In Vitro Maturation (IVM) of oocytes is an emerging procedure that has promising potential, where immature oocytes are retrieved from ovarian follicles and cultured. Therefore, if this procedure is employed, ovarian stimulation using expensive hormones can be avoided, and risks for ovarian hyperstimulation syndrome and side effects from medication (C. Grondahl, 2008) may be reduced. Using the IVM procedure, female cancer patients may preserve their oocytes without being exposed to high estrogen levels caused by ovarian stimulation (Ata *et al.*, 2010). Also, IVM of immature oocytes collected from a woman with polycystic ovarian syndrome (PCOS) resulted in a healthy live birth (Trounson *et al.*, 1994). The quality of embryo fertilized and developed in vitro depends on the quality of oocytes (Huang *et al.*, 2002). The quality of oocytes obtained following a traditional controlled ovarian hyperstimulation varies considerably both within and between patients. This can limit the overall success of the procedures and the ability to select the highest quality oocytes for fertilization or the highest quality embryos for embryo transfer. IVM could offer consistent maturation environment for immature oocytes and thus increase the supply of high quality oocytes of more uniform characteristics.

Although there have been a number of successful application of IVM technology in humans (Cha *et al.*, 1991; Chian *et al.*, 2009; Trounson, *et al.*, 1994; Veeck *et al.*, 1983), clinical outcomes such as pregnancy and implantation rates, following IVM are variable among different studies mainly due to suboptimal IVM conditions (Jurema & Nogueira, 2006). The optimization of IVM conditions and further understanding of the oocyte quality are crucial for the advancement of IVM technology and its application.

Key objectives toward achieving more efficient IVM will be to establish the molecular determinants of oocyte quality, identify specific biological processes or mechanisms that may be disrupted by ARTs, and identify specific modifications to procedures to eliminate these deficiencies.

The rhesus monkey is a good animal model for the study of human reproduction. Whereas rodent models, estrous mammals, and lower vertebrates differ markedly from humans in reproductive biology (e.g., IVM works very well in rodents), rhesus monkey reproductive biology is very similar to the human. The importance of a non-human primate model for modeling human granulosa cell function has been highlighted in numerous studies (M. L. Grondahl *et al.*, 2008; Johnson *et al.*, 2007; Neal *et al.*, 2008; Wen *et al.*, 2007). Using a non-human primate model, studies that are not possible in the human can be performed. In the rhesus monkey, VVM yields high quality oocytes from which embryos develop to blastocysts at a rate as high as 61% and subsequent term development (Bavister *et al.*, 1984; Schramm & Bavister, 1996a; Schramm *et al.*, 2003). On the other hand, oocytes retrieved after 7 days of in vivo FSH stimulation and then signaled to mature in vitro (IVM oocytes) show much less efficient development with a blastocyst formation rate of 15-40% (Schramm & Bavister, 1996b, 1999a; Schramm, *et al.*, 2003; Schramm *et al.*, 1994). Also, previous studies showed that embryos derived from IVM oocytes in the monkey are deficient in the timely onset of embryonic gene transcription (Schramm, *et al.*, 2003). The elucidation of the genes and pathways affected during IVM would increase our understanding of the nature and timing of follicular events that are critical for oogenesis, and would also provide valuable insights that may be applicable to improve IVM and other ART methods.

1.2.3 Oocyte Quality Screening Markers

The oocyte develops in close coordination with the somatic companion cells. Cumulus cells establish direct contact with the oocyte via trans-zonal processes and gap junctions until ovulation. The oocyte controls the overall development of the follicle and the differentiation of the cumulus cells (Eppig *et al.*, 2002; Gilchrist *et al.*, 2008; Gougeon, 1996; Matzuk, *et al.*, 2002; M. Zhang *et al.*, 2010). Cumulus cells, in return, provide the oocyte with a range of extracellular and intracellular molecules that support oocyte growth, regulate meiotic progression, and serve as essential metabolic precursors (Donahue & Stern, 1968; Leese & Barton, 1985; Su *et al.*, 2009).

In order to gain insight into the relationship between CCs and the oocyte, several gene expression studies have recently been carried out in different species (Adriaenssens *et al.*, 2011; Anderson *et al.*, 2009; Assidi *et al.*, 2010; Assidi *et al.*, 2011; Assou *et al.*, 2010; Assou *et al.*, 2008; Caixeta *et al.*, 2009; Peddinti *et al.*, 2010; Tamba *et al.*, 2010; Tesfaye *et al.*, 2009; X. Zhang *et al.*, 2005). However, discovery of a clear molecular relationship between the two cell types and identification of oocyte quality determinants are yet to come. The identification of CC markers that can accurately predict oocyte quality would provide an opportunity to develop a powerful and non-invasive method to select high quality oocytes for ART procedures, potentially leading to an increase in the success rate of ART treatments and better health of offsprings produced using ARTs.

1.3 Hypothesis and Specific Aims

Oocyte maturation and the initial phase of pre-implantation embryo development occur during the period of transcriptional silence. Therefore, both developmental processes must depend on maternal factors accumulated in the oocyte during oogenesis (Latham, 1999). I hypothesize that oocytes of different qualities possess distinct molecular characteristics and those molecular differences are responsible for different developmental outcomes. I also hypothesize that oocyte quality is determined by the genetically controlled accumulation of specific macromolecules, and is also affected by and reflected in the gene expression pattern in the supporting companion follicular cells, particularly cumulus and granulosa cells. In an attempt to understand better the molecular events responsible for proper development of oocyte and to identify potential molecular determinants of oocyte quality, I have performed transcriptome analyses based on the following specific aims.

1. Identification of genes and pathways differentially regulated in oocytes of different qualities

- Transcriptomes of rhesus MII-stage oocytes of high and low qualities were compared using cDNA microarrays (VVM-MII vs. IVM-MII).

2. Identification of somatic cell expressed correlates of oocyte quality

- Microarray analysis was performed comparing cumulus cells isolated from rhesus oocytes of high and low qualities (VVM-CC vs. IVM-CC).

3. Evaluation of genetic effects on oocyte quality

- Comparisons were made between transcriptomes of mouse GV and MII stage oocytes of three different genetic backgrounds (B6 vs. BDF1 vs. D2).

CHAPTER 2

MATERIALS AND METHODS

2.1 Collection of Rhesus Oocytes and Cumulus Cells

Adult female rhesus macaques were housed at the California National Primate Research Center (CNPRC). Only females with a history of normal menstrual cycles were selected for the study. Females were observed daily for signs of vaginal bleeding and the first day of menses was denoted cycle day 1. Recombinant human Follicle Stimulation Hormone (r-hFSH: Organon, West Orange, NJ) was administered (37.5 IU) twice daily, intramuscularly (IM) beginning on cycle day 1-4 for 7 days total (Figure 2.1).

For Pre-maturation (PM) or In Vitro Maturation (IVM) experiments, oocytes and cumulus cells (CCs) were collected on day 8. Animals were immobilized with ketamine hydrochloride (10 mg/kg) and cumulus oocyte complexes (COCs) were aspirated with an 18-gauge needle coated in 10,000 IU/ml heparin (Elkins-Sinn Inc., Cherry Hill, NJ) by ultrasound-guided oocyte collection (VandeVoort *et al.*, 2003). All COCs were collected into Tyrode lactate (TL)-HEPES medium (37°C) containing 0.1 mg/ml polyvinyl alcohol (PVA) and 5 ng/ml recombinant human FSH (r-hFSH; Organon). PM-CCs were obtained from GV oocytes immediately after aspiration of COCs.

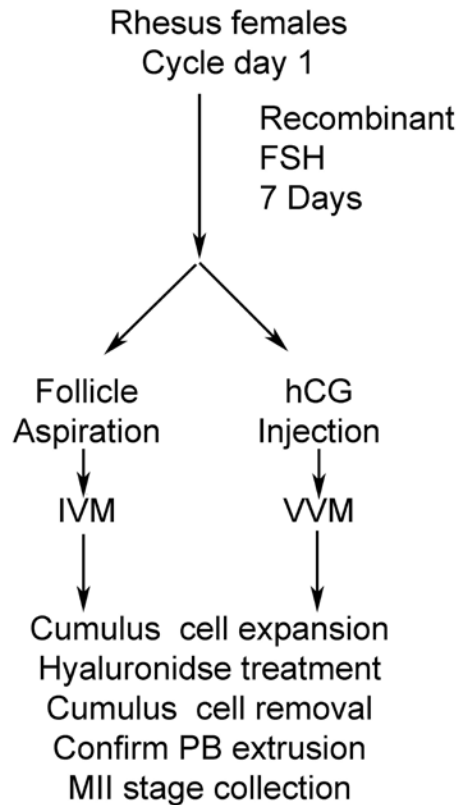
More immature oocytes were recovered at the GV stage and cultured for 24 h in 70- μ l drops under oil in CMRL medium (Boatman & Bavister, 1984) containing 10% bovine calf serum (Gem Cell, Woodland, CA), r-hFSH, r-hLH (0.03 IU/ml Pergonal, Ares-Serono), and 1 μ g/ml androstenedione (Steraloids, Newport, RI) [also reported as CMRLb medium (Schramm, *et al.*, 2003)]. After culture for 24 hrs, the COCs were placed individually into drops of TL-HEPES medium and CCs were removed from

oocytes by trituration through a small bore pipette. Only oocytes with one polar body were used for the IVM group.

For the collection of VVM oocytes and CCs, in addition to the hormonal treatment outlined above for immature oocyte collection, recombinant human chorionic gonadotropin (r-hCG) (1000 IU Ovidrel; Serono, Rockland, MA) was injected (IM) on treatment Day 8. COCs were aspirated from follicles at 28 – 30 h following r-hCG by ultrasound-guided aspiration (VandeVoort & Tarantal, 1991, 2001). Oocytes were retrieved from aspirates as described (VandeVoort, *et al.*, 2003). The EM Con filters (Verterinary concepts, Spring Valley, WI) were rinsed with 10 mg/ml hyaluronidase (MP Biomedicals, Solon, OH) and rinsed twice with TL-HEPES before oocytes were rinsed from the filter. Oocytes were recovered in 70 μ l drops of TL-PVA medium under oil and incubated at 37°C in a humidified atmosphere of 5% CO₂ in air.

Figure 2.1: Summary of procedures employed to obtain oocytes for array analysis.

After seven days of FSH stimulation, oocytes were aspirated on day 8 and subjected to IVM. Alternatively, females were treated with hCG and VVM oocytes aspirated on day 9. After IVM or VVM, cumulus cells have expanded and are removed by hyaluronidase treatment. Second polar body extrusion was confirmed and the oocytes were then lysed for analysis.



2.2 Collection of Mouse Oocytes and Eggs

Female mice of three genetic strains (C57BL/6, DBA/2 and B6D2F1) were purchased from the Jackson Laboratory (Bar Harbor, ME). Preliminary studies revealed that arrays from reciprocal F1 GV stage oocytes were highly similar and did not segregate from each other on hierarchical clustering. Hence, to simplify this study only B6D2F1 (C57BL/6 ♀ X DBA/2 ♂) oocytes were used, as these females can be readily obtained commercially. Ovaries were collected from 6-7 wk old female mice 48 h after the administration of 5 U equine chorionic gonadotropin (eCG; Sigma-Aldrich, St. Louis, MO). COCs were isolated from needle-punctured antral follicles in M2 medium containing 0.2 mM 3-isobutyl-1-methylxanthine (IBMX) and CCs were removed from fully grown GV stage oocytes by pipetting. MII stage eggs were collected from superovulated female mice at 8-10 wk of age. Superovulation was achieved by sequential administration of 5 IU eCG and hCG (Sigma-Aldrich) 48 h apart. CCs were removed using 100 IU/ml hyaluronidase (Sigma-Aldrich, St. Louis, MO) and the zona pellucidae of fully grown GV oocytes and MII eggs were removed using acid tyrode buffer (pH=2.5) (Hogan, 1994).

2.3 RNA Purification, Amplification and Array Hybridization

Total RNA was isolated from cumulus cells using the PicoPure RNA isolation kit (MDS Analytical Technologies, Sunnyvale, CA) according to the manufacturer's instruction. Oocytes or cumulus cells were lysed in 20 ul RNA extraction buffer and stored at -70°C until processing. Four biological replicates for each type of IVM or VVM rhesus monkey oocytes were prepared for the array. For each biological replicate, total RNA was pooled from eight MII oocytes obtained from at least three different monkeys. From each pool, half of the RNA was used for the reverse transcription, amplification

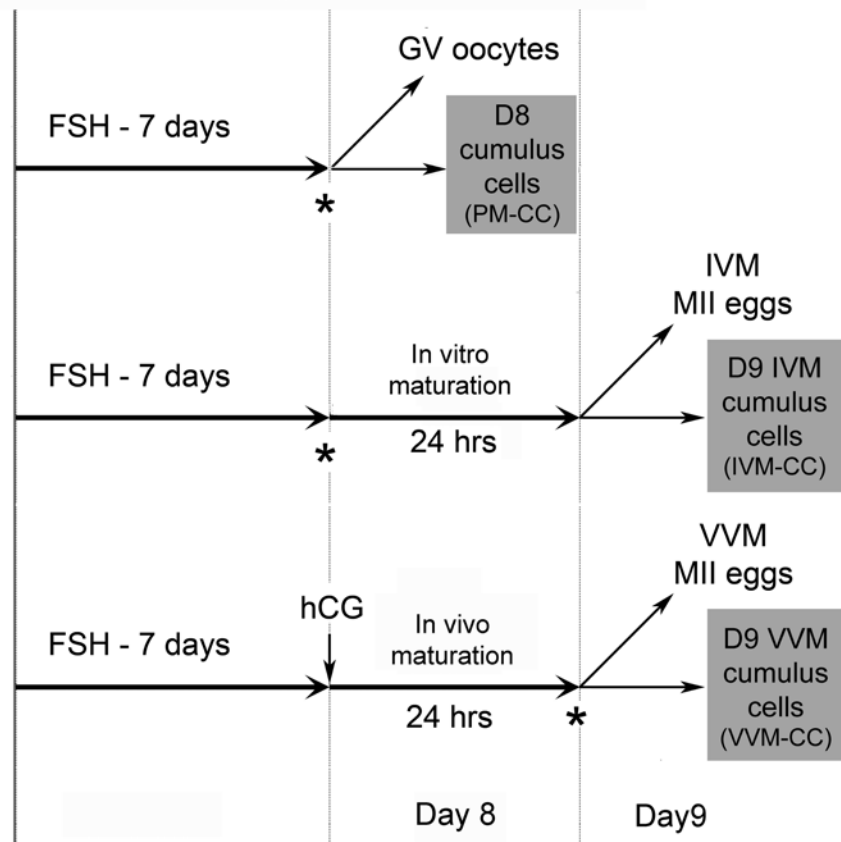
and array hybridization. Three types of rhesus monkey cumulus cells (PM-CC, IVM-CC and VVM-CC) were collected for the array (Figure 2.2). Each array sample contained multiple COCs obtained from one monkey. In total, eleven array samples (4 PM-CC, 3 IVM-CC and 4 VVM-CC) were collected from eleven different female monkeys. Fifty ng of total RNA from each cumulus cell array sample were subjected to the array amplification and hybridization. For the mouse array studies, twenty oocytes or eggs were lysed in each sample. Four biological replicates were collected from each of the three strains of mice (B6, D2 and F1) at both GV and MII stages.

Total RNA isolated from rhesus monkey or mouse oocytes or rhesus monkey cumulus cells was processed according to the Affymetrix cRNA linear amplification and labeling procedure (Eukaryotic Small Sample Target Labeling Assay, Affymetrix GeneChip Expression Analysis Technical Manual) with minor modifications as described previously (Y. S. Lee *et al.*, 2008). To summarize briefly, RNA was reverse transcribed and the cDNA subjected to two rounds of amplification, consisting of a first round of in vitro transcription, followed by random priming and a second round of reverse transcription and in vitro transcription with biotinylated nucleotides to achieve a linear amplification (initial 5 μ l volume for annealing, and reverse transcription for 30 min at 42° C followed by 30 min at 45° C). Ten μ g of the biotin-labeled cRNA sample were fragmented. Rhesus monkey cRNAs were hybridized to Affymetrix Rhesus Genome arrays and mouse cRNAs to Affymetrix Mouse Genome 430 v2 arrays. Fragmentation, hybridization, post-hybridization washing, staining and scanning were performed in the University of Pennsylvania Microarray Core Facility as described in the Affymetrix GeneChip Expression Analysis Technical Manual (Affymetrix, Santa Clara, CA).

Figure 2.2: Schematic summary of experimental design.

Cumulus cells were collected from rhesus monkey cumulus-oocyte complexes at day 8 after 7 days of r-hFSH treatment before final maturation (PM-CC), at day 9 after in vitro maturation (IVM-CC), and at day 9 after in vivo maturation following an ovulatory stimulus with hCG (VVM-CC).

FSH (Follicle-stimulating hormone), hCG (Human chorionic gonadotropin), D8 (Day 8), D9 (Day 9), IVM (In vitro maturation), VVM (In vivo maturation), * Aspiration of follicles



2.4 Microarray Data Analysis

2.4.1 Rhesus Monkey MII Oocyte Arrays

Array data were processed initially using the Microarray Suite 5 (MAS 5, Affymetrix) program with default analysis parameters and global scaling to target a mean equal to 150 signal units. The raw data from all arrays are available online at the GEO repository (Edgar *et al.*, 2002) under series GSE11895 (<http://www.ncbi.nlm.nih.gov/geo>). To minimize false positive signals, only genes called “present” in at least three out of four replicates were used for further analysis with all statistical packages. The MAS metric output was loaded into GeneSpring GX v7.3.1 (Agilent Technologies, Foster City, CA) with per chip normalization to the 50th percentile and per gene normalization to the median. The filtered MAS metrics output was loaded into TIGR-MEV v4.0 (Saeed *et al.*, 2003). The Significance Analysis of Microarray (SAM) algorithm (Tusher *et al.*, 2001) was applied to identify genes with significant differences among samples at the False Discovery Rate (FDR) < 5%. Genes were selected further as differentially expressed on the basis of t-test ($p < 0.05$). Fold-changes of expression were calculated following SAM analysis. The lists of differentially expressed genes were further evaluated using the Ingenuity Pathway Analysis (Ingenuity Systems, Redwood City, CA) and the Expression Analysis Systematic Explorer (EASE, version 2.0) programs to analyze gene ontology for over-representation (Hosack *et al.*, 2003).

2.4.2 Rhesus Monkey Cumulus Cells Arrays

Probe hybridization intensity data were imported into the Affymetrix Expression Console Software and summarized using Robust Multichip Analysis (RMA) algorithm with a global background correction and a quantile normalization (Bolstad *et al.*, 2003; Irizarry *et al.*, 2003). RMA algorithm allows the normalization of array signals across

multiple chips using a single global background reading (Affymetrix, 2006). The advantage of using RMA includes insignificant background variations, low noise and higher reproducibility of array signals (Affymetrix, 2005). Due to its ability to handle a large number of array samples in normalization and summarization, RMA was a better algorithm choice for the rhesus monkey cumulus cell array study in which numerous chips originating from multiple sample types were compared. MAS5 algorithm, on the other hand, normalizes each array independently and usually works well for a simple two-group comparison analysis (Affymetrix, 2002), such as the rhesus monkey MII oocyte array study. In order to minimize false detections, expression data were filtered based on Present/Absent calls determined by MAS5 algorithm at the default settings (detection p -value < 0.05 and $\tau = 0.015$). Only those probe sets called 'Present' in all biological replicates of one of the two groups in comparison were selected for the analysis. To minimize the chance of false positives in subsequent analyses, probe sets with maximum raw intensity values < 100 were omitted from the data set. To identify differentially expressed genes, SAM was performed (Tusher, *et al.*, 2001). In order to be able to work with a reasonable number of genes and derive meaningful array analysis results, more stringent statistical threshold settings were applied to filter the cumulus cell array data. Differentially expressed probe sets were identified at the FDR lower than 1% and the Student's t -test was used to select further for the genes with statistical significance ($P < 0.01$). Full datasets have been deposited in NCBI GEO database and are accessible through accession number GSE25288 (<http://www.ncbi.nlm.nih.gov/geo/>) and at www.preger.org. Pathway analysis and biological functional analysis were performed using the rhesus genome array annotations provided in IPA software (Ingenuity Systems, Redwood City, CA). For biological functional analysis, Fisher's exact test was performed with the p -value threshold of 0.05 to identify molecular and cellular functional categories with statistical significance.

2.4.3 Mouse GV and MII Oocytes Arrays

Four biological replicates were collected and processed for microarray from each group of oocytes obtained from three different strains in two different stages of development. Probe level data were summarized and normalized using the RMA algorithm with quantile normalization (Irizarry, *et al.*, 2003) provided in the Expression Console software (Affymetrix, Santa Clara, CA). RMA was chosen over MAS5 to normalize the mouse array data because this array study involves numerous arrays from various groups of samples, e.g. strains and stages. Detection calls (present, marginal or absent) were made for each probe set using MAS 5 algorithm provided in the Expression Console Software at the default setting (detection p-value < 0.05 and tau = 0.015). Probe sets called 'Present' in at least three out of four biological replicates were considered for further analysis. Genes differentially expressed among the three strains of mice were identified using SAM at FDR < 5% (Tusher, *et al.*, 2001). Pathway analysis and biological functional analysis were performed using the Ingenuity Pathway Analysis software (Ingenuity Systems, Redwood City, CA). For biological functional analysis, Fisher's exact test was performed with the p-value threshold of 0.01 to identify molecular and cellular functional categories with statistical significance. Hierarchical clustering and non-hierarchical K-means clustering analyses were performed using the GeneSpring GX v. 11. An unsupervised hierarchical cluster tree was produced based on the similarity measurement of Pearson correlation and the distance calculation with the default centroid linkage method (AgilentTechnologies, 2008). K-means clustering was used to group genes with similar expression profiles into clusters using the Pearson centroid distance calculation method. Ingenuity Pathway Analysis (IPA; Ingenuity Systems, Redwood, CA) was used to identify networks, pathways, and sub-sets of

affiliated genes that are over-represented amongst the lists of gene differences determined comparing the different genotypes at each stage.

2.5 Quantitative mRNA Expression Analysis

2.5.1 Rhesus Monkey IVM and VVM MII oocytes

Independent evaluation and confirmation of gene expression differences were performed using the quantitative real time RT-PCR (qRT-PCR) or Quantitative Amplification and Dot Blotting (QADB) assays. The QADB method is a quantitative RT-PCR based method that involves whole transcriptome amplification as cDNA, followed by dot blotting and quantitative analysis of cDNA probe hybridization. This method allows the assay of maximum number of genes with a small amount of materials. However, the QADB method requires higher mRNA abundance for efficient detection and quantitation than the qRT-PCR method does. The qRT-PCR was employed for lower abundance mRNAs not detectable by QADB: the mRNAs with array raw intensity values ≥ 500 were assayed by the QADB method while those with array signal values < 500 units were assayed using the qRT-PCR method.

For QADB analysis, 10 or 7 samples of 1-2 rhesus monkey oocytes per sample were assayed each for IVM and VVM oocytes, and representing oocytes from at least three females for each condition. It's been shown that the input in the range of 1-2 oocytes per sample does not affect results because the RT-PCR method amplifies the entire mRNA population quantitatively (Brady & Iscove, 1993; Iscove *et al.*, 2002). Complementary DNA probes were obtained by PCR (Table 2.1) from reverse transcribed rhesus monkey ovary, testis, or liver RNA. Blot preparation, probe preparation, hybridization, and quantitative analyses were performed as described (Zheng *et al.*, 2005a; Zheng *et al.*, 2004; Zheng *et al.*, 2005b; Zheng *et al.*, 2006). For

the genes assayed using the QADB method, student t-test was performed between IVM and VVM oocytes samples to determine a statistical significance of difference.

For the qRT-PCR assay, two pools of 10 rhesus monkey oocytes each, representing at least three females, were obtained for IVM and VVM oocytes. Total RNA was isolated using the PicoPure RNA isolation kit (Molecular Devices, Sunnyvale, CA) and assayed by qRT-PCR using pre-designed TaqMan gene expression assays and ABI Prism 7000 (Applied Biosystems, Foster City, CA). The mRNA abundance of a target gene was normalized to an internal gene control (*UBB*) for sample to sample comparisons and the relative expression ratio of IVM to VVM groups was obtained by the comparative C_T method (Livak & Schmittgen, 2001). Independent statistical analysis was performed to obtain p-values of difference between groups using Relative Expression Software Tool (REST) (Pfaffl *et al.*, 2002) for the genes assayed by quantitative RT-PCR method. The REST program calculates a relative expression ratio between the two groups of oocytes based on the normalized C_T values (ΔC_T) of biological replicate samples and this expression ratio is tested for significance by a pair wise fixed reallocation randomization test.

2.5.2 Rhesus Monkey IVM and VVM Cumulus Cells

Total RNAs isolated from rhesus monkey cumulus cells were subjected to a whole transcriptome amplification using the QuantiTect whole transcriptome kit (Qiagen, Valencia, CA) prior to qRT-PCR. Custom TaqMan gene expression assays were designed based on rhesus monkey cDNA sequences using Primer Express software v3.0 (Applied biosystems, Foster City, CA) (Table 2.2). Pre-designed TaqMan assays were used for the qRT-PCR of the mouse oocyte samples. Approximately 100 ng of cDNA prepared via whole transcriptome amplification was used for each sample with ABI StepOne Plus instrument according to the manufacturer's recommendations

(Applied biosystems, Foster City, CA). The mRNA abundance of a target gene was normalized to the endogenous mitochondrial ribosomal protein S18C gene (*MRPS18C*) to handle sample to sample variations. Rhesus monkey cumulus cell gene expression values were further analyzed for a relationship to oocyte quality. Single- and multiple-gene generalized estimating equations (GEE) were used to calculate the relationship of gene expression to oocyte quality. GEE is a special case of the generalized linear model taking into consideration the occurrence of a binary outcome (oocyte quality) from multiple events of a single experimental unit.

2.5.3 Mouse GV and MII stage Oocytes

Total RNA was extracted from twenty oocytes of each kind using PicoPure RNA extraction kit and ten oocyte equivalents of RNA were used in each of the QuantiTect whole transcriptome amplification reaction. About fifty ng of QuantiTect cDNAs were used in a single real time PCR reaction. At least four biological replicates were used for each strain and each stage in the relative quantitation analysis. Quantitative real time PCR was performed using TaqMan gene expression assays with ABI StepOne Plus instrument according to the manufacturer's protocol (Applied biosystems, Foster City, CA). The abundance of a target mRNA was normalized to the endogenous ribosomal protein 18s gene (*Rn18s*) for sample to sample comparisons. The relative expression ratios among different groups were obtained by the comparative C_T method (Livak & Schmittgen, 2001) using the StepOne software version 2.1 (Applied biosystems, Foster City, CA).

Table 2.1: Primers used to obtain cDNA probes for QADB

Gene Symbol		Primer Sequence	GenBank Accession no.	Probe size (bp)
<i>ATP6V0A4</i>	Forward	5'-GACCATGGGGAAGAGTTCAA-3'	XM_001105743	520
	Reverse	5'-GCTTCAGGTGAGCCAAGAAC-3'		
<i>AKR1C1</i>	Forward	5'-CAGAAGGCCCTATGTGTGGT-3'	XM_001104300	572
	Reverse	5'-TCACTTTTCCTGGTGGGTGT-3'		
<i>OSMR</i>	Forward	5'-ATGCCCAGCCTATTTGTCAC-3'	XM_001083745	423
	Reverse	5'-GGCATAAGCATAGGCAGAGC-3'		
<i>MT2A</i>	Forward	5'-CATGGATCCCAACTGCTCTT-3'	XM_001092096	283
	Reverse	5'-AAAAAGGAATGCAGCAAACG-3'		
<i>SLC1A5</i>	Forward	5'-AAACCCCTACCGCTTTCTGT-3'	XR_014069	648
	Reverse	5'-GTCCCTCCTGGGGTTTACAT-3'		
<i>SLC6A6</i>	Forward	5'-GCCACAGTATTTTGGGTTGG-3'	XM_001092530	199
	Reverse	5'-GAGGGCTCTGATTGGAGACA-3'		
<i>SPINK2</i>	Forward	5'-ATTGCGTTTCCCCTTTTTCT-3'	XM_001083400	180
	Reverse	5'-CACAAGTTATCTGGGCAGCA-3'		
<i>STAR</i>	Forward	5'-GGCTACTCAGCATCGACCTC-3'	XM_001090130	554
	Reverse	5'-CCTTGTACACACGCACTGCT-3'		
<i>TDRD1</i>	Forward	5'-TGGGACTGTGATGTAGCTG-3'	XM_001091904	619
	Reverse	5'-CTTCAACTCCTGGCCTCAAG-3'		
<i>UBB</i>	Forward	5' ATGGCCGCACTCTTTCTGACTACA 3'	BC000379	333
	Reverse	5'-CACTGCGAATGCCATGACTGAAGA-3'		

Table 2.2: Primer and Probe Sequences of the Custom-designed TaqMan assays used in qRT-PCR

Gene symbol	Forward Primer Sequence	Reverse Primer Sequence	Reporter Sequence
<i>ACPP</i>	AAGCCACCCCGTTCT	AACACAAAGAAGCGTATCAATCGA	ACATGACTGACAAAGAC
<i>AQP11</i>	GGAAGCCGCCTTATAGTTTCA	GGATGCCTCATTTCACAGTAATTT	CACTGGGACTTAAACA
<i>CCBE1</i>	TCTGAGCAGGTGCCATGATC	AACTTCCTTGCGGCCTTCA	AGGCTGAACCAATACACAGT
<i>CCDC126</i>	CCAAATCTCTGTTCTCTCTGTGTA	AACTTCTACCTGGCAATGGCATA	CTACCTTTATGTGAAGAAAT
<i>CLU</i>	GGTGTCCCAGCTGGCAA	CGTGGTGACCCGCAGATAG	CGCAAGGCGAAGAC
<i>CYP11A1</i>	GGCACCACATTCAACCTCATC	AAGGGCCAGAAGGTGAAGGA	TGCCTGAAAAGCC
<i>CYP19A1</i>	CTCTTAAAGAATGTTTTGGTCTCCATT	GCTTGTGAATTTTTCTTTGTGTACATGTAT	TAGTAGTCTGTGCATAAGGT
<i>EGR2</i>	TTGGTGCCTTGTGTGATGTAGAC	CTTCCATAAAGGCAACCCATT	ATGTTACAGGGTCTGCATG
<i>EGR3</i>	AAAGCAACAAAAGAAAATGCACTCT	CCCCATAGGTTTTCTGTTAAAA	CTTATGTGAACTGAGAGAAA
<i>FN1</i>	GCCTGTTCTGCTTCAAGTATTCA	CACCAAATCACAAGTTAGAATCACTTC	ACCGCTCAGTATTTTA
<i>FOSB</i>	TTCTCCCCCGCCTGTGT	ATGGGACAGTCAGAGAGGAGATAAG	CATCTGACCGTTTTTC
<i>FOSL2</i>	CCCAAGACCTGGCGTGAT	GAGACAGCTGCTCATCTCTCCTT	ACCATTGGCACCACCGT
<i>GMNN</i>	TGTTGAGAATTTTACTGCCGAAGT	CCAGAATTGGCATTATGTAGTTACGT	ACCTCCACTAGTTCTTT
<i>HRAS</i>	GGAAGCTGAACCCTCTTGATG	CGTCAGGAGAGCACACACTTG	CCCCGGCTGCATGA
<i>HSD11B1</i>	CTGAGCTCTTGTCCATGAAGACA	TCAGGTGTGACCCATGACTTTC	CTTCCCAGGGTATCTC
<i>HSD11B2</i>	AGGCCAAGGTTTCCCAAGTGT	GGGTCTGTTTGGGCTCATGA	CTGCGCCTCTCCACT
<i>HSD17B1</i>	GGGCTACCCTTCAATGACGTT	GACTCTCGCATAAGCC TTCGA	CCAGCAAGTTCGCG
<i>HSD3B2</i>	TGGCCCAACCAGAAGCTTT	TTGGGTAACAGCAAATCATATTGTCT	TGTCCTAATCATACGCAGAG
<i>HSDL1</i>	GGAGGCTGAGGCAGGAGAAT	GCACGATCTTGGCTCATCTCA	AGCCCGGGATGCAG
<i>IGF1</i>	GCAGCGCCGCATCAG	GTATGTAGGGTGGGTGTTGAGAGA	ATCCACTCTTCTAGGGATAT
<i>IGF1R</i>	TCAGCCCAACTGTTGATGCA	TCTTCTTACTGCTGTTGTGGTGT	TGCAAGGAAAGAAATT
<i>IGFBP3</i>	CAAAGTCAGGCTCAGGAGACT	CTCTGTGCAGCGTGTGTTCA	TGCTGCAGCCCTC
<i>IGFBP4</i>	TGGACTGAATGTGCCTAATGGA	GACCCAGGAAGCCCCTCAT	AAGACCCACGTGCTAGG

(Cont'd) Table 2.2: Primer and Probe Sequences of the Custom-designed TaqMan assays used in qRT-PCR

Gene symbol	Forward Primer Sequence	Reverse Primer Sequence	Reporter Sequence
<i>IGFBP5</i>	GGGTGAACAATTTTGT GGCTATTT	GGCCGGAGAAACCCTC AA	CCCTATAATTCTGACC CGCT
<i>IGFBP7</i>	GGACGATGCTGGAGAA TATGAGT	CGATGCTGAAGCCTGT CCTT	CCATGCATCCAATTC
<i>INSR</i>	ACCAGAATGTGACGGA GTTTGAT	TCTACCACCGTCCAGC TGTTG	CAGGATGCGTGTGGT T
<i>IRS1</i>	TTGGCAATTGAATGGA AGCA	GGAATCACCCATCTCC TTCTCTTT	TAAGAAGAGGAAATCA AAGTC
<i>IRS2</i>	CGGTCCTCGGCCTTAG TGA	CCTGCACTGGAATCCA ACAA	ATGGTCCAAGTATAGA CAGC
<i>KCNK3</i>	TGTGCTGGCCACTGAT TCC	CTCCTGCCCTGGTGAC CTAA	TTGAGTCTCACAACAG CCTA
<i>KLF6</i>	TGGCTGGGCTGGTATT TTGT	AAACCAGTTATGTGAG CGTTAGTCA	TCTTCCTGGAAATGAG CA
<i>MYST3</i>	TGCTTTTCCTGTTTTGT AACCTCTT	GCACCCCTTCCCCTTA GC	TGTTCTGGTGACTTG TA
<i>NEK6</i>	GGAAGGATGGGATGTA AAAAAGCT	CGCTAGGAAGTTGCAG AACCA	AGGGCTATCCTTTACA AAT
<i>PAPPA</i>	CCATATTATATCACTCC CAGTAGCACTT	CCAGAGATGGCCAATA GATGTCT	CTGGTGATCAAAAAC
<i>PPP1R14 B</i>	AGCAGCTTACGCGCCT CTAC	CTCATCCACATCAATCT CCAGTTCT	CTGCCAGGAAGAGGA
<i>PTGS2</i>	GTTTGTCTTAGGATA GGCCTGTGT	TATGGCACCTTCAGGC TAATGA	AGCCACAAAGAATA
<i>RORA</i>	AAAGCCTGAATACCTT CTGTTCCA	CAAGGCCAGGTTTTTC ACAATAT	TGGTGTCCAAATGGT
<i>SERBP1</i>	GTGGCAGCAGGACTGA CAAG	TGCCTCTGGGTCATCC ACAT	TCAAGTGCTTCTGCTC C
<i>SMAD7</i>	CAAGAAGGATTTGGTC CGTCATA	TAGAAGAAATGAAAGA AGAGTTAGGTGTCA	CCAAGGTACCATCTCT AGG
<i>STC1</i>	AGTTCTTTACTCGTCCC CTTTCATC	GAAAGTCTCCCACCCC ATCA	CTGGTACTCTGGCAA AT
<i>TAF10</i>	CTGCCCTCAGCGAGTA TGG	GGGTGGCTCAGGTGAA GTAGTG	ATCAATGTGAAGAAGC C
<i>TGFB1</i>	CAAGGGCTACCATGCC AACT	GTGTGTCCAGGCTCCA AATGT	CTGCCTGGGACCC
<i>TGFBR2</i>	GCAGAAGTTTGAATT AGGCAGAA	ACTCTCAGCCCACCCA CACT	CTCTGGGCACCTTAC
<i>TGFBR3</i>	TTCTGCAGGCTACACC CTTAATT	TTTCAACAACAGCTTCA GCATCA	CAGAGGCCATTTTGT

2.6 Transcription Factor Binding Motif Analysis

To identify potentially shared transcription factor binding motifs amongst the genes encoding mRNAs elevated in IVM oocytes, the list of official gene symbols was analyzed using the oPOSSUM analysis software (<http://www.cisreg.ca/cgi-bin/oPOSSUM/opossum>) (Ho Sui *et al.*, 2005). This software detects transcription factor binding sites (TFBS) over-represented among genes of interests and the identified TFBS are assigned with two statistical measurements, z-score and Fisher's exact probability (Ho Sui, *et al.*, 2005). The z-score tests for over-representation and the Fisher's exact probability value assesses a non-random association between the gene set and a given TFBS. For this analysis, I retrieved data for genes passing the threshold of $Z \geq 5.0$ and Fisher $P < 0.05$ for further examination.

2.7 3' UTR Analysis

2.7.1 3' UTR Analysis of mRNAs Over-expressed in Rhesus Monkey IVM Oocytes

The 3' UTRs of the 44 mRNAs that are over-expressed in IVM oocytes were examined. The mRNAs in the oocyte is highly subject to post-transcriptional regulation and the mRNA stability often depends on the presence of a CPE (McGrew & Richter, 1990; Oh *et al.*, 2000; Oh *et al.*, 1997; R. Simon *et al.*, 1992)] in the 3' UTR region of the mRNA. The CPE is responsible for binding maternal mRNAs into a messenger ribonucleoprotein complex with Maskin and CPE binding protein one (CPEB1) for storage, and subsequently regulates translational recruitment via a process that includes Maskin and CPEB phosphorylation, mRNA polyadenylation, and binding of translational initiation factors to the 5' mRNA cap (Barnard *et al.*, 2005; Cao & Richter, 2002; Fox *et al.*, 1992; Hodgman *et al.*, 2001; Richter, 1999). The 3'UTR exon sequences were retrieved for the 44 mRNAs over from the sequence database using the tools available

at <http://genome.ucsc.edu/cgi-bin/hgGateway?db=hg10>. These sequences were then examined for the presence of any of 14 published sequences that can function as CPEs in either mouse or frog [Table 2.3, (Oh, *et al.*, 2000; R. Simon, *et al.*, 1992)].

2.7.2 3' UTR Analysis of MII-stage Overdominance Genes in Mouse Oocytes

The mRNA sequences of mRNAs in MII-stage overdominance groups were retrieved from the NCBI Entrez database. Model mRNA sequences (i.e. IDs starting with XM) were excluded from the analysis. Whenever there are two or more mRNA sequences linked to the same gene, the longest sequence was selected for the analysis. The 3'UTR sequences were grouped into two groups, MII-ODL and MII-ODH, containing $n_L=377$ and $n_H=257$ 3'UTR sequences respectively.

For each potential motif m of length 5-15 nt

1. The number of 3'UTR sequences in MII-ODL group containing at least one m [$c_L(m)$] was counted.
2. The number of 3'UTR sequences in MII-ODH group containing at least one m [$c_H(m)$] was counted.
3. Frequencies of m in MII-ODL [$f_L(m)$] and MII-ODH [$f_H(m)$] were calculated as [$f_L(m) = c_L(m)/n_L$] and [$f_H(m) = c_H(m)/n_H$].
4. The log-ratio for frequencies of m [$f_{lr}(m)$] was calculated as [$f_{lr}(m)=\log_2(f_L(m)/f_H(m))$].
5. A goodness-of-fit statistical test was performed to compare two frequencies, $f_L(m)$ and $f_H(m)$; each statistical test returns one p-value.

To address the multiple comparisons issue, the Benjamini-Hochberg (BH) method for false discovery rate control was applied to the data. A cut-off threshold was set at the BH-adjusted p-value < 0.01 to identify the motifs with significant differences of frequencies in MII-ODL and MII-ODH 3'UTR sequences.

For a set of motifs M , its cover over MII-ODL was defined as the set of MII-ODL 3'UTR sequences that contain at least one motif from M . M 's coverage of ODL $cov_L(M)$ was further defined as the size of its cover over MII-ODL divided by the size n_L of MII-ODL. M 's coverage of MII-ODH was defined similarly. For a set of candidate motifs M_C , 45 significant motifs that only occur in 3'UTR sequences from MII-ODL (meaning that their f_H is 0, and flr value is undefined) and the top 100 significant motifs with highest flr values were selected. The following greedy iterative procedure was used to find an optimal set of motifs M :

1. Set $M = []$, $M' = M_C$.
2. Add to M the motif m from M' that maximizes $cov_L(M+[m]) - cov_H(M+[m])$.
3. Move m from M' to M : $M \leftarrow M+[m]$, $M' \leftarrow M'-[m]$
4. Repeat from step 2, until $M'=[]$.

Table 2.3: Published CPE motifs employed in analysis

AUUUUUUAU	UUUUUAU
UUUUUAAU	AUUUUAAU
UUUUAAU	UUUUUAU
AUUUUAA	AUUUUAAU
AUUUUUA	UUUUAAU
UUUUUUUUU	AUUUUUAAA
AUUUUUAA	UUUUUUUUU

CHAPTER 3
EFFECTS OF IN VITRO MATURATION ON GENE EXPRESSION
IN RHESUS MONKEY OOCYTES

3.1 Identification of Genes Differentially Expressed Between IVM and VVM Oocytes

High quality array data sets were generated for each kind of IVM and VVM rhesus monkey MII oocytes. Quality control parameters were well within acceptable range for all eight arrays hybridized for this study (Table 3.1). K-means hierarchical clustering confirmed the similarity among each type of oocytes. The biological replicates of IVM and VVM oocytes clustered appropriately with the same group of samples without any apparent outliers (Figure 3.1). Also, it indicates that there are sufficient differences between IVM and VVM oocytes to allow them to cluster separately.

Comparisons between rhesus monkey IVM and VVM oocytes revealed a remarkably small number of differentially expressed genes. At the FDR < 0.05 and P-value < 0.05, there were 59 genes that differed in mRNA expression between IVM and VVM oocytes out of 1.9×10^4 total probe sets employed for the SAM analysis. This only represents 0.39% of total genes detected in either IVM or VVM oocytes. Of this small set of differentially expressed mRNAs, ninety percent were more abundant in IVM oocytes. Only seven out of the 59 mRNAs were expressed more highly in VVM oocytes (Table 3.2) whereas the remaining 52 mRNAs were expressed more highly in IVM oocytes (Table 3.3).

Aldo-keto reductase family 1, member C1 (*AKR1C1*) mRNA showed the biggest difference in expression between IVM and VVM oocytes. The mRNA abundance of *AKR1C1* gene was initially calculated as 60-fold greater in VVM oocytes than in IVM oocytes. The average array raw intensity values for *AKR1C1* mRNA in IVM oocytes was very low (6.83) and it was called 'Absent' on the chip at the P-value < 0.05 threshold.

Therefore, the differential mRNA expression of *AKR1C1* between IVM and VVM oocytes was essentially qualitative. In addition to *AKR1C1*, Chromosome 6 open reading frame 117 (*C6orf117*) and Cholesterol 25-hydroxylase (*CH25H*) mRNAs were only detected in the VVM oocytes.

Amongst the genes more highly expressed in IVM oocytes, Suppressor of cytokine signaling 3 (*SOCS3*) had the largest fold change of difference between IVM and VVM oocytes (17-fold higher in IVM). The expression of *SOCS3* was not detected in VVM oocytes and, therefore, the differential expression of this gene was also qualitative. Out of 39 mRNAs that were more highly expressed in IVM oocytes and had array intensities ≥ 100 , *SOCS3* and *MPPE1* (Metallophosphoesterase 1) were the only two that showed the qualitative difference: the two mRNAs are only expressed in IVM oocytes and not expressed in VVM oocytes.

Table 3.1: Quality control parameters for array hybridization (Rhesus monkey IVM and VVM MII eggs)

	% P-call	Scale Factor	Background
VVM oocytes	33.61-40.35	0.873-1.59	43.64-65.28
IVM oocytes	36.49-37.71	0.957-1.372	48.32-59.84
Normal Range	30 - 60	0.5 – 5.0	20 - 100

Figure 3.1: Hierarchical clustering (HCL) of in vitro (IVM) and in vivo (VVM) matured oocytes.

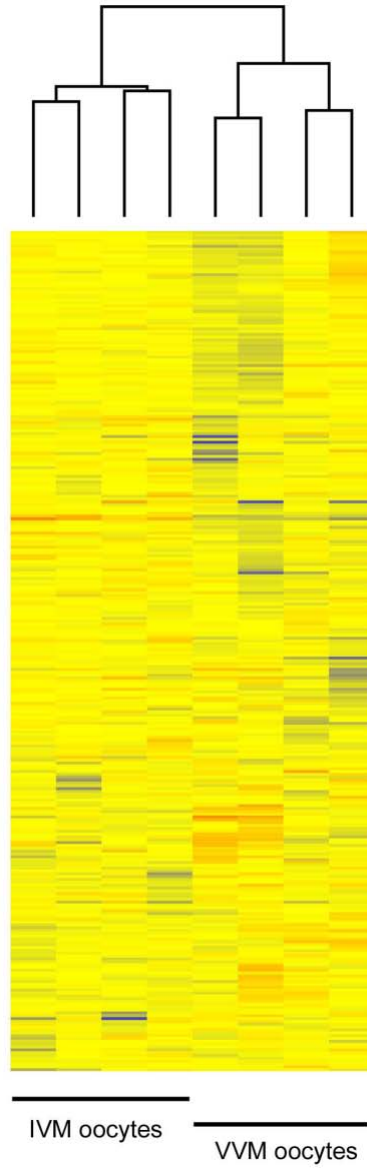


Table 3.2: Genes expressed higher in VVM oocytes than in IVM oocytes

Gene Symbol	Gene Description	Ratio VVM / IVM	Average Raw Intensity	
			IVM	VVM
<i>AKR1C1</i>	aldo-keto reductase family 1, member C1	60.19	6.83	410.78
<i>ATP6V0A4</i>	ATPase, H ⁺ transporting, lysosomal V0 subunit a isoform 4	2.77	190.23	527.55
<i>C6orf117</i>	chromosome 6 open reading frame 117	26.78	15.80	423.18
<i>CH25H</i>	cholesterol 25-hydroxylase	7.60	15.00	114.05
<i>FLJ37035</i>	FLJ37035 protein	1.91	65.53	125.15
<i>ZGPAT</i>	zinc finger, CCCH-type with G patch domain	2.43	32.05	77.73
<i>ZNF542</i>	zinc finger protein 542	2.59	21.85	56.68

Table 3.3: Genes expressed higher in IVM oocytes than in VVM oocytes

Gene Symbol	Gene Description	Ratio IVM /VVM	Average Raw Intensity	
			IVM	VVM
<i>C10orf125</i>	similar to human C10orf125	3.28	57.95	17.65
<i>CD5L</i>	CD5 antigen-like (scavenger receptor cysteine rich family)	4.90	33.95	6.93
<i>CD83</i>	CD83 antigen (activated B lymphocytes, immunoglobulin superfamily)	2.59	189.43	73.25
<i>CKAP4</i>	similar to cytoskeleton-associated protein 4	2.01	1230.20	612.50
<i>CUGBP2</i>	CUG triplet repeat, RNA binding protein 2	2.06	520.53	252.90
<i>CYP19A1</i>	cytochrome P450, family 19, subfamily A, polypeptide 1	4.93	668.80	135.78
<i>CYP3A43</i>	cytochrome P450, family 3, subfamily A, polypeptide 43	3.95	108.75	27.55
<i>CYP3A5</i>	cytochrome P450, family 3, subfamily A, polypeptide 5	12.20	79.93	6.55
<i>DUSP1</i>	dual specificity phosphatase 1	3.39	1197.73	353.10
<i>EFNA1</i>	similar to ephrin A1 isoform a precursor	3.05	83.93	27.53
<i>FLJ35767</i>	FLJ35767 protein	2.42	270.73	111.68
<i>GAP43</i>	growth associated protein 43	7.12	57.88	8.13
<i>GRIN2A</i>	similar to human glutamate receptor, ionotropic, N-methyl D-aspartate 2A	2.22	696.93	313.65
<i>HSD11B2</i>	hydroxysteroid (11-beta) dehydrogenase 2	5.49	1031.48	187.73
<i>ID3</i>	similar to inhibitor of DNA binding 3	2.95	259.35	88.05
<i>IL26</i>	interleukin 26	3.80	39.58	10.43
<i>IL6ST</i>	Interleukin 6 signal transducer (gp130, oncostatin M receptor)	2.35	255.70	108.75
<i>INHBA</i>	Inhibin, beta A (activin A, activin AB alpha polypeptide)	10.17	589.98	58.00
<i>KCNK3</i>	Potassium channel, subfamily K, member 3	2.91	248.13	85.20
<i>LDLR</i>	low density lipoprotein receptor (familial hypercholesterolemia)	5.05	321.20	63.55
<i>LOC704308</i>	hypothetical protein LOC704308 related to H19	4.54	11113.85	2448.85
<i>LOC92017</i>	similar to RIKEN cDNA 4933437K13	7.91	615.25	77.78
<i>LOH11CR1J</i>	LOH11CR1J gene, loss of heterozygosity, 11, chromosomal region 1 gene J product	1.62	328.33	203.00
<i>MDM4</i>	Mdm4, transformed 3T3 cell double minute 4, p53 binding protein	1.95	422.90	217.05
<i>MITD1</i>	hypothetical protein BC018453	1.70	2850.83	1672.28
<i>MPPE1</i>	metallophosphoesterase 1	15.04	108.30	7.20

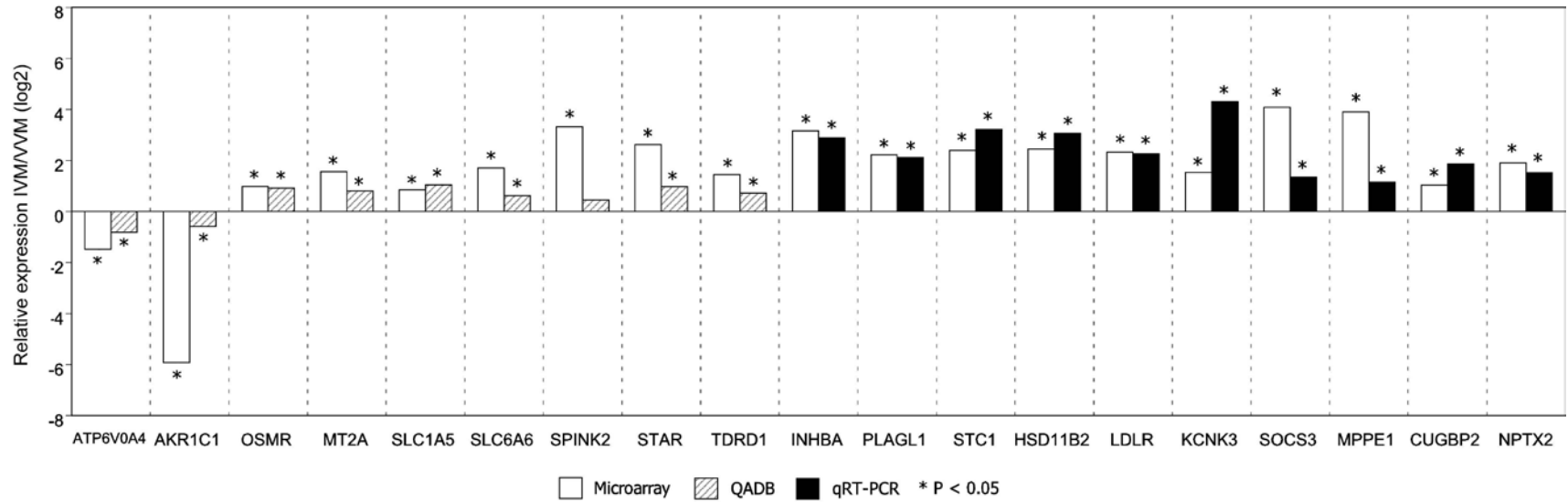
(Cont'd) Table 3.3: Genes expressed higher in IVM oocytes than in VVM oocytes

Gene Symbol	Gene Description	Ratio IVM /VVM	Average Raw Intensity	
			IVM	VVM
<i>MT2A</i>	metallothionein 2A	2.96	10511.85	3551.68
<i>MYLIP</i>	myosin regulatory light chain interacting protein	1.79	5456.40	3053.88
<i>NBEAL1</i>	similar to amyotrophic lateral sclerosis 2 (juvenile) chromosome region, ca, idate 17	2.04	26.63	13.03
<i>NPTX2</i>	neuronal pentraxin II	3.75	617.18	164.50
<i>OSMR</i>	Oncostatin M receptor	1.99	1164.08	583.63
<i>PGAP1</i>	GPI deacylase	2.19	51.75	23.63
<i>PLAGL1</i>	similar to pleiomorphic adenoma gene-like 1 isoform 2	4.67	90.75	19.43
<i>RG9MTD3</i>	similar to RNA (guanine-9-) methyltransferase domain containing 3	2.16	250.18	115.68
<i>RPL13</i>	ribosomal protein L13	2.55	1029.68	404.28
<i>RPS6KA5</i>	ribosomal protein S6 kinase, 90kDa, polypeptide 5	1.84	2376.53	1292.05
<i>SLC12A5</i>	solute carrier family 12, (potassium-chloride transporter) member 5	1.87	1568.50	839.98
<i>SLC1A5</i>	similar to Neutral amino acid transporter B(0) (ATB(0))	1.81	3025.90	1670.58
<i>SLC6A6</i>	Solute carrier family 6 (neurotransmitter transporter, taurine), member 6	3.27	86.38	26.40
<i>SND1</i>	Staphylococcal nuclease domain containing 1	1.97	141.68	71.88
<i>SOCS3</i>	suppressor of cytokine signaling 3	17.08	152.45	8.93
<i>SPINK2</i>	serine peptidase inhibitor, Kazal type 2 (acrosin-trypsin inhibitor)	10.06	1004.35	99.83
<i>STAR</i>	similar to steroidogenic acute regulator isoform 1	6.19	1180.63	190.63
<i>STC1</i>	stanniocalcin 1	5.28	649.05	123.03
<i>TDRD1</i>	similar to tudor domain containing 1	2.73	298.58	109.30
<i>TMEM26</i>	similar to transmembrane protein 26	11.99	186.43	15.55
<i>USP54</i>	ubiquitin specific peptidase 54	2.37	54.70	23.10
<i>ZNF26</i>	zinc finger protein 26 (KOX 20)	1.82	657.63	361.48
n/a	Transcribed locus	1.55	73.35	47.23
n/a	Transcribed locus, moderately similar to NP_858931.1	2.04	505.88	247.55
n/a	NFS1 nitrogen fixation 1 isoform b precursor [Homo sapiens]	1.74	1165.70	669.55
n/a	Transcribed locus	2.48	68.95	27.83

3.2 Quantitative mRNA Expression Analysis

Nineteen of the 59 differentially expressed mRNAs were examined by the QADB and/or qRT-PCR methods (Figure 3.2). The QADB method was used to analyze the expression of nine genes that had the average array intensities >500 and the other ten were assayed using the qRT-PCR method. Out of the 19 mRNAs examined, eighteen showed significant differences in expression ($P < 0.05$) in the same direction as indicated by the array data. The Serine peptidase inhibitor, Kazal type 2 (*SPINK2*) mRNA displayed differential expression but the difference did not reach statistical significance.

Figure 3.2: Comparison of differences in mRNA expression revealed by microarray analysis (white) and independent measurements using the QADB (striped) or qRT-PCR (black) assays. [* indicates a statistically significant difference between IVM and VVM groups (P < 0.05)]



3.3 Biological Functions of Differentially Expressed Genes in Rhesus Monkey MII Oocytes

In order to investigate whether certain biological functions might be preferentially affected by mRNA overexpression in IVM oocytes, the EASE analysis was performed on the 42 genes that are annotated for function. EASE performs statistical tests to identify biological categories over-represented in a list of genes with respect to the background population of genes (Hosack, *et al.*, 2003). Out of 42 genes analyzed, 33 were involved in at least one biological function over-represented in IVM oocytes compared to VVM oocytes (Table 3.4). The EASE analysis identified steroid metabolism as the biological function enriched in the IVM oocytes with the highest significance. Three of the genes (*CYP19A1*, *HSD11B2*, *STAR*) in this functional category also participate in the steroid biosynthesis, which was also one of the biological functions significantly over-represented in the genes more highly expressed in IVM oocytes. Other major biological functions over-represented in IVM oocytes were cell-cell signaling, homeostasis, cell growth and response to stress (Table 3.4). There were also additional functional categories that are not identified by the EASE analysis yet encompassed by the genes over-expressed in IVM oocytes. Those functions were macromolecular transport (*KCNK3*, *LDLR*, *NPTX2*, *SLC12A5*, *SLC1A5*, *SLC6A6*), cellular adhesion (*CD83*, *PGAP1*), RNA binding and control of translation (*CUGBP2*, *RG9MTD3*, *RPS6KA5*, *TDRD1*, *SND1*), cytoskeleton/cell architecture (*MYLIP*), transcription (*SND1*), and proteolysis (*MDM4*, *USP54*).

Table 3.4: EASE analysis output for genes over-expressed in IVM oocytes

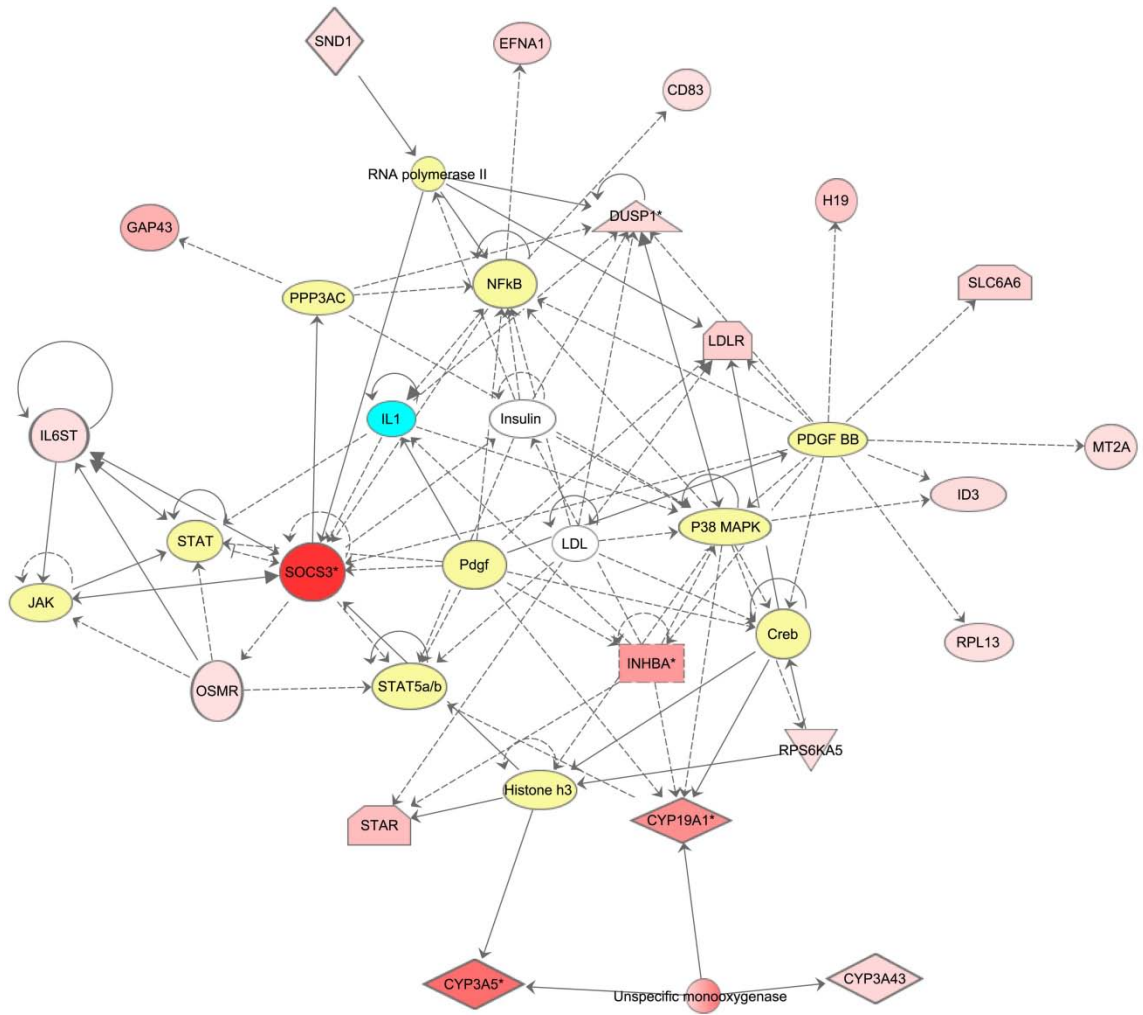
GO Biological process	EASE score	Gene Symbols
steroid metabolism	9.87E-04	<i>CYP19A1; CYP3A5; HSD11B2; LDLR; STAR</i>
cellular process	6.09E-03	<i>CD5L; CD83; CKAP4; DUSP1; EFNA1; GAP43; GRIN2A; HSD11B2; IL26; IL6ST; INHBA; KCNK3; LDLR; MDM4; MT2A; NPTX2; OSMR; PLAGL1; RPL13; RPS6KA5; SLC12A5; SLC1A5; SLC6A6; SOCS3; STAR; STC1; TDRD1</i>
response to external stimulus	1.01E-02	<i>CD5L; CD83; CYP3A43; CYP3A5; DUSP1; GAP43; IL26; IL6ST; INHBA; RPS6KA5; STC1</i>
cell-cell signaling	1.16E-02	<i>EFNA1; GRIN2A; HSD11B2; IL26; INHBA; KCNK3; STC1</i>
steroid biosynthesis	2.14E-02	<i>CYP19A1; HSD11B2; STAR</i>
cell growth and/or maintenance	2.15E-02	<i>CKAP4; DUSP1; GAP43; GRIN2A; INHBA; KCNK3; LDLR; MDM4; MT2A; OSMR; PLAGL1; RPL13; SLC12A5; SLC1A5; SLC6A6; SOCS3; STAR; STC1</i>
cell ion homeostasis	3.82E-02	<i>MT2A; SLC12A5; STC1</i>
ion homeostasis	3.82E-02	<i>MT2A; SLC12A5; STC1</i>
cell homeostasis	4.47E-02	<i>MT2A; SLC12A5; STC1</i>
response to stress	4.53E-02	<i>CD5L; CD83; DUSP1; GAP43; IL26; INHBA; RPS6KA5</i>
homeostasis	4.66E-02	<i>MT2A; SLC12A5; STC1</i>

The number of genes over-expressed in VVM oocytes was too small to be analyzed by the EASE. Among the seven genes in this group, there were at least three that are associated with known biological functions. The *AKR1C1* gene encodes an enzyme that catalyzes the reduction of aldehydes and ketones to alcohols by utilizing NADH or NADPH. The AKR1C1 protein is involved in the metabolism of progesterone and an isoform of 3 α -hydroxysteroid dehydrogenases (3 α -HSDs) which convert steroid hormones to their inactive forms (Penning *et al.*, 2000). AKR1C1 is also one of several enzymes (HSD17B1, AKR1C3, HSD17B3, AKR1C1, AKR1C2 and AKR1C4) that can catalyze the conversion of androstenedione to testosterone (Nakamura *et al.*, 2009; Penning, *et al.*, 2000). The *ATP6V0A4* gene encodes a subunit of a vacuolar ATPase that mediates acidification of intracellular compartments that's responsible for various intracellular processes such as protein sorting, zymogen activation and receptor-mediated endocytosis. Mutations in *ATP6V0A4* gene are associated with defects in renal functions and hearing loss (Stover *et al.*, 2002). Cholesterol 25-hydroxylase (CH25H) converts cholesterol to 25-hydroxysterol, leading to the repression of cholesterol biosynthesis and lipid metabolism (Lund *et al.*, 1998).

A further insight into the biological functions of the genes over-expressed in IVM oocytes were sought by performing the Ingenuity Pathway Analysis (IPA). The IPA analysis revealed that 21 of the 42 differentially expressed mRNAs with known annotation interact with one another in biological functions related to cell growth, maintenance and cell-cell signaling (Figure 3.3). Based on this analysis, it is suggested that numerous components affecting cell growth and signaling may be altered in IVM oocytes. Included in this network are the genes products that mediate cell signaling such as SOCS3 and INHBA. SOCS3 is a key component of JAK/STAT signaling pathway and INHBA relays cellular signals to other mediators such as STAR and

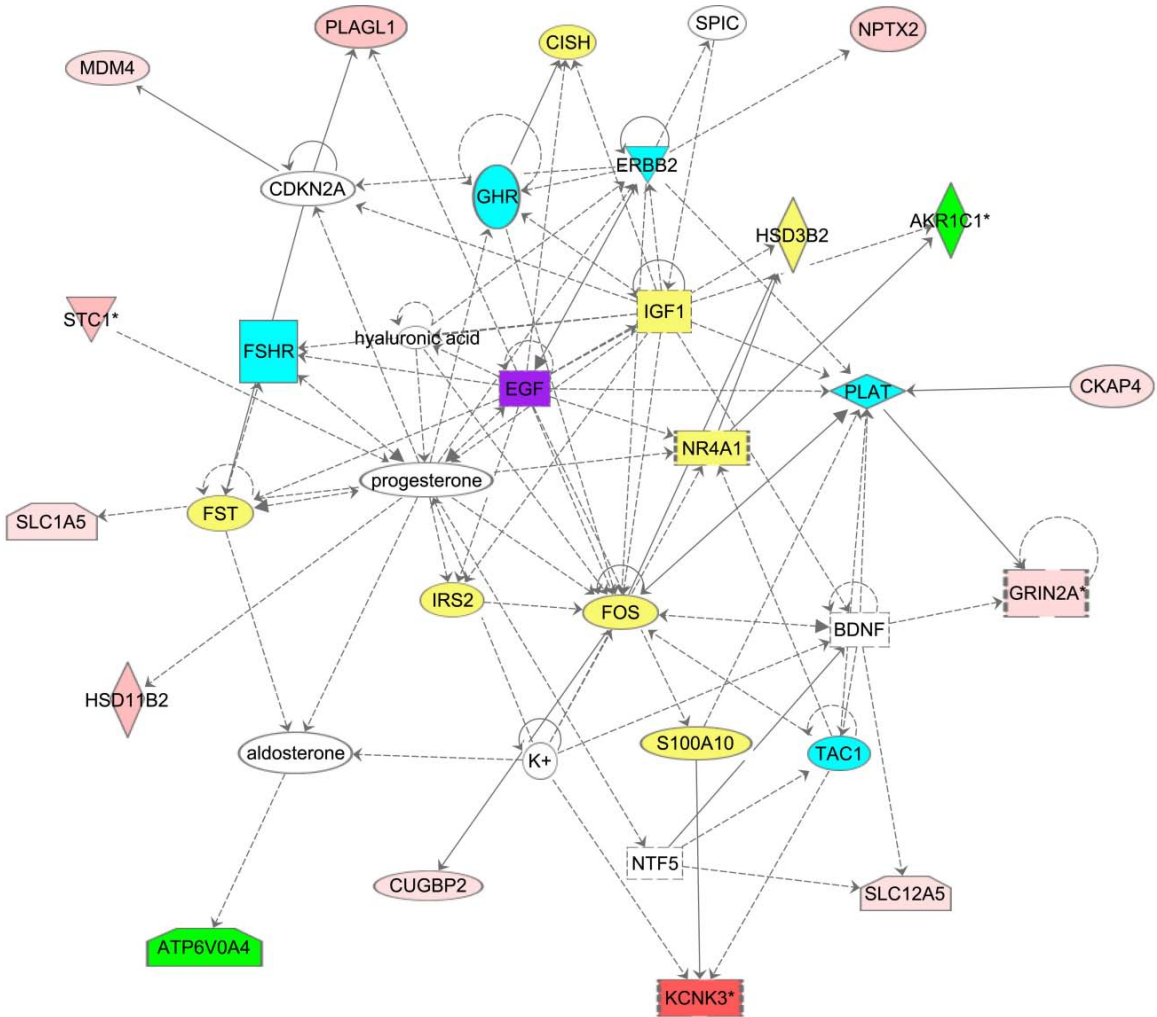
CYP19A1. Insulin, NFkB, p38/MAPK, CREB, and PDGFB are also involved in the regulation of the differentially expressed genes in this network.

Figure 3.3: Ingenuity pathway analysis gene interaction network 1 (Red: genes upregulated in IVM oocytes, Yellow: genes expressed in both oocytes and cumulus cells, Blue: genes expressed in cumulus cells but not in oocytes).



Many of the genes in the second IPA network are involved in the endocrine and paracrine regulation of cell growth and differentiation, and steroid metabolism (Figure 3.4). Based on my array data, key regulators such as progesterone, FSHR and other growth factors, e.g. EGF, IGF1 and BDNF included in this network are either not expressed in the oocyte or are not differentially expressed between IVM and VVM oocytes. This suggests that the functional pathways in which these factors are involved may become compromised in IVM oocytes due to the altered interactions the oocyte with somatic cells rather than due to their altered expression in the oocyte. It is notable that the genes over-expressed in IVM oocytes are predominantly distal targets of these factors (distant from center of network), indicating that IVM oocytes may be accompanied by an altered response to endocrine or paracrine factors. Therefore, the predominant difference between IVM and VVM oocytes may originate from the compromised cell-cell interactions, that this difference may, in turn, affect cell growth and differentiation.

Figure 3.4. Ingenuity pathway analysis gene interaction network 2 (Red: genes upregulated in IVM oocytes, Green: genes upregulated in VVM oocytes, Yellow: genes expressed in both oocytes and cumulus cells, Blue: genes expressed in cumulus cells but not in oocytes, Purple: genes expressed in oocytes but not in cumulus cells).



3.4 Transcription Factor Binding Motif Analysis

In order to determine whether there was any coordinated regulation at the level of transcription in IVM oocytes, a transcription factor binding motif analysis was performed using the oPUSSUM software. Only those genes that were more highly expressed in IVM oocytes and annotated with approved gene symbols were subjected to the analysis. The oPUSSUM retrieved data for 36 out of 44 submitted genes and based on this data I identified a set of five transcription factors that might have contributed to the differential mRNA expression in IVM oocytes (Table 3.5). Four of these were quite prevalent, with binding sites being detected in 25 or more of the 36 genes analyzed, and two of these (NKX2-5 and NOBOX) passed the more stringent cutoff of $Z \geq 10.0$.

3.5 3' UTR Analysis

The 3' UTR analysis of 44 mRNAs over-expressed in IVM oocytes revealed that a number of the affected mRNAs possess quite long 3'UTRs, with an average length of 1213 nt, a median value of 962 nt, and a range of 111-8227 nt (Table 3.6). Thirty six (82%) mRNAs contained one or more putative CPEs. Of these, six (*CUGBP2*, *MYLIP*, *PGAP1*, *PLAGL1*, *RPS6KA5*, *STC1*, *TMEM26*) contained 5 or more putative CPEs, and five (*LDLR*, *MDM4*, *MPPE1*, *SOCS3*, *USP54*) contained 3-4 CPEs. The average number of CPEs per nt of 3' UTR was 0.0025 with a mean value of 0.0018. Eleven of the 44 mRNAs analyzed (*CUGBP2*, *IL6ST*, *MDM4*, *MT2A*, *MYLIP*, *OSMR*, *PGAP1*, *PLAGL1*, *RPS6KA5*, *TMTM26*, and *USP54*) exceed twice the median value and the four (*IL6ST*, *MDM4*, *MT2A*, and *RPS6KA5*) exceed the average value. There was no significant correlation found between the fold change of difference in array values to the length of 3' UTR or the number of CPEs.

Table 3.5: Transcription factor binding sites (TFBS over-represented in the genes showing elevated expression in IVM oocytes relative to VVM oocytes at $Z \geq 5.0$ and Fisher $P < 0.05$)

Transcription Factor	No. Genes	Z Score	Fisher p- value
NKX2-5	34	10.52	2.29E-02
NOBOX	30	12.39	4.83E-02
FOXA2	26	8.763	3.73E-02
FOXD1	25	9.225	2.58E-02
AR	5	9.6	1.21E-02

Table 3.6: Characteristics of published 3'UTRs for human homologs of mRNAs over-expressed in IVM oocytes

Gene Symbol	3'UTR length (bp)	no. CPE	no. CPE / total bp
<i>CD5L</i>	1050	1	0.0010
<i>CD83</i>	1681	3	0.0018
<i>CKAP4</i>	1012	3	0.0030
<i>CUGBP2</i>	3589	15	0.0042
<i>CYP19A1</i>	1335	3	0.0022
<i>CYP3A43</i>	549	1	0.0018
<i>CYP3A5</i>	111	0	0.0000
<i>DUSP1</i>	664	2	0.0030
<i>EFNA1</i>	843	1	0.0012
<i>FLJ35767</i>	1099	0	0.0000
<i>GAP43</i>	423	0	0.0000
<i>GRIN2A</i>	1576	2	0.0013
<i>HSD11B2</i>	548	2	0.0036
<i>ID3</i>	476	1	0.0021
<i>IL26</i>	496	1	0.0020
<i>IL6ST</i>	214	2	0.0093
<i>INHBA</i>	647	1	0.0015
<i>KCNK3</i>	1269	1	0.0008
<i>LDLR</i>	2498	3	0.0012
<i>MITD1</i>	112	0	0.0000
<i>MDM4</i>	541	3	0.0055
<i>MPPE1</i>	972	3	0.0031
<i>MT2A</i>	127	1	0.0079
<i>MYLIP</i>	1496	7	0.0047
<i>NBEAL1</i>	930	3	0.0032
<i>NPTX2</i>	1239	3	0.0024
<i>OSMR</i>	426	2	0.0047
<i>PGAP1</i>	8227	36	0.0044
<i>PLAGL1</i>	1124	5	0.0044
<i>RG9MTD3</i>	1265	1	0.0008
<i>RPL13</i>	398	0	0.0000
<i>RPS6KA5</i>	1247	10	0.0080
<i>SLC12A5</i>	542	0	0.0000
<i>SLC1A5</i>	627	1	0.0016
<i>SLC6A6</i>	365	0	0.0000
<i>SND1</i>	549	1	0.0018
<i>SOCS3</i>	1636	3	0.0018
<i>SPINK2</i>	271	0	0.0000
<i>STAR</i>	1572	1	0.0006
<i>STC1</i>	2849	8	0.0028
<i>TDRD1</i>	952	1	0.0011
<i>TMEM26</i>	3672	17	0.0046
<i>USP54</i>	1091	4	0.0037
<i>ZNF26</i>	1086	1	0.0009
AVERAGE	1214	3.48	0.0025
MEDIAN	962	1.50	0.0018

3.6 Expression of Imprinted Genes

Imprinted genes are critical for the embryo development and growth and the differential DNA methylation of imprinted genes must be correctly established during gametogenesis (Bao *et al.*, 2000; Obata *et al.*, 1998; Sapienza *et al.*, 1989; Surani *et al.*, 1990). Aberrant imprinting was observed in oocytes and embryos following IVM in mouse and other species (Borghol *et al.*, 2006; Imamura *et al.*, 2005; Khosla *et al.*, 2001). In order to investigate whether there is a disrupted regulation of imprinted genes in rhesus monkey IVM oocytes, the array raw intensity values for maternally and paternally imprinted genes were examined (Tables 3.7 and 3.8). The list of known imprinted genes was obtained from the 'geneimprint' imprinted gene databases (<http://www.geneimprint.com/site/genes-by-species.Homo+sapiens>). Among the maternally imprinted genes, there were two known (*PLAGL1*, *MEST*) and two predicted (*C20ORF82*, *C6ORF117*) imprinted genes that were over-expressed in IVM oocytes. The *H19* gene well-known to be paternally imprinted and a gene predicted to be paternally imprinted (*ANKRD11*) were also over-expressed in IVM oocytes.

Table 3.7: Expression of maternally imprinted genes in IVM and VVM oocytes

Gene Symbol	Imprinting status	Average Raw Intensity		IVM / VVM ratio	p-value
		VVM	IVM		
<i>DIRAS3</i>	Imprinted	393.05	403.48	1.03	0.8646
<i>DLK1</i>	Imprinted	2992.70	499.13	0.17	0.1373
<i>IGF2</i>	Imprinted	1084.20	1208.83	1.11	0.3902
<i>MEST*</i>	Imprinted	3403.18	4796.15	1.41	0.0008
<i>NDN</i>	Imprinted	115.30	110.10	0.95	0.9216
<i>PEG3</i>	Imprinted	919.73	916.10	1.00	0.9915
<i>PLAGL1*</i>	Imprinted	19.43	90.75	4.67	0.0029
<i>SGCE</i>	Imprinted	84.53	57.23	0.68	0.4517
<i>SNRPN</i>	Imprinted	2194.28	2083.08	0.95	0.6783
<i>SNURF</i>	Imprinted	2194.28	2083.08	0.95	0.6783
<i>ZIM2</i>	Imprinted	45.60	37.10	0.81	0.3650
<i>APBA1</i>	Predicted	40.83	34.63	0.85	0.6109
<i>BRP44L</i>	Predicted	11.98	20.13	1.68	0.3164
<i>C20orf82*</i>	Predicted	15.88	36.00	2.27	0.0362
<i>C6orf117*</i>	Predicted	423.18	15.80	0.04	0.0091
<i>C9orf116</i>	Predicted	54.65	39.70	0.73	0.3406
<i>C9orf85</i>	Predicted	25.15	32.18	1.28	0.6190
<i>CDH18</i>	Predicted	151.18	164.20	1.09	0.5463
<i>DGCR6</i>	Predicted	248.35	131.70	0.53	0.0717
<i>EGFL7</i>	Predicted	36.78	24.35	0.66	0.4256
<i>EVX1</i>	Predicted	43.68	57.65	1.32	0.4546
<i>FAM59A</i>	Predicted	318.15	279.65	0.88	0.4662
<i>FOXP1</i>	Predicted	6.98	9.23	1.32	0.6189
<i>FUCA1</i>	Predicted	1217.38	1458.58	1.20	0.2174
<i>GATA3</i>	Predicted	10.48	16.95	1.62	0.4923
<i>HES1</i>	Predicted	37.80	21.53	0.57	0.1105
<i>KBTBD3</i>	Predicted	378.95	224.85	0.59	0.2690
<i>LOC51145</i>	Predicted	16.00	29.88	1.87	0.3557
<i>LY6D</i>	Predicted	34.75	34.35	0.99	0.9587
<i>MYEOV2</i>	Predicted	1300.38	965.68	0.74	0.1430
<i>NKAIN3</i>	Predicted	22.70	26.35	1.16	0.7562
<i>PURG</i>	Predicted	115.45	114.18	0.99	0.9671
<i>PYY2</i>	Predicted	16.95	25.53	1.51	0.5271
<i>RBP5</i>	Predicted	13.85	16.83	1.21	0.7239
<i>RPL22</i>	Predicted	5076.30	4922.63	0.97	0.8103
<i>SIM2</i>	Predicted	55.35	67.30	1.22	0.7295
<i>SOX8</i>	Predicted	150.53	175.78	1.17	0.4963
<i>SPON2</i>	Predicted	917.80	764.13	0.83	0.4443
<i>TMEM157</i>	Predicted	73.93	62.75	0.85	0.5082
<i>TMEM52</i>	Predicted	396.05	371.15	0.94	0.7557
<i>TMEM60</i>	Predicted	720.53	526.10	0.73	0.1955
<i>ZNF225</i>	Predicted	46.10	41.03	0.89	0.8139

Table 3.8: Expression of paternally imprinted genes in IVM and VVM oocytes

Gene Symbol	Imprinting status	Average Raw Intensity		IVM / VVM ratio	p-value
		VVM	IVM		
<i>ATP10A</i>	Imprinted	28.13	44.50	1.58	0.1154
<i>CDKN1C</i>	Imprinted	57.55	112.40	1.95	0.1388
<i>GNAS</i>	Imprinted	5444.98	5545.08	1.02	0.8761
<i>H19*</i>	Imprinted	2448.85	11113.85	4.54	0.0053
<i>KCNK9</i>	Imprinted	208.05	163.80	0.79	0.4489
<i>MEG3</i>	Imprinted	520.13	337.28	0.65	0.2299
<i>OSBPL5</i>	Imprinted	873.60	943.55	1.08	0.5677
<i>PPP1R9A</i>	Imprinted	333.18	402.43	1.21	0.4031
<i>SLC22A18</i>	Imprinted	168.20	150.45	0.89	0.7161
<i>TP73</i>	Imprinted	197.65	175.58	0.89	0.7975
<i>UBE3A</i>	Imprinted	1028.75	1068.65	1.04	0.7969
<i>ZNF264</i>	Imprinted	954.15	1039.53	1.09	0.6175
<i>ACD</i>	Predicted	464.55	440.83	0.95	0.5554
<i>C20orf20</i>	Predicted	340.08	307.03	0.90	0.2576
<i>CDK4</i>	Predicted	380.75	249.00	0.65	0.2922
<i>CHMP2A</i>	Predicted	199.45	173.70	0.87	0.3599
<i>DVL1</i>	Predicted	560.98	463.20	0.83	0.3184
<i>E2F7</i>	Predicted	26.95	40.40	1.50	0.1969
<i>FASTK</i>	Predicted	144.18	153.53	1.06	0.6125
<i>FGFRL1</i>	Predicted	212.95	200.53	0.94	0.5832
<i>GLI3</i>	Predicted	59.23	40.88	0.69	0.4103
<i>HOXA11</i>	Predicted	39.85	46.28	1.16	0.6925
<i>IFITM1</i>	Predicted	63.70	89.28	1.40	0.4182
<i>KIAA1530</i>	Predicted	66.83	74.33	1.11	0.4541
<i>KIAA1545</i>	Predicted	139.40	111.83	0.80	0.2838
<i>LDB1</i>	Predicted	697.43	854.13	1.22	0.2384
<i>PAOX</i>	Predicted	63.58	38.80	0.61	0.1298
<i>PHPT1</i>	Predicted	629.80	570.70	0.91	0.4594
<i>PTPN14</i>	Predicted	75.00	58.80	0.78	0.1408
<i>RAB1B</i>	Predicted	1116.30	902.10	0.81	0.2373
<i>SLC4A2</i>	Predicted	106.80	99.53	0.93	0.7184
<i>ZFP36L2</i>	Predicted	160.83	112.70	0.70	0.4367
<i>ANKRD11*</i>	Provisional Data	171.13	271.93	1.59	0.1038
<i>CTNNA3</i>	Provisional Data	31.25	53.75	1.72	0.7765
<i>ZNF215</i>	Provisional Data	604.28	622.35	1.03	0.0164

3.7 Discussion

This study provided the comparison of transcriptomes of IVM and VVM oocytes in a non-human primate model for the first time and yielded several novel findings relevant to the molecular basis for differences in oocyte quality. The analysis revealed that there was a relatively small set of mRNAs differentially expressed between two kinds of rhesus monkey oocytes. It is interesting to consider that such a dramatic difference in oocyte quality arises with so few mRNA differences and after such a seemingly minor procedural change. IVM oocytes lack one day of development in vivo compared to VVM oocytes and this small difference seems to create a significant reduction in the success rate of fertilization and embryonic development in IVM oocytes (Schramm, *et al.*, 2003). The results from this array study suggest that the difference in oocyte quality may arise from specific changes made during oocyte development rather than from a wide range of differences in mRNA expression.

The array analysis identified several functional categories for which regulation may be altered in IVM oocytes. The biological function most significantly affected by IVM is steroid biosynthesis and metabolism. Genes for steroid synthesis and metabolism such as *CYP19A1* and *CYP3A5* are overexpressed in IVM oocytes. *CYP19A1* catalyses the formation of C18 estrogens from C19 androgens and has a critical role in steroidogenesis in the ovary. *CYP3A5* is part of a larger family of genes involved in steroid metabolism and is expressed in the human ovary (Bieche *et al.*, 2007; A. J. Lee *et al.*, 2003). Use of CMRLb medium (contains androstenedione) in the oocyte culture increases the developmental competence of IVM oocytes (Schramm, *et al.*, 2003). Androstenedione may provide a molecular precursor for steroidogenesis (Meinhardt & Mullis, 2002) and may be indirectly responsible for the high levels of expression of both *CYP19A1* and *CYP3A5* genes. In addition to the cytochrome P450

aromatases, more genes involved in steroid metabolism, *LDLR* and *STAR* and are also over-expressed in IVM oocytes. *LDLR* contributes to steroidogenesis by transporting LDL into the cell via endocytosis (Brown & Goldstein, 1979). LDL is a major carrier of cholesterol that is subsequently used as the precursor for steroid and androgen biosynthesis. *STAR*, a key regulator of cholesterol metabolism and steroid synthesis, is regulated by LDL at the transcriptional level (Reyland *et al.*, 2000). The *HSD11B2* gene also participates in steroid synthesis and metabolism. *HSD11B2* protein catalyzes the conversion of cortisol to corticosterone and thus modulates intracellular glucocorticoid levels. A study showed that the mRNA expression of another gene overexpressed in IVM oocytes, *STC1*, is in turn regulated by glucocorticoids in rat sertoli cells (Groves *et al.*, 2001).

Another biological function affected by IVM is cell-cell interactions and signaling. The biofunction over-representation analysis identified 11 genes (*CD5L*, *CD83*, *EFNA1*, *GP43*, *IL26*, *IL6ST*, *INHBA*, *NPTX2*, *OSMR*, *PGAP1*, *STAR*) that participate in cell-cell interactions, indicating that the communication between oocyte and surrounding follicle cells may be disrupted. The *CD83* and *PGAP1* gene regulate cell adhesion which is an important component of oocyte and follicle development. The overexpression of mRNAs encoding growth factors and hormones (*IL26*, *INHBA*, *NPTX2*, *STC1*), growth factor receptors (*OSMR*), and modulators of cellular responses to such factors (*HSD11B2*, *IL6ST*, *SOCS3*, *STAR*) suggests that the in vitro response of oocytes and embryos to external stimuli may be significantly altered.

Cellular ion homeostasis is another critical function for oocyte and embryo development. The intracellular pH regulation and a series of other cellular processes become disrupted due to the misregulation of genes encoding various ion channels, for example, the decreased expression of the mRNA encoding the hydrogen ion channel *ATP6V0A4*, the increased expression of potassium ion channel mRNAs (*KCNK3*,

SLC12A5) and amino acid transporter mRNAs (*SLC1A5*, *SLC6A6*). *STC1* is involved in calcium and phosphate homeostasis and has a role in maintaining the intracellular pH (Yoshiko & Aubin, 2004), and, therefore, its overexpression in IVM oocytes may compromise the cellular homeostasis. This result suggests that the removal of the oocyte from the follicle for IVM may prematurely terminate important cell-cell interactions that foster the emergence of full oocyte developmental competence. Also, it indicates that it may be necessary to adjust the ionic composition of culture medium in order to enhance the developmental competency of IVM oocytes and embryos.

The IPA analysis also supports the notion that IVM oocytes are compromised in lipid metabolism, cell-cell interaction and signaling. The first IPA network (Figure 3.3) showed that *INHBA* and *SOCS3* regulate cell growth and signaling by exerting a range of effects via many other factors that are expressed in the oocyte but not up-regulated, and other exogenous factors like IL1, Insulin, and LDL. The second network (Figure 3.4) displayed a network of processes regulated by various hormones and growth factors, including the stress response via *PLAGL1*, *NPTX2*, *KCNK3*, *STC1*, *AKR1C1*, *SLC1A5*, and *MDM4*. In both IPA networks, the overexpressed genes were mostly located at the periphery of the networks. This implies that those genes may be downstream mediators of cellular processes regulated by the signaling pathways involving *SOCS3* and *INHBA*, and also that the genes might be regulated by the interactions between cumulus cells and the oocyte. Also suggested in the IPA network analysis is that the signaling pathways disrupted in IVM oocytes involve progesterone, FSH, EGF and aldosterone, insulin and PDGF.

The increased expression of some mRNAs may reflect an incomplete establishment of mechanisms for regulating maternal mRNA stability and content. The *CUGBP2* gene encodes an RNA binding protein that binds to and increases the stability of *PTGS2* (a.k.a. *COX-2*) mRNA, and inhibits its translation (Mukhopadhyay *et al.*, 2003).

TDRD1 is found in nuage/germinal granules of both male and female germ cells (Chuma *et al.*, 2006), and the mouse *Tdrd1* interaction with *Mili* was found to be a critical regulator of spermatogenesis (J. Wang *et al.*, 2009). SND1 is also a main component of RISC (RNA induced silencing complex) and plays an important role in microRNA function (Tsuchiya *et al.*, 2007). This result indicates that the developmental competence of the oocyte may be acquired progressively during maturation as previously suggested by Schramm and Bavister (Schramm & Bavister, 1999b), and that the key events of this process may continue up to the time of ovulation. Therefore, it may be concluded that oocyte quality becomes compromised when the COC is aspirated a day before ovulation and those final key events get interrupted.

The 3'UTR analysis revealed that putative CPE motifs were detected in more than 80% of the mRNAs over-expressed in IVM oocytes, consistent with the result found among actively translating maternal mRNAs in mouse MII stage oocytes (Potireddy *et al.*, 2006). However, there was no apparent relationship between the difference in mRNA abundance and the length of 3'UTR or the number of CPEs present. Thus, there seems to be no specific characteristic relating to CPE elements that are responsible for the increased expression of this particular group of mRNAs in IVM oocytes.

The finding that maternally imprinted genes, *PLAGL1* and *MEST*, are overexpressed in IVM oocytes suggests that premature removal of the oocyte from the follicle may disrupt essential events such as genomic imprinting. It's been previously suggested that assisted reproduction methods could alter DNA methylation of imprinted genes in human oocytes (Fortier *et al.*, 2008; T. Li, *et al.*, 2005). *PLAGL1* is a member of a co-regulated group of imprinted genes, and its expression may affect the expression of other imprinted genes (Varrault *et al.*, 2006). There are several possible reasons for the unanticipated expression of the maternally imprinted *PLAGL1* in the oocyte. Its expression in the oocyte may result from aberrant activation of the biallelic promoter P2

(Valleley *et al.*, 2007). Although the expression of *PLAGL1* is observed only from the paternal allele in most tissues, tissue-specific biallelic transcription has been reported (Valleley, *et al.*, 2007). It could also be the result of the delayed degradation of maternal transcripts or the interruption of the DNA methylation process in IVM oocytes. In addition to *PLAGL1*, *MEST1* and two additional potentially maternally imprinted genes were over-expressed in IVM oocytes, while expressed at the background level in VVM oocytes. The misregulated expression of these imprinted genes implies that suboptimal IVM conditions could cause incorrect imprinting in embryos. It's been demonstrated previously that imprinting of some genes may occur quite late during oogenesis (Lucifero *et al.*, 2002), which result suggests a possibility that the assisted reproductive technologies involving IVM may disrupt imprinting.

By comparing transcriptomes of IVM and VVM oocytes, I identified a set of genes differentially expressed between two kinds of rhesus monkey oocytes as well as the biological functions and pathways potentially compromised in oocytes of suboptimal developmental competence. The findings of this study indicated that the removal of the COCs from the follicular environment before the key pathway interactions are complete may terminate critical developmental processes in the oocyte, which may, in turn, cause detrimental effects on the development of its consequent embryo. Also, the exposure of COCs to IVM conditions may disrupt genomic imprinting, causing overexpression of several imprinted genes. This study provides novel insight into the nature of oocyte-follicle cell interactions, the potential molecular and cellular consequences of altering these interactions, and the basis for compromised developmental competence following IVM procedures in a non human primate model. These results also raise concerns about applying IVM clinically without addressing such developmental defects, but indicate that these deficiencies may be overcome by further improvement in IVM culture systems.

CHAPTER 4

EXTENSIVE EFFECTS OF IN VITRO OOCYTE MATURATION ON RHESUS MONKEY CUMULUS CELL TRANSCRIPTOME

4.1 Overview of the Array Analysis

All quality control parameters were within the acceptable ranges for the eleven array samples of rhesus monkey cumulus cells (Table 4.1). The average detection rate for pre-maturation cumulus cells (PM-CC) samples was 47 % corresponding to approximately 25,000 probe sets. The detection rates for in vitro matured cumulus cells (IVM-CC) and in vivo matured cumulus cells (VVM-CC) samples were 38 % and 41 %, respectively. A hierarchical clustering analysis (HCL) and three-dimensional Principal Component Analysis (PCA) revealed that the Biological replicates cluster to their corresponding groups without any apparent outliers (Figures 4.1 and 4.2).

I observed that cumulus cells undergo a dramatic change in their transcriptome during the last 24 hours of maturation. A total 3,252 out of 19,076 annotated genes (17 %; 4,431 probe sets) on the rhesus monkey array were either up or down regulated during VVM and 14.5 percent (2,772 genes; 3,840 probe sets) of all genes were modulated during IVM. There were more genes down-regulated than up-regulated during the cumulus cell maturation process (Table 4.2). Of the probe sets differentially regulated during VVM, 74 % (2,459 unique genes; 3,284 probe sets (2,776 annotated)) were down-regulated while only 26 % (793 unique genes; 1,147 probe sets (883 annotated)) were up-regulated. A similar relationship was observed during IVM (1,865 genes (2,592 probe sets) down-regulated compared to 907 genes (1,248 probe sets) up-regulated).

Table 4.1: Quality control parameters for array hybridization (Rhesus monkey IVM and VVM MII cumulus cells)

Sample type	% Present	# probe sets with present calls	Scale Factor	Average Background
PM-CC	46.1-48.1	24,365-25,425	0.5-0.6	39.0-41.6
IVM-CC	36.3-41.3	19,210-21,814	2.2-3.7	34.7-40.4
VVM-CC	40.3-42.7	21,279-22,568	0.9-1.8	43.3-70.2
Normal range	30-60	15,856-31,711	0.5-4.8	20-100

Figure 4.1: Hierarchical Clustering Analysis (rhesus monkey PM, IVM, VVM-CC)

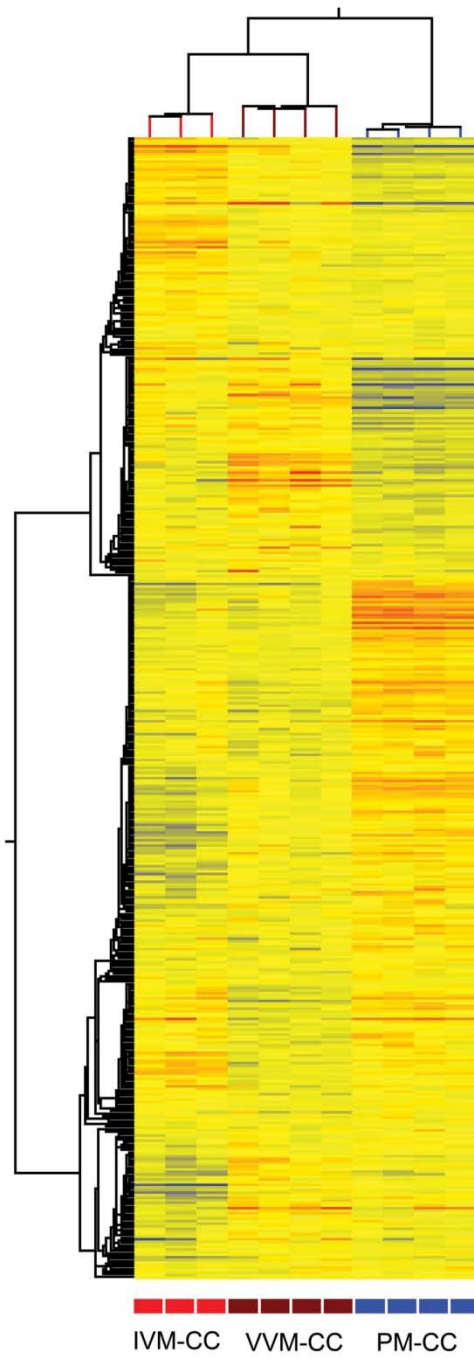


Figure 4.2: Principal Component Analysis (rhesus monkey PM, IVM, VVM-CC)

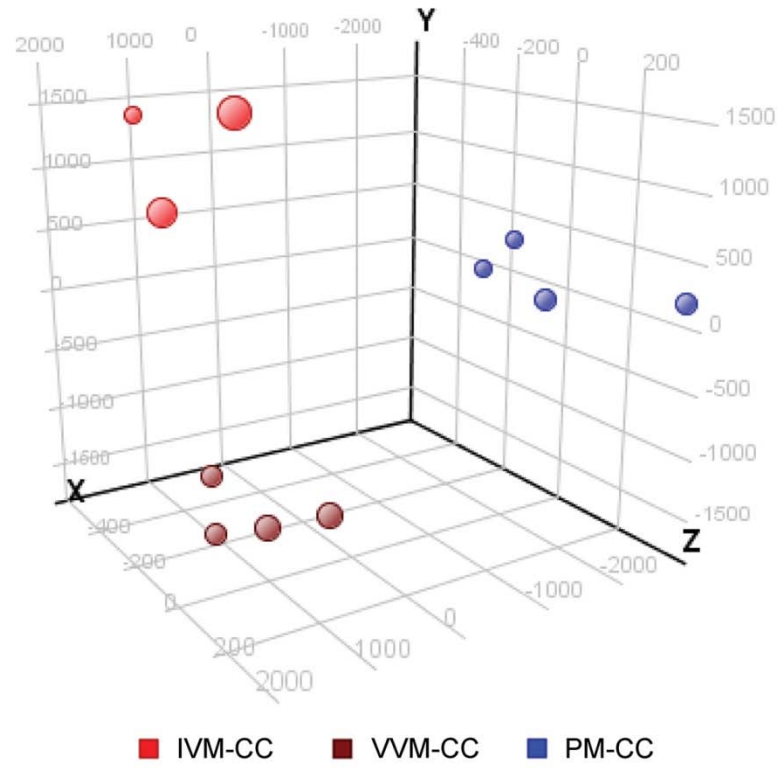


Table 4.2: Probe sets significantly up- or down-regulated in rhesus monkey cumulus cells during VVM or IVM

Maturation type	Comparison	# probe sets analyzed*	# differentially expressed probe sets [§] (# Unique genes)					
			Total		Fold change ≥ 2		Fold change ≥ 10	
			Up	Down	Up	Down	Up	Down
VVM	PM-CC vs. VVM-CC	14,521	4431 (3,252)		2840 (2,068)		154 (109)	
			1,147 (793)	3,284 (2,459)	762 (513)	2078 (1,555)	93 (64)	61 (45)
IVM	PM-CC vs. IVM-CC	14,457	3840 (2,772)		2,766 (1,963)		121 (91)	
			1,248 (907)	2,592 (1,865)	711 (489)	2,055 (1,474)	33 (24)	88 (67)

* Filtered for Present calls in all replicates of one group and the raw array intensity value ≥ 100

[§] FDR < 1% and P < 0.01

4.2 Identification of Differentially Regulated Gene Sets

In order to assess the biological processes or functions significantly affected in cumulus cells by IVM and VVM, the IPA analysis was applied to the cumulus cell array data set. To simplify and focus my analysis, 485 genes (1,099 probe sets) with inconsistent expression results in redundant probe sets were omitted from further consideration, and only the genes that differed in expression at the threshold of 2-fold or greater were employed for IPA. Affymetrix chips contain multiple probe sets mapped to different regions of the same gene and it's not uncommon to find different probe sets yield different expression results. There are various reasons that may cause this. First, different probe sets may represent different splice variants. In this case, different expression values may indicate two cell types favor different mRNA variants for the same gene. However, only a small set of redundant probe sets were designed for multiple splice variants. Many others were designed to target different regions on the same transcript. For those redundant probe sets targeting for the same transcript, it is possible that one probe set might have a better probe specificity and/or hybridization strength than the other. These differences in the probe quality may result in different expression measurements on the array. There are also other factors that may yield inconsistent results, for example, the distance of a targeted region from the poly-A tail, sequence similarity to different genes in the same family and the location of the probe set on the array, etc. In a study where redundant probe set behaviors were surveyed, the authors concluded that the inconsistent expression values of redundant probe sets most likely result from the incorrect gene models used to design the array probe sets (Cui & Loraine, 2006). The purpose of this study was to identify the genes and pathways that show the most significant differences between IVM and VVM rather than studying the expression patterns of specific genes. To fulfill this objective, I focus my

analysis on the genes that showed consistent array values by eliminating those with inconsistent values from the analysis.

Comparisons were first made between PM-CC and IVM-CC or between PM-CC and VVM-CC to understand the transitions that occur during IVM or VVM. Based on the results from these comparisons, array data sets were categorized as correctly or incorrectly regulated, and as either up- or down-regulated during maturation. Once the differences in developmental transitions were characterized, VVM-CC and IVM-CC were also compared directly to each other.

4.2.1 Identification of Genes Incorrectly Regulated During IVM

The first two groups of genes incorrectly regulated during IVM include those for which mRNA expression changed (increased or decreased from PM-CC) during IVM but not changed during VVM. These genes are categorized as 'IVM unique' genes (Figure 4.3). The 'IVM unique' group contains 1,551 probe sets (1,216 annotated) corresponding to 1,126 unique genes, a half of which were down-regulated and the other half was up-regulated (Supplemental Tables S1a and S1b). The next two groups of incorrectly regulated genes are those that changed (increased or decreased from PM-CC) during VVM but not changed during IVM (Figure 4.3; VVM-unique). A total 1,607 unique genes (2,142 probe sets; 1,760 annotated) are in the VVM-unique category. Compared to the IVM-unique genes, a higher proportion (1,423 probe sets; 1,112 unique genes) of the 'VVM-unique' genes was down-regulated during maturation than up-regulated (719 probe sets; 495 unique genes) (Supplemental Tables S2a and S2b).

In addition to the 'IVM unique' and 'VVM unique' genes, there were more incorrectly regulated genes. A small number of genes (28 probe sets corresponding to 28 unique genes) was regulated in opposite directions (Figure 4.4) and thus considered incorrectly regulated during IVM. Twenty one of these genes were up-regulated during

IVM but down-regulated during VVM and seven genes were down-regulated during IVM while up-regulated during VVM (Supplemental Tables S3a and S3b).

4.2.2 Identification of Correctly Regulated Genes

Genes for which mRNA expression changed in the same direction during IVM and VVM were classified as 'correctly regulated.' The 'correctly regulated' genes were identified by comparing the probe sets that showed significant changes in gene expression going from PM-CC to IVM-CC to those that showed significant changes and going from PM-CC to VVM-CC. These genes may represent a minimally required set of changes for cumulus cell accompanying oocyte maturation. About four percent (2,289 out of 52,865) of the probe sets or 8.6 percent (1,648 out of 19,076) of all annotated genes on the rhesus array were regulated during both IVM and VVM (Figure 4.3; IVM+VVM common). The majority of these (2,261 probe sets (1,824 annotated), 1,620 unique genes) was regulated in the same direction during IVM and VVM, either increased or decreased in expression during maturation (Figure 4.4, Supplemental Tables S4a and S4b). Among the relatively small pool of up-regulated genes (n=293), serglycin (*SRGN*, a.k.a. *PRG1* or Proteoglycan 1) showed the highest up-regulation in gene expression as high as 287-fold.

Figure 4.3: Venn diagram to identify differential patterns of mRNA regulations in cumulus cells during IVM and VVM.

Probe sets for which mRNA abundance either changed only during IVM (IVM-unique: pink) or only during VVM (VVM-unique: blue) represent the genes that may be incorrectly regulated during IVM. Probe sets for which mRNA expression changed during both IVM and VVM may be either correctly or incorrectly regulated genes depending on the directionality of the change.

IVM unique (pink): Number of probe sets differentially regulated only during in vitro maturation. VVM unique (blue): Number of probe sets differentially regulated only during in vivo maturation. IVM+VVM common (purple): probe sets differentially regulated during both in vitro and in vivo maturations. F.C.: Fold change of difference. * Probe sets more highly expressed in day 9 in vitro matured cumulus cells. § Probe sets more highly expressed in day 9 in vivo matured cumulus cells

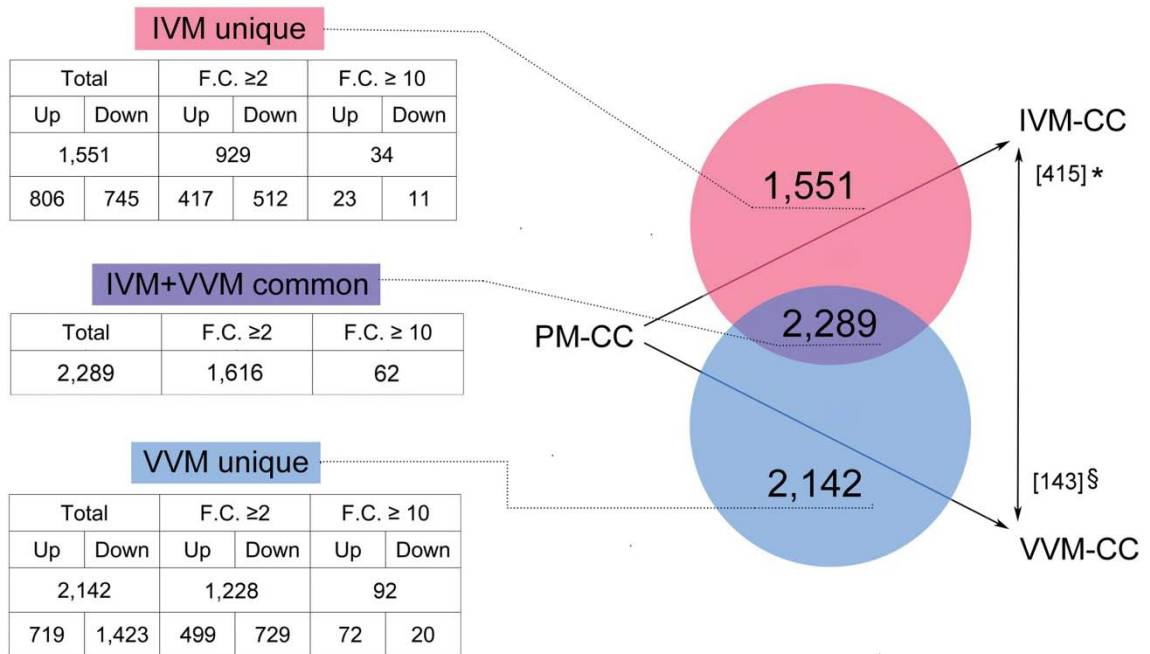
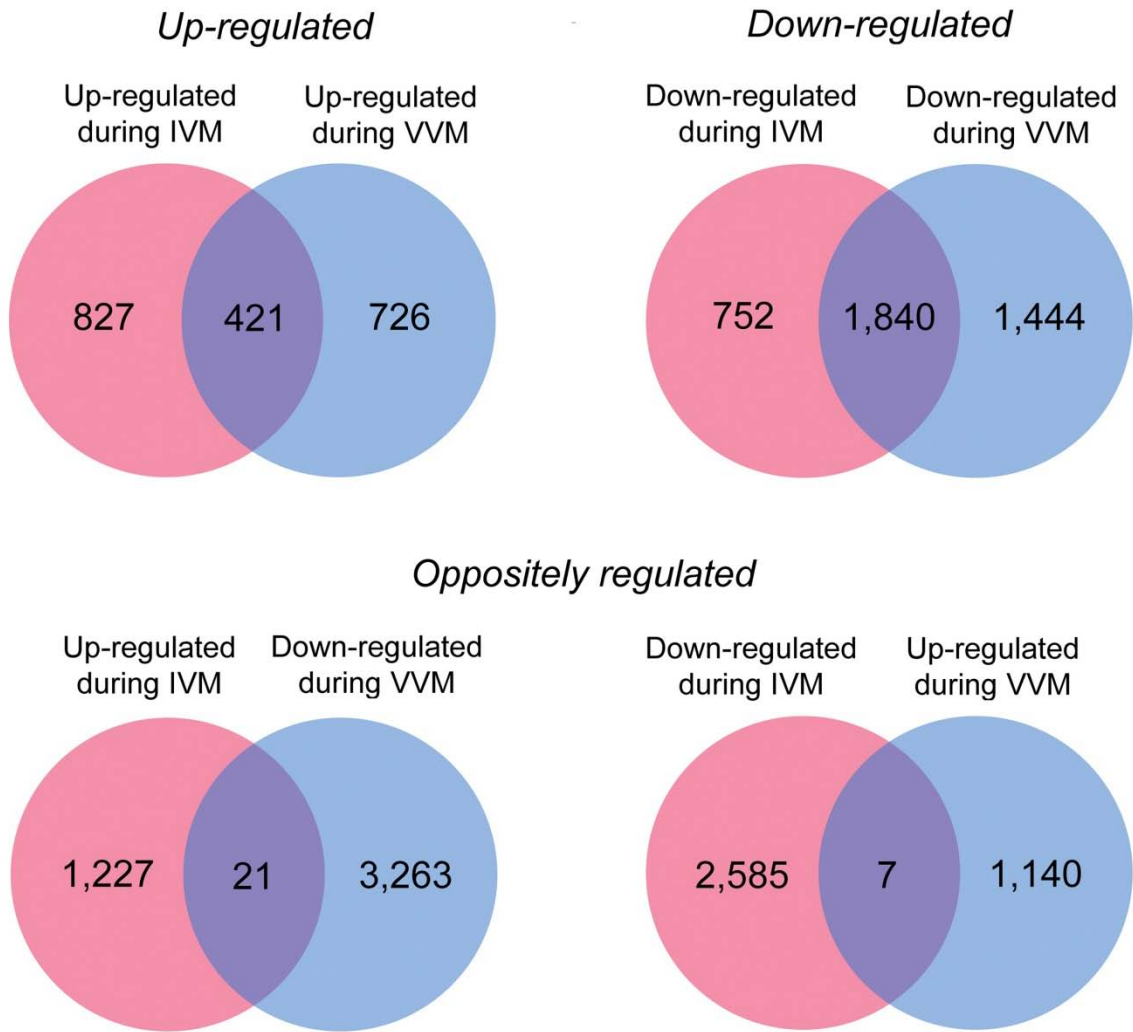


Figure 4.4: Venn diagrams to identify genes regulated in the opposite directions during IVM and VVM. Probe sets regulated in the same direction during IVM and VVM (421 probe sets up-regulated during both IVM and VVM and 1,840 probe sets down-regulated during both IVM and VVM) are considered as correctly regulated genes. Twenty eight probe sets regulated in the opposite directions during IVM and VVM are incorrectly regulated genes.



4.2.3 Direct comparison of IVM and VVM cumulus cells & Identification of more incorrectly regulated genes

The array analyses discussed in previous sections focused on the differences in the transition from PM-CC to IVM-CC and VVM-CC. Those analyses may indicate genes or pathway interactions misregulated during IVM and help us understand what may cause the poor developmental outcomes of IVM oocytes. Identification of mRNAs showing altered abundance with IVM, on the other hand, may provide us markers that predict oocyte quality.

Despite the large number of genes showing incorrect modes of regulation relative to PM-CC, the final outcome of maturation was a much smaller set of differentially expressed mRNAs. There were 558 probe sets (452 unique genes) that showed differential mRNA abundance between IVM and VVM cumulus cells. Of these 76 % were more abundant in IVM cells than in VVM cells (Table 4.3). The disparity between the number of VVM-CC versus IVM-CC differences and the number of differences in the transitional comparisons to PM-CC arises because many of the differences seen comparing the transitions reflect quantitative differences in regulation rather than qualitative differences in gene expression. IPA analysis revealed that biofunctions such as RNA post-transcriptional modification and lipid metabolism were over-represented among the genes more highly expressed in IVM-CC (Table 4.4). For the genes more highly expressed in VVM-CC, 'gene expression' and 'cell death' were among the top biofunctions over-represented. 'Cellular growth and proliferation' was a category shared by both cumulus cell types but each cell type had different genes for the category.

An additional group of oppositely regulated genes (89 probe sets corresponding to 68 unique genes) was identified (Supplemental Tables S5a and S5b) during this comparison analysis. These genes were not identified as "incorrectly regulated" in the

previous analyses due to either a small fold change or P-value greater than the cut-off setting of 0.01, in the comparison to PM-CC, but significant end-stage differences between VVM-CC and IVM-CC. More than half of these newly identified oppositely regulated genes (58 genes) were up-regulated during IVM while being down-regulated during VVM. Therefore, there were a total of 117 genes regulated in the opposite directions during IVM and VVM. Of those genes, 79 were up-regulated during IVM but down-regulated during VVM while 38 were down-regulated during IVM but up-regulated during VVM.

Table 4.3: Probe sets differentially expressed between IVM and VVM cumulus cells

Comparison	# probe sets analyzed*	# differentially expressed probe sets [§] (# unique genes)					
		Total		Fold change ≥2		Fold change ≥ 10	
		Higher in IVM	Higher in VVM	Higher in IVM	Higher in VVM	Higher in IVM	Higher in VVM
VVM-CC vs IVM-CC	13,042	558 (452)		343 (286)		10 (8)	
		415 (344)	143 (108)	236 (202)	107 (84)	4 (3)	6 (5)

* Filtered for Present calls in all replicates of one group and the raw array intensity value ≥100

[§] FDR < 1% and P <0.01

Table 4.4: Molecular and cellular functions over-represented among genes differentially regulated between IVM and VVM cumulus cells (Fold change of difference ≥ 2).

	Category	P-value	Genes
Higher in IVM-CC	RNA Post-Transcriptional Modification	2.93E-06-2.2E-03	<i>EXOSC2,BOP1,POP5,NOP56,DDX56,METTL1,EBNA1BP2,IMP4,AARS</i>
	Lipid Metabolism	3.8E-05-4.11E-02	<i>POR,OXT,A4GALT,CYP19A1,SLC37A4,HSD11B2,SMPD2,FDXR,PGR,HSD3B2</i>
	Small Molecule Biochemistry	3.8E-05-4.11E-02	<i>SRM,NME1,TKT,CNP,PTHLH,AQP11,G6PD,GRK5,UMPS,SMPD2,FDXR,PGR,POR,OXT,NUDT5,YARS,CYP19A1,A4GALT,ECE2,SLC37A4,HSD11B2,AARS,HSD3B2,AHCY</i>
	Cellular Movement	6.41E-04-4.11E-02	<i>ITGAE,OXT,NME1,ARPC1B,CYP19A1,A4GALT,PTHLH,POSTN,NUAK1,ITGA5,ENG,LIMK1</i>
	Cellular Growth and Proliferation	7.1E-04-4.11E-02	<i>DCBLD2,NME1,KCNK3,PTHLH,COPE,LIMK1,PGR,POR,GADD45GIP1,HINT1,CYP19A1,TRAF4,POSTN,HSD11B2,ENG,ACTN1,AHCY,ST3GAL2,FSTL3,DDX56,CNP,PSME2,SMAD7,ITGA5,SMPD2,FDXR,PDLIM4,OXT,CCND3,LOXL1,S100A11</i>
Higher in VVM-CC	Gene Expression	5.04E-06-3.62E-02	<i>SIAH1,ZNF281,EGR3,FOXJ2,BTG1,GNAQ,TBL1X,BACH1,TGFBR2,FOSB,EGR2,KLF7,GADD45A,RORA,MYST3,PTPN1,ITGAV,JARID2,FOSL2,JUND,CTDSP2,CITED2,SSB,CREBZF</i>
	Cell Death	1.77E-05-4.41E-02	<i>GNE,SIAH1,SFRS5,EGR3,GNAQ,BTG1,HERPUD1,FOSB,TGFBR2,EGR2,KLF7,GADD45A,RND3,PTPN1,ITGAV,BNIP3L,FOSL2,JUND,IRS2,ATR,CITED2,PEG3</i>
	Cellular Growth and Proliferation	1.62E-04-4.41E-02	<i>SIAH1,SFRS5,FRZB,ALDH1L1,TGFBR2,EGR2,GADD45A,PTPN1,ITGAV,JARID2,FOSL2,JUND,IRS2,CITED2,ACPP,GNE,TSPAN5,EGR3,BTG1,GNAQ,MAP3K7IP3,FOSB,BNIP3L,TFPI,ATR</i>
	Cellular Development	1.64E-04-4.02E-02	<i>ATP1B1,EGR3,GNAQ,BTG1,TBL1X,TGFBR2,RC3H1,EGR2,GADD45A,RND3,RORA,MYST3,PTPN1,ITGAV,FOSL2,JUND,IRS2,ATR,CITED2</i>
	Cell Cycle	2.07E-04-4.41E-02	<i>SIAH1,GADD45A,PROS1,ITGAV,JARID2,FOSL2,JUND,IRS2,ATR,CITED2</i>

4.3 Biofunctional Analysis of Differentially Expressed Gene Sets

4.3.1 Functional Characteristics of Correctly Regulated Genes

Bio-function analysis of correctly regulated genes revealed that 'Cell cycle' was a biological function enriched at the highest significance among the genes down-regulated during both IVM and VVM (Table 4.5). Genes positively associated with cell cycle progression (GO:0045786; e.g., *AKT1*, *CDC2*, *CDC20*, *CDC25A*, *CDC25C*, *CDC45L*, *CENPF*, *NUSAP1*, *PGGT1B*) were down-regulated, and some genes negatively associated with cell cycle progression (*BUB3*, *ESR1*, *BCL2*, *CHMP1A*, *CDKN1B*, *ILKAP*, *BUB1*) were also down-regulated during maturation. Cell cycle regulatory genes also comprised the most highly affected biological function among the genes up-regulated during maturation. The mRNA abundances of *CDKN1A* and *APBB1* genes, which promote cell cycle-arrest (GO:0045787), were increased during maturation.

Table 4.5: Top ten molecular and cellular functions over-represented in genes correctly regulated during IVM (Fold change of difference ≥ 2).

	Category	P-value	# Genes
<i>Down-regulated</i>	Cell Cycle	4.98E-16 -7.86E-03	132
	Cellular Assembly and Organization	5.66E-11 -8.07E-03	79
	DNA Replication, Recombination, and Repair	5.66E-11 -7.86E-03	108
	Cellular Movement	3.25E-10 -3.25E-10	20
	Cell Death	3.08E-09 -7.86E-03	144
<i>Up-regulated</i>	Cell Death	1.44E-06 -1.94E-02	34
	Small Molecule Biochemistry	8.97E-05 -1.85E-02	20
	Cellular Assembly and Organization	1.22E-04 -1.9E-02	16
	Cellular Movement	1.69E-04 -1.9E-02	12
	Cell Cycle	1.8E-04 -1.85E-02	19

4.3.2 Functional Characteristics of Incorrectly Regulated Genes

IPA biofunction over-representation analysis was performed on the incorrectly regulated genes (IVM-unique and VVM-unique) that have the fold change of difference greater than two (Table 4.6). For VVM-unique genes, DNA replication, recombination and repair was the most significantly affected functional category. Among IVM-unique genes, cellular growth and proliferation genes were significantly regulated. Differences in pathway regulation were plotted for easier evaluation (Figure 4.5). DNA replication, recombination and repair was most different between IVM and VVM cumulus cells in both the confidence interval and gene number. Eighty one genes involved in DNA replication, recombination and repair were either up or down-regulated during VVM while only nine were regulated during IVM. In VVM cumulus cells, most of the genes in this biofunctional category are involved in DNA repair or synthesis and replication. IVM cumulus cells regulated a handful of genes involved in DNA packaging or genome instability (Table 4.7). For the cell cycle functional category, not only was the total number of affected cell cycle genes greater in VVM cumulus cells than IVM cells, there was also slightly higher expression of genes that delay cell cycle in VVM cumulus cells compared to IVM cumulus cells (Table 4.7).

IVM and VVM cells differed particularly in the regulation of the genes involved in the G1/S transition of the cell cycle (Table 4.8). VVM-CC showed a preference in up-regulating many genes involved in the cell cycle arrest at the G1/S transition phase, while IVM cumulus cells showed the opposite trend, up-regulating more genes that promote the G1/S cell cycle progression. Interestingly, although IVM-CC did not regulate the same genes as the VVM-CC, they up-regulated a distinct set of G1/S cell cycle arrest genes, such as Insulin-like growth factor-binding protein 3 (*IGFBP3*) and Transforming growth factor beta 1 (*TGFB1*). Additionally, IVM-CC successfully down-

regulated some genes that promote progression at the G1/S transition. This analysis suggests that IVM cumulus cells may utilize pathways or mechanisms distinct from VVM cumulus cells as the oocyte matures. The reduced oocyte developmental competence may result from the fact that these alternate pathways used by IVM CCs may not be as efficient as the normal pathway used by VVM CCs for supporting oocyte development and this may be the reason why IVM cumulus cells yield reduced quality.

The modulation of distinct sets of genes by IVM and VVM cells was also observed in other biofunctional categories. Changes in the 'cell death' and 'cell growth and proliferation' functions were associated with distinct sets of genes during IVM and VVM (Tables 4.9 and 4.10), but the overall directionality seemed to be regulated similarly. For example, the percentages of pro-apoptotic and anti-apoptotic genes in IVM-CC were almost the same as those in VVM-CC (Table 4.7). Genes involved in growth promotion and growth inhibition were likewise distinct but distributed in similar proportions in IVM and VVM cells. These observations suggest that IVM cumulus cells regulate the maturation process using gene sets distinct from those used by VVM cumulus cells.

Table 4.6: Molecular and cellular functions enriched in VVM-unique and IVM-unique genes (Fold change of difference ≥ 2).

Category		P-value	# Genes
<i>VVM-unique genes</i>	DNA Replication, Recombination, and Repair	2.65E-08 -6.42E-03	81
	Cell Cycle	2.22E-06 -7.03E-03	84
	Cellular Growth and Proliferation	1.37E-05 -7.06E-03	201
	Cell Death	1.69E-05 -6.63E-03	170
	Lipid Metabolism	1.04E-04 -7.03E-03	38
<i>IVM-unique genes</i>	Cellular Growth and Proliferation	1.88E-06 -1.6E-02	158
	Cellular Assembly and Organization	4.04E-06 -1.6E-02	68
	Cell Death	7.81E-06 -1.6E-02	138
	Cell Cycle	2.89E-05 -1.63E-02	65
	Cellular Development	2.89E-05 -1.63E-02	63

Figure 4.5: Comparison biofunctional analysis of VVM-unique vs IVM-unique genes (F.C. ≥ 2) using Ingenuity Pathway Analysis (IPA) Program. Biofunctions over-represented in VVM-unique and IVM-unique genes share similar categories and significance level (represented in p-values) despite their distinct gene sets. (The number on the top of each bar graph represents the number of genes in the corresponding biofunctional category.)

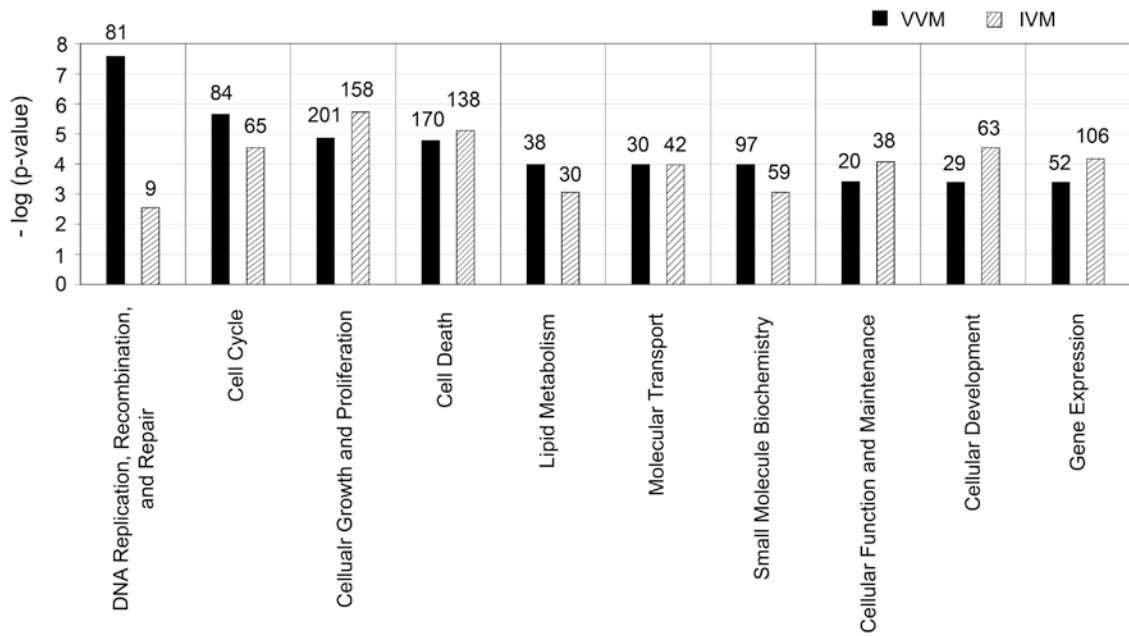


Table 4.7: Number of genes over-represented in cell cycle, cell death and cellular growth and proliferation.

Cell cycle		VVM-unique	IVM-unique
Up-regulated	Delay in cell cycle progression	25/36 (69%)	7/26 (27%)
	Increased cell cycle progression	7/36 (19%)	14/26 (54%)
Down-regulated	Delay in cell cycle progression	17/48 (35%)	11/40 (28%)
	Increased cell cycle progression	16/48 (33%)	22/40 (55%)
Cell Death		VVM-unique	IVM-unique
Up-regulated	Pro-survival	7/72 (10%)	7/59 (12%)
	Anti-apoptosis	20/72 (28%)	17/59 (29%)
	Pro-apoptosis	25/72 (35%)	21/59 (36%)
Down-regulated	Pro-survival	11/98 (11%)	5/79 (6%)
	Anti-apoptosis	22/98 (22%)	31/79 (39%)
	Pro-apoptosis	30/98 (31%)	29/79 (37%)
Cellular growth and proliferation		VVM-unique	IVM-unique
Up-regulated	Decreased growth	21/86 (24%)	11/74 (15%)
	Decreased proliferation	25/86 (29%)	9/74 (12%)
	Increased growth	17/86 (20%)	17/74 (23%)
	Increased proliferation	21/86 (24%)	22/74 (30%)
Down-regulated	Decreased growth	16/115 (14%)	10/84 (12%)
	Decreased proliferation	18/115 (16%)	15/84 (18%)
	Increased growth	32/115 (28%)	18/84 (21%)
	Increased proliferation	41/115 (36%)	26/84 (31%)
DNA replication, repair and recombination		VVM-unique	IVM-unique
Up-regulated	DNA replication	7/30 (23%)	0/2 (0%)
	DNA synthesis	14/30 (46%)	0/2 (0%)
	DNA packaging	0/30 (0%)	1/2 (50%)
	DNA repair	7/30 (23%)	0/2 (0%)
	Instability of genomes	0/30 (0%)	1/2 (50%)
Down-regulated	DNA replication	12/51 (24%)	0/7 (0%)
	DNA synthesis	12/51 (24%)	0/7 (0%)
	DNA packaging	0/51 (0%)	2/7 (29%)
	DNA repair	14/51 (27%)	0/7 (0%)
	Instability of genomes	0/51 (0%)	5/7 (71%)

Table 4.8: Comparison of G1/S cell cycle regulation genes over-represented during VVM and IVM.

Cell cycle		VVM-unique	IVM-unique
Up-regulation	G1/S arrest	<i>PTGS2(+212)</i> , <i>ANXA1(+47)</i> , <i>PRKCA(+16)</i> , <i>ADD45B(+15)</i> , <i>IFI16(+12)</i> , <i>CEBP(+12)</i> , <i>GAS1(+7)</i> , <i>PRKCH(+8)</i> , <i>GALS3(+7)</i> , <i>GALS1(+3)</i> , <i>SOD2(+3)</i>	<i>IGFBP3(+36)</i> , <i>PLAGL1(+4)</i> , <i>PURA(+3)</i> , <i>TGFB1(+3)</i>
	G1/S progression	<i>CAMK2D(+2)</i>	<i>SMAD7(+10)</i> , <i>ITGA5(+8)</i> , <i>FN1(+4)</i> , <i>TAF10(+3)</i> , <i>PLAC1(+3)</i> , <i>GMNN(+3)</i> , <i>CCND1(+2)</i>
Down-regulation	G1/S arrest	---	<i>DDX3(-7)</i> , <i>TXNIP(-4)</i> , <i>LATS2(-4)</i> , <i>APC(-2)</i>
	G1/S progression	<i>ESR2(-8)</i> , <i>CBX2(-4)</i> , <i>SMC1A(-4)</i> , <i>E2F2(-4)</i> , <i>CCND2(-4)</i> , <i>CCND3(-3)</i> , <i>CCNE1(-3)</i> , <i>TP53(-3)</i> , <i>POLE(-3)</i>	<i>PIM1(-8)</i> , <i>KLF4(-6)</i> , <i>KRAS(-4)</i> , <i>PPP3CA(-3)</i> , <i>SIRT1(-3)</i> , <i>MYC(-3)</i> , <i>FKBP1A(-2)</i>

(In parentheses: Fold change of difference in mRNA abundance during maturation; (+) up-regulation, (-) down-regulation)

Table 4.9: Genes involved in cell death

Cellular death F.C. >=2	
VVM-UP	IVM-UP
<p><i>PHLDA1, CRYAB, PLP1, LGALS3, IFI16, TGFB3, BCL6, TGFB2, SOD2, CAMK2D, EXOC2, IRS2, PRLR, RAD51C, GNE, HEYL, MIF, DAPK1, P4HB, UNC13B, GSN, BCAP29, STC1, RND3, NCOA1, RTN4, SGPP1, PRKCH, PIK3CD, LRIG1, FYN, ADAM17, ID2, INPP1, GADD45B, PTGER3, SAT1, GALNT2, CASP4, MKL1, CLIC4, PALLD, NFKBIA, IGF1, GADD45A, CDK5, ERBB4, ANXA1, GAS1, CEBPA, IP6K2, CITED2, PRKCA, TBC1D9, GNAQ, CD36, MAPK9, DNAJB9, SH3BP5, STAR, KITLG, CDC42BPA, LDLR, KLF7, DHCR24, PPM1B, BNIP3L, SH3RF1, PTGS2, ATR, MAOA, LGALS1</i></p>	<p><i>F2R, ATXN3, MAP1B, HRAS, TAF10, PGR, BLOC1S2, MAP2K2, TGFB1, KRT18, NEK6, SUB1, TNFRSF10C, TXN, MAP3K2, DDIT4, ITPR2, IFT74, CNP, IFT57, ITGA5, THBD, IFNAR2, RASD1, YARS, TTF1, IGFBP3, S100A11, PDCD5, EPHX1, PRDX2, NME1, S100A6, FN1, KCNK3, GPX1, CTNNA1, IRAK1, HINT1, GMNN, HSPE1, PURA, TNFRSF6B, PLAGL1, SDC1, NQO1, SMAD7, G6PD, TRIB3, BCL3, FKBP1B, GPI, ARHGDI</i></p>
VVM-DOWN	IVM-DOWN
<p><i>LIG1, PRPF19, FGF2, CDC7, RAD9A, NGF, BIRC5, CTSD, CYP19A1, HSD11B2, DNMT1, E2F2, UNG, IL11RA, M6PR, TP53, STAT5A, SLC6A8, UCP2, BGN, TBP, TUB, KIF3A, PCNA, CCNE1, ADAM12, MSH2, MAD1L1, PSAP, ZNF346, CYCS, ESR2</i></p>	<p><i>GAB2, QKI, SFRS5, KIF1B, PIK3R1, SRF, KRAS, LATS2, MYC, BNIP3, PEG10, PIM1, ABCC1, FOSL2, PRDM1, JUND, HIPK1, MCL1, PEG3, ATG12, UBE4B, TIA1, EGR3, BTG1, VEGFC, RFC1, WASF1, KLF4, BAG4, MLL, TP53BP2, APC, FOSB, CDH2, POU2F1, ZFR, CD9, ZAK, HPRT1, RGN, CDC2L6, INSR, AZI2, KLF10, DUSP6, PTN, DDX3X, UGCG, FKBP1A, CASD1, CDC25B, ATP7A, EFNB2, SERPINB9, ARF6, YES1, NLK, BMPR1A, RYBP, LAMP1, STK24, SUMO1, MLLT3, PPM2C, POT1, PPP3CA, IRF2, TXNIP, ATP2C1, RABGEF1, LAMP2, PRKCI, NF1, BCL10, TFCP2, NR4A1, SIRT1</i></p>

Table 4.10: Genes involved in cellular growth and proliferation

Cellular Growth and Proliferation F.C. >=2	
VVM-UP	IVM-UP
<p><i>PHLDA1, CRYAB, OSTF1, PLP1, LGALS3, TGFBR3, IFI16, MAP4K4, BCL6, NEU1, TGFBR2, SOD2, AMK2D, JARID2, IRS2, OSMR, PRLR, ACP, GNE, PDIA5, HEYL, GLA, MIF, TSPAN5, HHIP, GSN, TFPI2, MAP3K7IP3, STC1, NCOA1, PRKCH, PIK3CD, TFPI, LRIG1, C3AR1, EREG, HSD11B1, LGR4, SPTBN1, FYN, ADAM17, ID2, ADD45B, EPB41L3, BTG3, EVI5, SAT1, RARRES1, PROX1, PDCD10, KLF9, NFKBIA, CDK5, IGF1, PTPRJ, GADD45A, ERBB4, ANXA1, GAS1, STARD13, CEBPA, KISS1, IFITM1, ERRF1, IP6K2, ASPH, CITED2, PRKCA, ARID5B, RGS2, IL13RA1, SPRY1, CD36, GNAQ, MAPK9, KITLG, F11R, TNS3, DHCR24, TSPYL2, BNIP3L, PTGS2, RNF14, CTSC, ATR, CXADR, MIR21, LGALS1</i></p>	<p><i>F2R, HRAS, ARHGEF1, LIMK1, PGR, ZBTB17, PLAC1, MAP2K2, TGFB1, TCEB3, POSTN, LAMB1, TXN, PDXK, ENG, CBR1, MAP3K2, FSTL3, ADAMTS1, SURF1, CNP, PSME2, PLEC1, PFDN5, ITGA5, GRK5, IFNAR2, THBD, RASD1, MYL9, OXT, TTF1, IGFBP3, EBNA1BP2, TNFAIP6, S100A11, PRDX2, DCBLD2, S100A6, NME1, FN1, KCNK3, RPL29, ACE2, TPR, GPX1, COPE, CTNNA1, MCFD2, ARD1A, PLEKHO1, IRAK1, UCHL1, HINT1, GADD45GIP1, RASAL1, DDR2, MEG3, PURA, TNFRSF6B, COX17, ST3GAL2, PLAGL1, PPP2R5C, DGKA, G6PD, SMAD7, BCL3, UBE2L6, PDF, FKBP1B, GPI, TBC1D8, MAGED4B</i></p>
VVM-DOWN	IVM-DOWN
<p><i>USP21, LIG1, FGF2, SOCS2, CDC7, RAD9A, RUVBL1, NGF, SEMA4C, BIRC5, POR, CTSD, SIVA1, MXD3, PROK1, HSD11B2, TRIT1, GTPBP4, SALL2, TP53, STAT5A, C14ORF169, S1PR2, KHDRBS1, CDCA7, ATIC, MLLT1, PDLIM4, EI24, CCNE1, PCNA, CCND3, CCND2, MAD1L1, RPS6KA5, IRF8, NUP98, ESR2</i></p>	<p><i>CBX7, GAB2, EPS8, SFRS5, SUV39H1, PIK3R1, SRF, KRAS, ADIPOR1, MYC, LIFR, BNIP3, AGPS, PEG10, PIM1, NEO1, FOSL2, PRDM1, JUND, HIPK1, FRS2, MXI1, MCL1, PGK1, RBM3, EGR3, GABPB2, BTG1, VEGFC, RFC1, MAFF, ATAD2, KLF4, MLL, TPX2, DDX17, APC, FOSB, UBR5, CDH2, CCNG2, CD9, HPRT1, UHMK1, CTDSPL, CDC2L6, INSR, YTHDF2, MORC3, FRZB, DUSP6, KLF10, PTN, DDX3X, FKBP1A, UGCG, FZD1, CDC25B, EFNB2, AGGF1, BMPR1A, MLLT3, SUMO1, PPP3CA, IRF2, TXNIP, PLA2G1B, ERO1L, HUNK, STRAP, RABGEF1, DLG5, ARF1, SIX5, PRKCI, ABI1, NF1, BCL10, NR4A1, FGF11, NRIP1, YME1L1, TCF7L2, SIRT1</i></p>

Next, in order to explore the functional relevance of genes most highly altered during IVM, a more stringent fold change criterion (≥ 10 -fold) was applied to the IVM-unique and VVM-unique genes. This identified Periostin (*POSTN*) and FBJ murine osteosarcoma viral oncogene homolog B (*FOSB*) as molecules prominently up-regulated or down-regulated, respectively, during IVM (Supplemental Tables S6a and S6b). Many of the genes up-regulated at ≥ 10 -fold during IVM encode extracellular matrix proteins (*POSTN*, *EFEMP1*, *SPON2*, *LAMB1*), membrane proteins (*KCNK3*, *TMEM26*, *TTMA*, *THBD*) or those related to ECM proteins (*IGFBP3*, *TNFAIP6*, *MMP20*). Ingenuity pathway analysis showed that this group of genes is over-represented in molecular functions such as cellular growth and proliferation, cellular development and cell-to-cell signaling. There were only four genes down-regulated ≥ 10 -fold during VVM. Three out of these are transcription factors. *FOSB* and *EGR3* mRNA expression is maintained at a higher level in VVM cumulus cells compared to IVM cumulus cells (Supplemental Table S6b). In addition to *FOSB* and *EGR3*, other early transcription factors *FOSL2* and *JUND* mRNAs were down-regulated during IVM but maintained at a more steady level during VVM.

The characteristics of the genes differentially regulated during VVM are distinct from those regulated during IVM. For both the genes up-regulated and the genes down-regulated during VVM with the highest degree of changes in mRNA expression, lipid metabolism was the most highly over-represented function (Table 4.11, Supplemental Tables S7a and S7b). Genes up-regulated during VVM by ≥ 10 -fold were enriched in the biological functions of lipid metabolism and small molecule biochemistry. Those genes are *HSD11B1*, *STAR*, *EREG*, *PTGS2*, *CEBPA*, *PTGER3*, *ANXA1*, *ACSL1*, *CD36*, *RORA*, *PRKCA*, *IGF1*, *ABHD5*, *UGP2*, *SLC16A10* and *CLDN1* (Table 4.11 and Supplemental Table S7a). They are involved in various subcategories of lipid metabolism function, such as the synthesis, metabolism and transport of lipids, β -oxidation of fatty acids, the

synthesis and metabolism of cholesterol and prostaglandins, etc. It is also notable that a well-known cumulus cell maturation marker *PTGS2* (prostaglandin-endoperoxide synthase 2) was identified as differentially up-regulated during VVM but not during IVM. The genes down-regulated during VVM (F.C. ≥ 10) are connected in a network involved in small molecule biochemistry and lipid metabolism (Table 4.12 and Figure 4.6). Cytochrome P450 family 19 subfamily A polypeptide 1 (*CYP19A1*) and hydroxysteroid (11-beta) dehydrogenase 2 (*HSD11B2*), for example, interact with sex steroid hormones such as progesterone, beta-estradiol and prolactin (Burton *et al.*, 1998; X. Li *et al.*, 2001; Tseng & Mazella, 2002; H. Wang *et al.*, 2009). Also, *CYP19A1* may increase the expression of progesterone receptor (PGR) (X. Li *et al.*, 2002). This is consistent with my finding that *PGR* mRNA expression was significantly upregulated in IVM-CC, in which *CYP19A1* mRNA expression failed to get down-regulated.

Included in the group of oppositely regulated genes were those involved in RNA post-transcriptional modification (*POP5*, *AARS*), carbohydrate metabolism (*NUDT5*, *TKT*, *PTHLH*, *SLC37A4*) and cell-to-cell signaling interaction (*ITGAE*, *PTHLH*). Only 10 of 68 genes were down-regulated during IVM but up-regulated during VVM. Among these were genes involved in post-translational modification (*SERP1*, *PTPN1*, *HERPUD1*, *NCSTN*) and cell morphology (*DLG1*, *EGR2*, *PTPN1*) (Supplemental Tables S5a and S5b).

Table 4.11: Molecular and cellular functions over-represented among genes up or down-regulated during VVM with the fold change of difference greater than 10.

	Category	P-value	Genes
Up-regulated	DNA Replication, Recombination, and Repair	2.65E-08-6.42E-03	<i>RGS2,GADD45B,EPB41L3,IFI16,CD36,RARRES1,TFPI2,F11R,IGF1,ANXA1,CEBPA,ERRFI1,PTGS2,CXADR,EREG,C3AR1,HSD11B1,ACPP,PRKCA</i>
	Cell Cycle	2.22E-06-7.03E-03	<i>RGS2,ABHD5,IGF1,RORA,ANXA1,CEBPA,CD36,PTGS2,HSD11B1,ACSL1,STAR</i>
	Cellular Growth and Proliferation	1.37E-05-7.06E-03	<i>SLC16A10,ABHD5,RGS2,PTGER3,CD36,STAR,IGF1,UGP2,CLDN1,RORA,ANXA1,CEBPA,PTGS2,HSD11B1,ACSL1,PRKCA</i>
	Cell Death	1.69E-05-6.63E-03	<i>SLC16A10,ABHD5,RGS2,PTGER3,CD36,STAR,IGF1,UGP2,RORA,ANXA1,CEBPA,PTGS2,ACSL1,HSD11B1,PRKCA</i>
	Lipid Metabolism	1.04E-04-7.03E-03	<i>CD36,RARRES1,SERPINA3,TFPI2,SHC4,F11R,IGF1,ANXA1,ERRFI1,PTGS2,EREG,FUT4,PRKCA</i>
Down-regulated	Cell Morphology	7.34E-04-2.61E-02	<i>CACNA2D2,CYP19A1,RYR2,IHH</i>
	Cellular Development	7.34E-04-1.39E-02	<i>CYP19A1,IHH</i>
	Cellular Function and Maintenance	7.34E-04-6.59E-03	<i>SFRP4,CYP19A1</i>
	Cellular Growth and Proliferation	7.34E-04-4.77E-02	<i>SFRP4,CACNA2D2,NDP,CYP19A1,RYR2,IHH,CDCA7,SLC29A1</i>
	Lipid Metabolism	7.34E-04-3.61E-02	<i>CYP19A1</i>

Figure 4.6: IPA network for genes down-regulated only during VVM. (Molecule names are listed in Table 4.12)

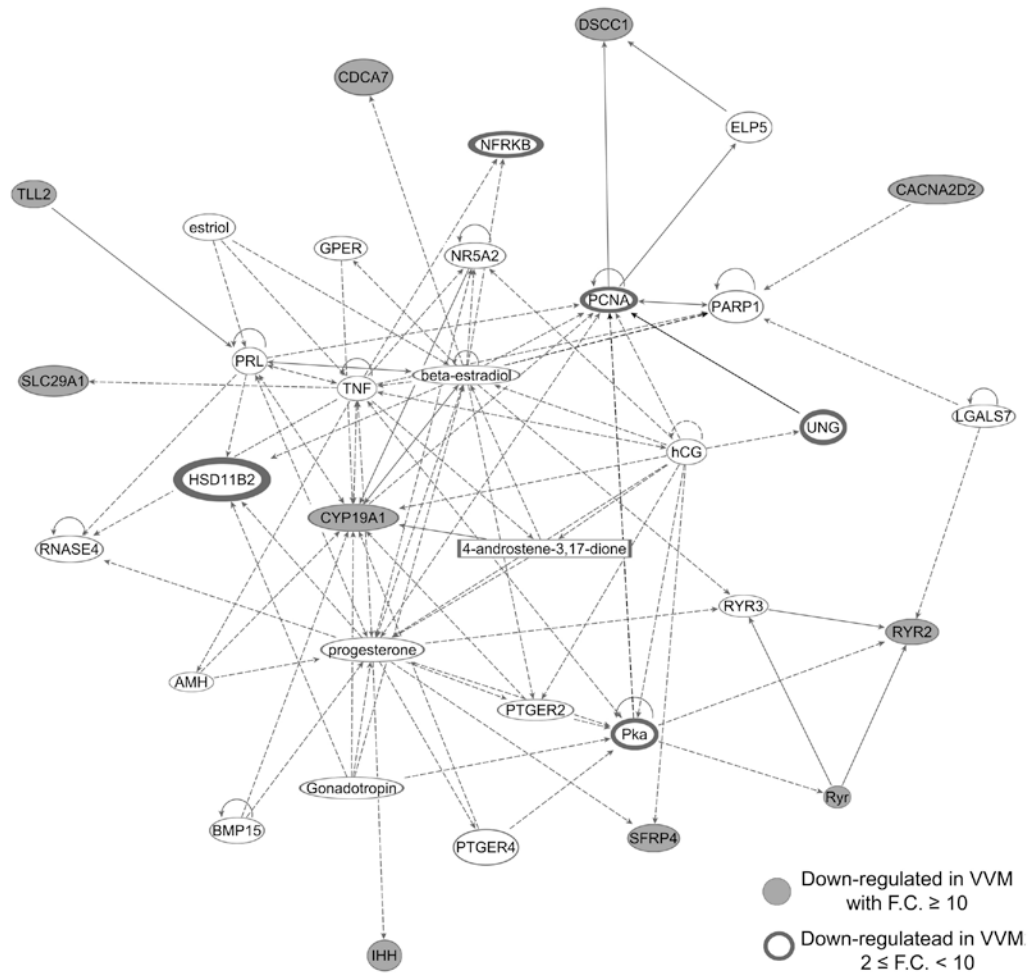


Table 4.12: Molecules in an IPA network constructed from genes down-regulated only during VVM (Figure 4.6). A * denotes genes from Table S7b

Molecule	Gene Name	Cellular Location
4-androstene-3,17-dione		
AMH	anti-Mullerian hormone	Extracellular Space
beta-estradiol		
BMP15	bone morphogenetic protein 15	Extracellular Space
CACNA2D2*	calcium channel, voltage-dependent, alpha 2/delta subunit 2	Plasma Membrane
CDCA7*	cell division cycle associated 7	Nucleus
GONADOTROPIN		
CYP19A1*	cytochrome P450, family 19, subfamily A, polypeptide 1	Cytoplasm
DSCC1*	defective in sister chromatid cohesion 1 homolog (S. cerevisiae)	
ELP5		
estriol		
GPER	G protein-coupled estrogen receptor 1	Plasma Membrane
hCG		
HSD11B2	hydroxysteroid (11-beta) dehydrogenase 2	Cytoplasm
IHH*	Indian hedgehog	Extracellular Space
LGALS7	lectin, galactoside-binding, soluble, 7	Extracellular Space
NFRKB	nuclear factor related to kappaB binding protein	Nucleus
NR5A2	nuclear receptor subfamily 5, group A, member 2	Nucleus
PARP1	poly (ADP-ribose) polymerase 1	Nucleus
PCNA	proliferating cell nuclear antigen	Nucleus
Pka		Cytoplasm
PRL	prolactin	Extracellular Space
progesterone		
PTGER2	prostaglandin E receptor 2 (subtype EP2), 53kDa	Plasma Membrane
PTGER4	prostaglandin E receptor 4 (subtype EP4)	Plasma Membrane
RNASE4	ribonuclease, RNase A family, 4	Extracellular Space
Ryr		
RYR2*	ryanodine receptor 2 (cardiac)	Plasma Membrane
RYR3	ryanodine receptor 3	Plasma Membrane
SFRP4*	secreted frizzled-related protein 4	Plasma Membrane
SLC29A1*	solute carrier family 29 (nucleoside transporters), member 1	Plasma Membrane
TLL2*	tolloid-like 2	Extracellular Space
TNF	tumor necrosis factor	Extracellular Space
UNG	uracil-DNA glycosylase	Nucleus

4.4 Identification of Oocyte Quality Markers by qRT-PCR and Statistical Analysis

Rhesus monkey IVM oocytes have limited developmental competence compared to VVM oocytes. The analysis of cumulus cells associated with the oocyte may, therefore, lead to the development of molecular markers predictive of oocyte quality. A panel of 43 genes was selected as candidates for markers to distinguish cumulus cell phenotypes associated with different oocyte quality. The qRT-PCR results confirmed differential expression for these genes between IVM-CC and VVM-CC (Figure 4.7).

Single- and multiple-gene generalized estimating equations (GEE) were used to calculate the relationship of gene expression to oocyte quality based on the mRNA expression values measured by qRT-PCR. GEE is a special case of the generalized linear model taking into consideration the occurrence of a binary outcome (oocyte quality) from multiple events of a single experimental unit. Of the 43 genes tested, univariate generalized estimating equations analysis (GEE) identified 24 genes which mRNA expression levels were significantly related to oocyte quality (IVM vs. VVM) (Figure 4.7 genes with asterisks and Table 4.13). Changes in the mRNA expression of these genes are associated with increases or decreases in oocyte quality as indicated by the odds ratio. Therefore, any of the 24 genes may be used as a molecular marker of oocyte quality.

In addition, stepwise multiple GEE identified three genes (*NEK6*, *AQP11* and *IGF1*) that can be used in combination to predict oocyte quality at a higher statistical confidence (Table 4.14). The following equation may be used to predict the probability of having a high quality oocyte: $P(\text{high quality oocyte}) = \frac{e^{5.608 + .645[\text{NEK6}] + .100[\text{AQP11}] - 2.17[\text{IGF1}]}{1 + e^{5.608 + .645[\text{NEK6}] + .100[\text{AQP11}] - 2.17[\text{IGF1}]}}$.

Figure 4.7: Quantitative analysis of selected mRNAs by quantitative RT-PCR. Genes marked with * are those 24 found by univariate analysis to be highly predictive of oocyte quality (Table 4.13). [Patent pending]

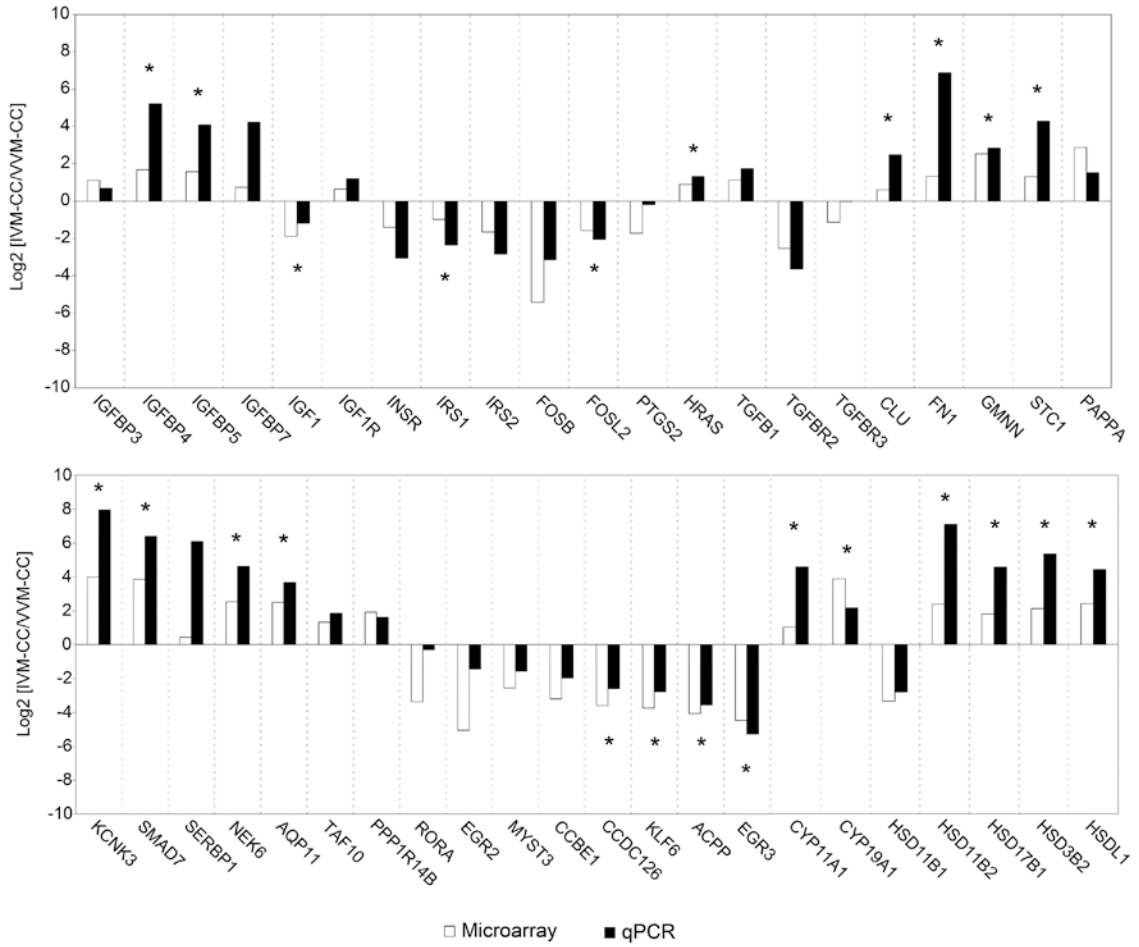


Table 4.13: Univariate GEE analysis of gene expression data related to oocyte quality.

Genes	Odds ratio	95% Confidence limits		P-value
<i>NEK6</i>	1.193	1.056	1.346	0.0044
<i>AQP11</i>	1.629	1.140	2.327	0.0074
<i>CCDC126</i>	0.862	0.761	0.976	0.0187
<i>KLF6</i>	0.800	0.647	0.988	0.0385
<i>ACPP</i>	0.161	0.031	0.835	0.0296
<i>EGR3</i>	0.911	0.831	0.998	0.0458
<i>IGFBP4</i>	2.073	1.014	4.240	0.0458
<i>IGF1</i>	0.606	0.398	0.922	0.0195
<i>IRS1</i>	0.344	0.215	0.551	<.0001
<i>FOSL2</i>	0.960	0.934	0.987	0.0039
<i>HRAS</i>	1.174	1.019	1.352	0.0265
<i>CLU</i>	1.765	1.552	2.008	<.0001
<i>FN1</i>	1.102	1.082	1.122	<.0001
<i>HSD17B1</i>	2.510	1.673	3.765	<.0001
<i>HSDL1</i>	1.146	1.121	1.171	<.0001
<i>HSD11B2</i>	1.091	1.072	1.111	<.0001
<i>STC1</i>	2.035	1.111	3.725	0.0213
<i>CYP11A1</i>	1.168	1.137	1.199	<.0001
<i>GMNN</i>	1.158	1.108	1.210	<.0001
<i>HSD3B2</i>	1.912	1.139	3.208	0.0141
<i>CYP19A1</i>	11.221	3.682	34.196	<.0001
<i>IGFBP5</i>	1.029	1.003	1.055	0.0265
<i>KCNK3</i>	1.000	1.000	1.000	0.0152
<i>SMAD7</i>	1.033	1.009	1.057	0.0066

[Patent pending]

Table 4.14: Multiple variable GEE analysis of gene expression data related to oocyte quality.

Genes	Odds ratio	95% Confidence limits		P-value
<i>NEK6</i>	1.905	1.316	2.759	0.0006
<i>AQP11</i>	1.105	1.036	1.179	0.0025
<i>IGF1</i>	0.114	0.025	0.518	0.0049

4.5 Discussion

Transcriptome analyses of rhesus monkey cumulus cells, PM-CC, IVM-CC and VVM-CC, provided results that may improve our understanding of the oocyte maturation process and its relationship to oocyte quality. Array analyses results indicated that a large number of genes (558 probe sets, 452 genes, 4.5 % of total genes detected) were identified to be differentially expressed in the direction comparison of IVM-CC and VVM-CC. Many more differences were observed when the two developmental transitions were compared, PM-CC to IVM-CC versus PM-CC to VVM-CC, indicating that many more genes undergo changes in mRNA expression during maturation than what is revealed just by comparing IVM-CC and VVM-CC. A total of 2,830 genes was incorrectly regulated (1,607 VVM-unique+1,127 IVM-unique +96 oppositely regulated), which is over 20% of the genes detected on the array. This result shows that cumulus cell development becomes robustly disrupted during the terminal 24 h maturation period during IVM. The large difference observed between IVM-CC and VVM-CC contrasts with a small set of differentially expressed mRNAs reported for the rhesus monkey oocytes (Chapter 3 above and (Y. S. Lee, *et al.*, 2008)). This result indicates that reduced oocyte quality may not be reflected highly at the level of oocyte mRNA expression because key regulations in the oocyte may be at the post-translational level, whereas changes in cumulus cell affecting oocyte quality may occur at the mRNA level.

The array data also indicated that there was a delay in the regulation of mRNA expression pattern in IVM-CCs. A higher proportion of VVM-unique genes are normally down-regulated during VVM but not down-regulated during IVM, indicating that IVM-CCs may be delayed or defective in down-modulating the mRNA expression of some genes. The group of VVM-unique and IVM-unique genes might have resulted in part from a failure of IVM cumulus cells in timely gene regulation or mRNA degradation.

A deficient expression of several essential transcription factors were observed in IVM-CC. The expression of these early transcription factors is required for maturation and terminal differentiation of mural granulosa cells (Hattori *et al.*, 2000; Russell *et al.*, 2003; Sharma & Richards, 2000), indicating that IVM-CC may be deficient in completing the maturation process. The genes with the greatest expression differences were well-known cumulus cell differentiation markers *FOSB*, *FOSL2*, *JUND*, *PTGS2*, and *EGR2*, which failed to be regulated correctly during IVM. This indicates that IVM-CCs may not attain an identical phenotype as VVM-CC during maturation. An increased mRNA expression of *PTGS2*, *STAR*, *HAS2* and *GREM1* is associated with cumulus cell expansion process in the mouse and is regulated by GDF9 secretion from the oocyte (Elvin *et al.*, 1999; Joyce *et al.*, 2001; Pangas *et al.*, 2004; Segi *et al.*, 2003). Although *HAS2* and *GREM1* mRNAs were detected on the arrays, there was not a high degree of up-regulation associated with either IVM or VVM. In contrast, *PTGS2* and *STAR* genes showed the highest relative increase in mRNA expression in VVM-CC compared to the PM-CC. It was demonstrated that cumulus expansion could occur in IVM COCs without the increased mRNA expression of these genes (Nyholt de Prada *et al.*, 2009) and the association between cumulus expansion and gene expressions regulated by GDF9 does not appear to be as direct in the primate as indicated in the mouse. However, it was shown that a higher mRNA expression of *PTGS2*, *HAS2* and *GREM1* was associated with better quality oocytes and embryos in humans (McKenzie *et al.*, 2004).

The next finding from the cumulus cell array analysis is that remarkable compensatory changes in gene expression occurred during IVM. I observed this particularly for cell cycle arrest at the G1/S phase transition, cell death, and cell growth and proliferation categories. This indicates that IVM-CC may reach similar physiological states as VVM-CC, but the two cell types may differ significantly at the level of individual regulatory gene expression.

In IVM-CC, genes involved in cell-cell interactions were misregulated in mRNA expression and this misregulation may compromise the communication between the oocyte and cumulus cells. The transcriptome analysis of IVM oocytes revealed that there may be a compromised mRNA expression of genes regulating cell-cell interaction [Chapter 3 and (Y. S. Lee, *et al.*, 2008)]. A similar result was observed in IVM-CC in which changes in mRNA expression of growth factors and other ligands, their receptors, and other interactive cell-surface molecules were detected. For example, the *DLG1* gene (Discs, large homolog 1) is responsible for the structural integrity of adherens junctions and tight junctions. IVM-CC failed to up-regulate this gene during maturation, further indicating a compromised cell-to-cell interaction between IVM oocytes and cumulus cells.

Among the genes up-regulated in both IVM and VVM-CC, *SRGN* showed the greatest fold changes in mRNA expression from PM-CC to IVM or VVM-CC. The *SRGN* mRNA is less highly up-regulated with IVM, 128-fold increase during IVM and 287-fold increase during VVM (Supplemental Table S4a). The *SRGN* (PRG1) protein is best known for its role in formation of mast cell secretory granules and a granule-mediated apoptosis via the association with granzyme B and perforin (Metkar *et al.*, 2002; Raja *et al.*, 2002). *SRGN* binds to hyaluronic acid as well as its receptor CD44, and can inhibit the adhesion of cells to extracellular matrix proteins (Ernst *et al.*, 1995; Toyama-Sorimachi *et al.*, 1995). Various cellular processes are influenced by *SRGN*, such as matrix formation, cell-cell and cell-matrix adhesion, cell proliferation and migration and the protein is also implicated in ovarian development, ovulation and fertilization (Salustri *et al.*, 1999). that the regulation of proteoglycan by gonadotropins suggests the involvement of these molecules in folliculogenesis (Mueller *et al.*, 1978). In addition, *SRGN* binds circulating lipoproteins and regulate their cellular uptake and concentration in follicular fluid (Williams & Fuki, 1997). It was shown that higher low-density lipoprotein

(LDL) concentrations in follicular fluid are associated with decreased oocyte fertilization rate (Volpe *et al.*, 1991). However, the direct association or mechanisms of serglycins in steroidogenic activity of cumulus cells are not fully understood yet.

Another major finding from this array analysis is that many of the genes that are mis-regulated to the greatest degree during IVM are involved in lipid metabolism. Lipid metabolism is implicated as a key regulation pathway in cumulus cell maturation. Especially, steroidogenesis and prostaglandin synthesis are must be carefully regulated for COCs to achieve complete maturation. Cytochrome P450 genes are key genes involved in that process and *CYP19A1* in particular was incorrectly regulated during IVM. The *CYP19A1* mRNA expression was significantly down-regulated during VVM but not during IVM. The *CYP19A1* gene is implicated in steroidogenesis, particularly the synthesis of estrogen, which plays a critical role in regulating homeostatic pathways and influence fertility, lipid metabolism and other key biological pathways (Simpson *et al.*, 2005). During follicular development, the *CYP19A1* mRNA expression in ovarian mural granulosa cells is up-regulated by FSH and prostaglandin E2 (PGE2) (Z. Cai *et al.*, 2007; Parakh *et al.*, 2006). However, with the surge of LH/hCG, *CYP19A1* gene expression must be rapidly down-regulated. The down-regulation of *CYP19A1* gene expression in mural granulosa cells is a characteristic of ovarian follicular differentiation (Andric *et al.*, 2010; Ndiaye *et al.*, 2005). The failure of IVM-CC to down-regulate *CYP19A1* expression further indicates that IVM-CCs are likely compromised in their terminal differentiation.

In addition to *CYP19A1*, other numerous genes involved in lipid metabolism were also incorrectly regulated during IVM (Figure 4.8). For example, *LDLR* (Low Density Lipoprotein Receptor) and *STAR* (Steroidogenic Acute Regulatory Protein) genes are responsible for regulating the transfer of cholesterol. LDLR is a cell surface protein that takes up cholesterol-carrying LDL molecules (Brown & Goldstein, 1986) and STAR

mediates the transfer of cholesterol to the inner mitochondrial membrane from outer membrane (Strauss *et al.*, 1999). The expression of these two mRNAs was up-regulated during VVM but not up-regulated during IVM. Additional lipid metabolism genes misregulated during IVM (Figure 4.8) are *CYP11A1* and *HSD3B2* encoding enzymes that convert cholesterol to progesterone. The *CYP11A1*, *HSD3B2* mRNAs were over-expressed in IVM-CC, as was the mRNA for progesterone receptor (*PGR*). A decreased *PGR* gene expression is associated with better embryo quality in humans (Hasegawa *et al.*, 2005), therefore, the over-expression of *PGR* and the enzymes involved in the progesterone production in IVM-CC may explain reduced developmental competence of IVM oocytes and embryos. The association of a higher *PGR* mRNA expression with COCs of a reduced developmental competence is consistent with the observation that higher quality human embryos came from COCs with reduced levels of progesterone receptor (Hasegawa, *et al.*, 2005). The *PGR* is not detected in mouse cumulus cells, although it is present in the granulosa cells of preovulatory follicles after the hCG stimulus (Teilmann *et al.*, 2006) and similar transient expression in response to LH has also been demonstrated in the rat. (Park-Sarge & Mayo, 1994; O. K. Park & Mayo, 1991) The rhesus monkey cumulus cell microarray results appear to delineate another significant difference between primates and rodents.

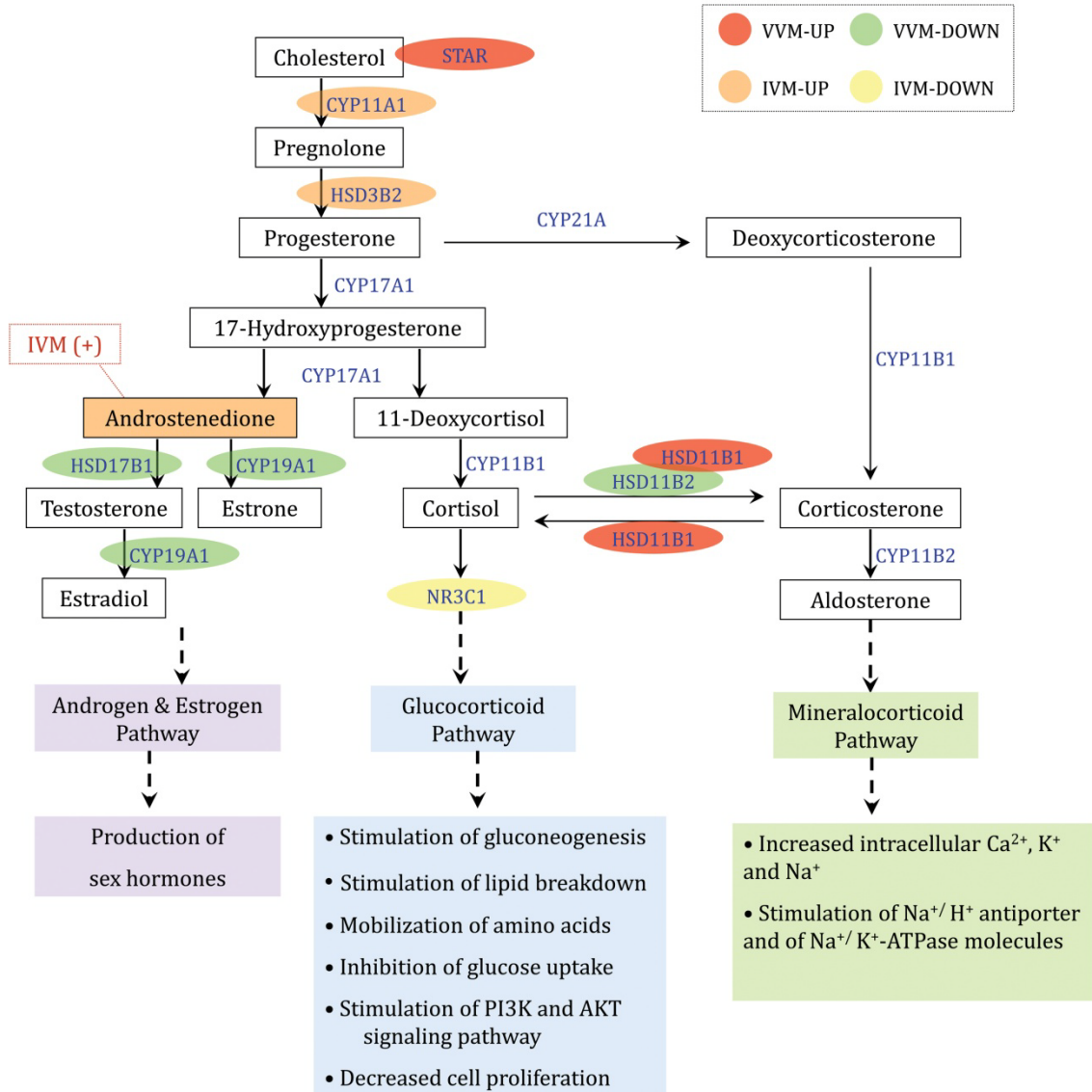
The array data also indicated that the synthesis of sex hormones was not suppressed during IVM. The mRNA expression of *HSD17B1* and *CYP19A1*, that encode enzymes that convert androstenedione into testosterone or estradiol, was down-regulated during VVM but not down-regulated during IVM. It appears there is a continued production of androgens during IVM, whereas the androgen production is shut down during VVM. The abnormal regulation of lipid metabolism in IVM-CC may affect glucocorticoid and mineralocorticoid pathways. Glucocorticoids are steroid hormones that play a critical role in maintaining physiological homeostasis. Glucocorticoids mediate

their functions by interacting with their receptors. Cortisol (or hydrocortisone) is the active form of glucocorticoids that can bind and activate glucocorticoid receptors and corticosterone is the inactive form. Hydroxysteroid (11-beta) dehydrogenase 1 (HSD11B1) predominately converts inactive cortisone to active cortisol, while hydroxysteroid (11-beta) dehydrogenase 2 (HSD11B2) converts active cortisol to inactive cortisone (Figure 4.8). Glucocorticoids activated by HSD11B1 can up-regulate the expression of *PTGS2*; both *HSD11B1* and *PTGS2* mRNAs were up-regulated during VVM but not during IVM.

Based on the results from this array study, a panel of 24 genes which mRNA expression correlates highly with oocyte quality was identified. These genes are candidate oocyte quality markers which may be used for screening and identifying high or low quality oocytes. These markers may be implemented in a non-invasive assay using cumulus cells isolated from an individual COCs. The use of these oocyte quality markers may allow clinical selection of high quality oocytes in various fertility treatment procedures (Schultz, 2005) and in evaluating IVM conditions for oncofertility programs (Woodruff, 2010), etc. These oocyte quality markers may also aid in optimizing reproductive biology methods to enhance production of valuable agricultural species or enhance species conservation approaches. Evolutionary conservation of most of these genes (Supplemental Table S8) indicates the feasibility of application across species.

Figure 4.8: Misregulation of Genes Involved in Steroidogenesis during IVM.

Numerous genes involved in steroidogenesis are incorrectly regulated during IVM. The misregulation of these genes may, in turn, compromise downstream pathways such as the production of androgen and estrogen, glucocorticoid and mineralocorticoid pathways.



CHAPTER 5
EFFECTS OF HYBRID GENOTYPE ON GENE EXPRESSION
IN MOUSE OOCYTES AND EGGS

5.1 Overview of Array Results

All quality control parameters were in the acceptable range for the array data set (Table 5.1). The rate of signal detection was consistent (41.1-47.6%, 18,404-21,451 probe sets), and the scale factors and average background readings were likewise within the acceptable ranges. Hierarchical cluster analysis (Figure 5.1) revealed that the GV and MII stage samples separated from each other as expected, and that the samples for each strain also separated from each other, indicating significant genetic variation in transcriptomes. For both GV and MII stages, the DBA2 (D2) strain clustered on a separate branch from the C57BL/6 (B6) and B6D2F1 (F1) samples, indicating that B6 and F1 oocytes were more similar to each other than to D2 oocytes. Principal component analysis (Figure 5.2) revealed tight clustering by strain and stage of oocyte, indicating excellent reproducibility of the data. Additionally, the F1 oocytes of both stages displayed a phenotype that was largely intermediate between the two parental strains.

Next, SAM analysis was applied to evaluate the numbers of genes with significant differences between the three genotypes at each stage. The two parental strains displayed the widest disparity in comparisons, with over half the detected probed sets differing at the 5% FDR and nearly 38% differing at the level of 1% FDR (Table 5.2). This is consistent with earlier comparisons between inbred strains for other tissues (Grice *et al.*, 2007; Mulligan *et al.*, 2006). At the level of both 5% FDR and 1% FDR, B6 and F1 oocytes were most similar to each other, and the D2 oocytes were quite different from either of these two genotypes. For example, at the FDR of 1% only 579 (<3%)

probe sets differed between B6 and F1 GV stage oocytes, compared to >7.5% comparing D2 and F1 oocytes. I also noted that the fraction of probes differing between the parental genotypes and the hybrid genotype increased dramatically with development from GV to MII stage. For example, comparing B6 to F1, the fraction of probe sets showing differences at FDR 1% increased from <3% to more than 11%, and for D2 the increase was from 7.5% to >31%. The increase in difference between parental genotypes was less dramatic (38 versus 42%), indicating a large change in the hybrid oocytes during maturation relative to the two parental strains.

Table 5.1: Quality control parameters for array hybridization (Mouse GV and MII oocytes)

Sample type*	% Present**	# probe sets with present calls	Scale Factor***	Average Background
B6 GV oocytes	44.9 - 47.6	20,248 - 21,451	0.26 - 0.29	39.69 - 61.99
F1 GV oocytes	45.8 - 46.2	20,673 - 20,849	0.25 - 0.30	44.95 - 58.55
D2 GV oocytes	44.5 - 45.5	20,064 - 20,518	0.29 - 0.36	38.45 - 45.17
B6 MII eggs	41.2 - 42.9	18,562 - 19,348	0.29 - 0.51	40.08 - 50.92
F1 MII eggs	40.8 - 42.9	18,404 - 19,349	0.29 - 0.39	39.65 - 47.99
D2 MII eggs	41.1 - 42.7	18,558 - 19,271	0.37 - 0.51	31.69 - 37.09
Normal range	30-60	13,530-27,060	0.11 – 1.01	20-100

*B6 (C57BL/6), F1 (B6D2F1), D2 (DBA/2), GV (Germinal Vesicle), MII (Metaphase II)

** A probe pair is present (P) if perfect match (PM) is significantly larger than mismatch (MM).

*** Scale factor is a measure of how mean intensities vary across the arrays. They should be within 3-fold of the mean of all arrays.

Figure 5.1: Hierarchical Clustering Analysis (Mouse GV and MII oocytes)

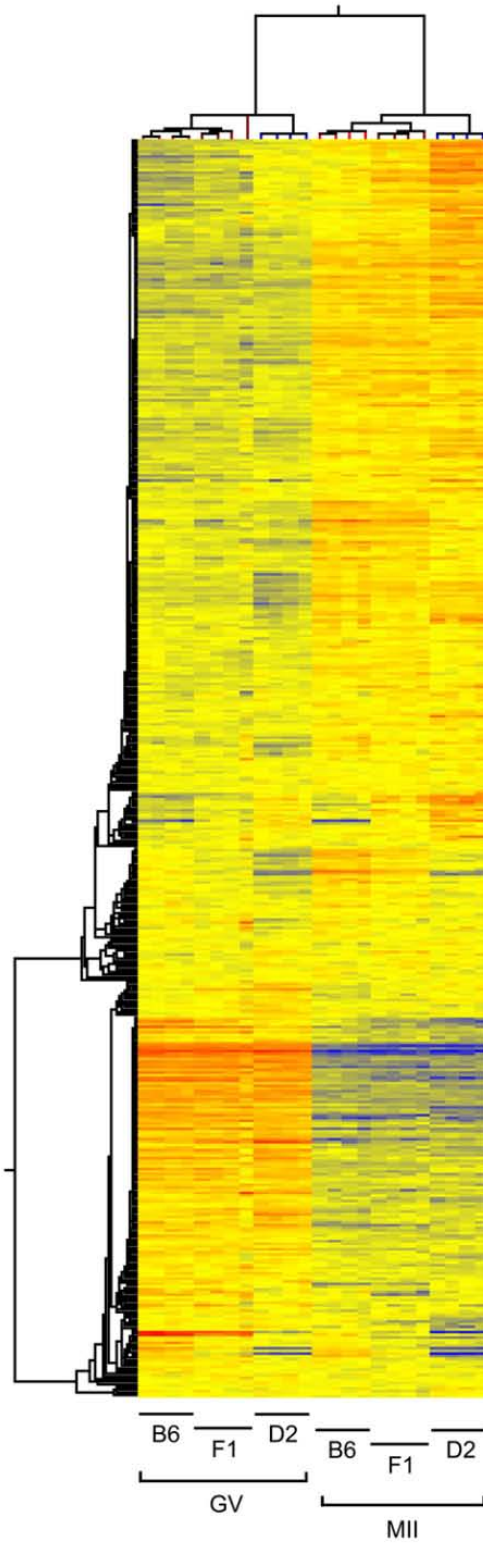


Figure 5.2: Principal Component Analysis (Mouse GV and MII oocytes)

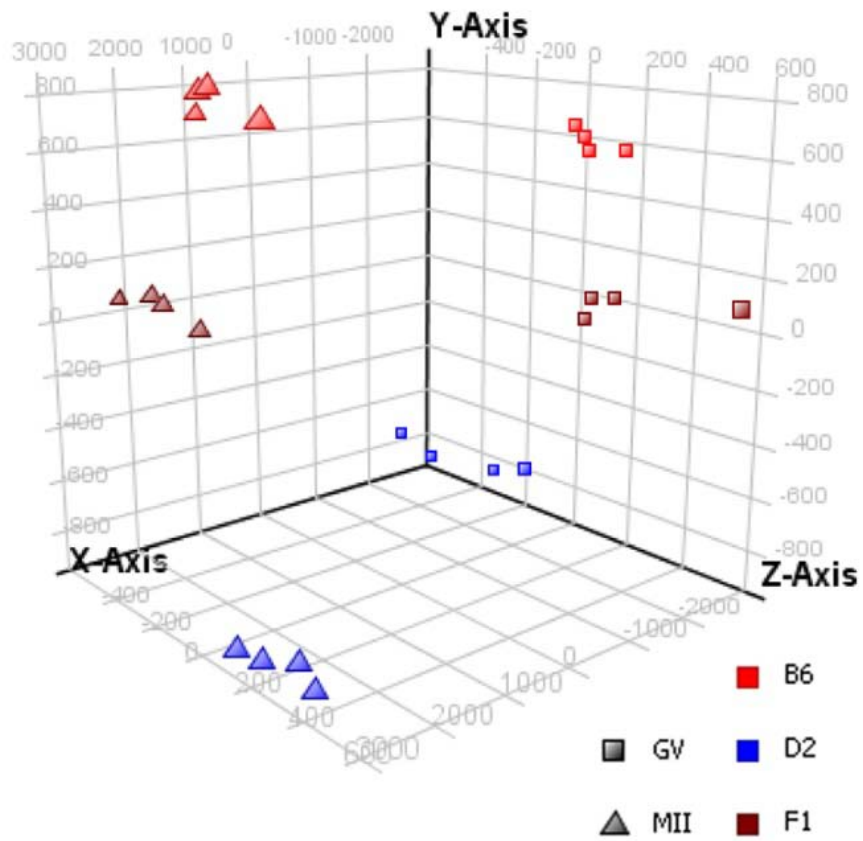


Table 5.2: Number of differentially expressed genes among oocytes/eggs of three genotypes identified by Significance Analysis of Microarray (SAM)

Comparison	# Probe sets analyzed	# Differentially expressed probe sets	
		FDR < 5%	FDR < 1%
B6-GV vs D2-GV	20,989	13,383	7,958
B6-GV vs F1-GV	20,674	1,915	579
D2-GV vs F1-GV	20,719	4,928	1,568
B6-MII vs D2-MII	19,305	12,338	8,180
B6-MII vs F1-MII	19,041	6,498	2,173
D2-MII vs F1-MII	19,083	10,339	5,986

5.2 Overdominance Effects in Gene Expression

5.2.1 Identification of Overdominance Genes

Genes that show overdominance were identified by comparing array data for the oocytes of different strains. For differences passing the FDR threshold of 5%, those genes that differed by at least 1.25-fold between the F1 oocytes and both parental strains, and with a P-value < 0.05 were identified (Table 5.2 and 5.3). This revealed a total of 45 overdominant genes for the GV stage and a total of 646 overdominant genes for the MII stage (Table 5.4, Supplemental Table S9a-b and S10a-b). The numbers of genes with expression either higher or lower in F1 oocytes were similar. Of all genes with overdominant gene expression pattern, only five genes displayed overdominance at both stages (Table 5.5). Three of these were lower in F1 oocytes at both stages, whilst one switched from low to high and one switched from high to low with maturation. The large increase in the number of overdominant genes was consistent with the observation that there is more difference in gene expression at the MII stage than at the GV stage, and also consistent with the observation that F1 oocytes diverged from the parental genotypes to a greater degree at the MII as compared to GV stage.

Table 5.3: Identification of Overdominance and Dominance Genes

Type of hybrid expression patterns		Group name	Ratio of array raw intensity values				
			[F1/B6]		[F1/D2]		[B6/D2]
Overdominant expressions	Low in F1	ODL	$[F1/B6] \leq 0.8$ $P < 0.05$	AND	$[F1/D2] \leq 0.8$ $P < 0.05$	-	-
	High in F1	ODH	$[F1/B6] \geq 1.25$ $P < 0.05$	AND	$[F1/D2] \geq 1.25$ $P < 0.05$	-	-
B6-dominant expressions	High in D2	FBL	$0.8 < [F1/B6] < 1.25$ $P \geq 0.05$	AND	$[F1/D2] \leq 0.8$ $P < 0.05$	AND	$[B6/D2] \leq 0.8$ $P < 0.05$
	Low in D2	FBH	$0.8 < [F1/B6] < 1.25$ $P \geq 0.05$	AND	$[F1/D2] \geq 1.25$ $P < 0.05$	AND	$[B6/D2] \geq 1.25$ $P < 0.05$
D2-dominant expressions	High in B6	FDL	$[F1/B6] \leq 0.8$ $P < 0.05$	AND	$0.8 < [F1/D2] < 1.25$ $P \geq 0.05$	AND	$[B6/D2] \geq 1.25$ $P < 0.05$
	Low in B6	FDH	$[F1/B6] \geq 1.25$ $P < 0.05$	AND	$0.8 < [F1/D2] < 1.25$ $P \geq 0.05$	AND	$[B6/D2] \leq 0.8$ $P < 0.05$

Table 5.4: Number of Overdominance and Dominance Genes

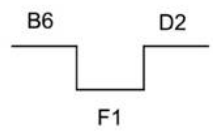
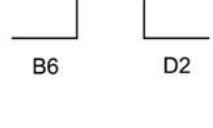
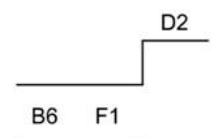

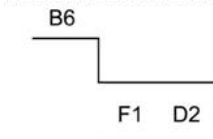
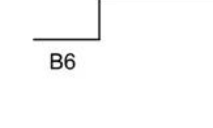
Type of hybrid expression patterns		Group name	# Probe sets (# Unique genes)		
			GV	MII	
Overdominant expressions	Low in F1	ODL	21 (21)	423 (384)	
	High in F1	ODH	25 (24)	311 (262)	
B6-dominant expressions	High in D2	FBL	1,146 (969)	1,903 (1,553)	
	Low in D2	FBH	923 (823)	1,087 (935)	
D2-dominant expressions	High in B6	FDL	219 (194)	668 (597)	
	Low in B6	FDH	192 (174)	576 (519)	

Table 5.5: Genes that showed the overdominant mRNA expression pattern in both GV and MII stages.

Probe Set ID	Gene Symbol	Gene Title	GV	MI I
1439041_at	<i>Slc39a10</i>	Solute carrier family 39 (zinc transporter), member 10	F1 high	F1 low
1434975_x_at	<i>4933439C20Rik</i>	RIKEN cDNA 4933439C20 gene	F1 low	F1 high
1459211_at	<i>Gli2</i>	GLI-Kruppel family member GLI2	F1 low	F1 low
1436966_at	<i>Peli2</i>	Pellino 2	F1 low	F1 low
1453094_at	<i>Foxn3</i>	Forkhead box N3	F1 low	F1 low

Comparing further the genes showing overdominance at the two stages provides insight into how the hybrid genotype affects the transition from GV to MII stage (Table 5.6). Over half (396/686; 57.7%) displayed overdominance at one stage but expression values intermediate between the parental strains at the other stage (T29-32, Table 5.6). Most (n=382) displayed intermediate values at the GV stage, consistent with increasing effects of overdominance at the MII stage (T31 and T32, Table 5.6).

The next most prevalent patterns observed were for genes showing equal expression across the three strains at the GV stage transitioning to overdominant reduced (n=103) or increased (n=85) expression at the MII stage, with these 188 genes accounting for nearly 28% of all the overdominant genes (T23 and T24, Table 5.6). Genes in these two groups with equal expression transitioning to overdominant high or low expression in F1 oocytes were further categorized into 4 sub-clusters defined by K-means hierarchical clustering (Figures 5.3 and 5.4). In some cases, mRNA expression was increased to a greater degree in F1 oocytes than in parental genotypes (T24 cluster A) or decreased to a greater degree in F1 oocytes (T23 clusters C & D). Gene expression in F1 oocytes increased (T23 cluster B) or declined (T24 cluster C) to a lesser degree in other cases compared to the oocytes of parental genotypes. The mRNA expression of some genes was maintained throughout the transition in F1 oocytes while increased or decreased in the oocytes of the parental genotypes (T23 cluster A and T24 cluster D). The opposite pattern was also observed: the mRNAs categorized as T24 cluster B showed small changes during maturation in the oocytes of parental strains while increased in F1 oocytes.

Table 5.6: Theoretically possible types of transitions in gene expression (Total overdominance genes: 775 probe sets corresponding to 686 unique genes)

Transition Type	From	To	# Probe sets	# Unique genes
	GV	MII		
T1	ODL	ODL	3	3
T2	ODL	ODH	1	1
T3	ODH	ODL	1	1
T4	ODH	ODH	0	0
T5	ODL	FBL	0	0
T6	ODL	FBH	1	1
T7	ODL	FDL	4	4
T8	ODL	FDH	0	0
T9	ODH	FBL	8	8
T10	ODH	FBH	0	0
T11	ODH	FDL	0	0
T12	ODH	FDH	0	0
T13	FBL	ODL	6	6
T14	FBH	ODL	35	34
T15	FDL	ODL	1	1
T16	FDH	ODL	1	1
T17	FBL	ODH	17	14
T18	FBH	ODH	6	6
T19	FDL	ODH	0	0
T20	FDH	ODH	2	2
T21	ODL	Equal	2	2
T22	ODH	Equal	5	5
T23	Equal	ODL	113	103
T24	Equal	ODH	99	85
T25	ODL	No expression	4	4
T26	ODH	No expression	0	0
T27	No expression	ODL	3	2
T28	No expression	ODH	7	7
T29	ODL	Intermediate	6	6
T30	ODH	Intermediate	10	8
T31	Intermediate	ODL	260	234
T32	Intermediate	ODH	179	148

ODL: Overdominance; Low in F1; ODH: Overdominance; High in F1

FBL: B6-dominance; High in D2; FBH: B6-dominance; Low in D2

FDL: D2-dominance; High in B6; FDH: D2-dominance; Low in B6

No expression: No expression in all three strains; Equal: Equal expression across three strains

Intermediate: F1 expression in between two parental strains

GV: Germinal Vesicle stage oocytes; MII: Metaphase II eggs

Figure 5.3: K-means clustering analysis for the genes which mRNA expression was equal during the GV stage but reduced in F1-overdominance at the MII stage. (T23)

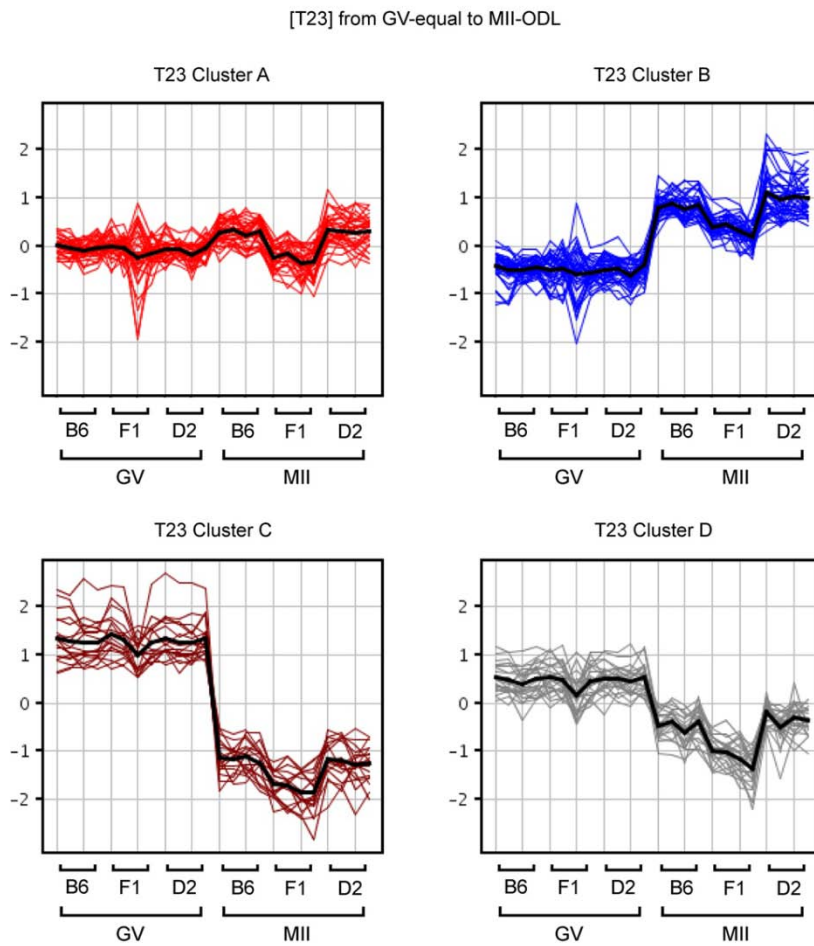
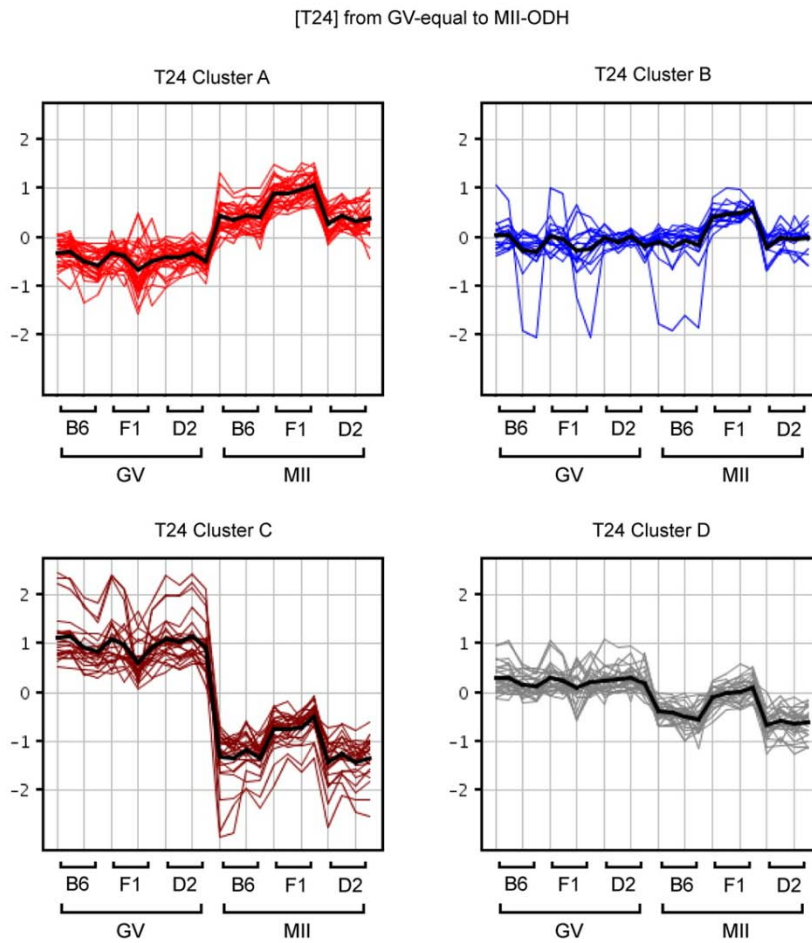


Figure 5.4: K-means clustering analysis for the genes showing equal mRNA expression at the GV stage but elevated with F1-overdominance at the MII stage. (T24)



K-means clustering indicated that the overdominance at MII stage is not obtained via a single specific pattern but rather result from various patterns of mRNA regulation that are specific for each mRNA and for genetic background of oocyte where the mRNA regulation occurs. To investigate how individual mRNAs are regulated differentially depending on genetic backgrounds during oocyte maturation, the directionality and degree of mRNA regulation was obtained for the genes in T23 and T24 groups (Supplemental Tables S11 and S12). The positive log ratio of average array intensity values at MII and GV stages indicates the up-regulation of mRNA during the GV-to-MII transition and the negative log ratio indicates a down-regulation. For each mRNA, a log ratio of array intensity values was calculated for each of the three different genetic backgrounds.

In more than 50% of the genes in T23 group (from GV-equal to MII-ODL), oocytes from both parental strains failed to down-regulate as much mRNA as F1 oocyte could (Table 5.7; F1-DOWN >> Parental-DOWN and F1-DOWN & Parental-UP). Among these, 10 mRNAs were up-regulated in oocytes of parental genetic backgrounds instead of being down-regulated as in the F1 oocytes. In another 38%, oocytes from parental strains up-regulated mRNA abundance at a much greater extent compared to F1 oocytes. On the other hand, more than 50% of the genes in T24 group (from GV-equal to MII-ODH) obtained its overdominance high in F1 expression pattern due to a greater reduction in mRNA abundance in B6 and D2 oocytes than in F1 oocytes. In some cases, F1 oocytes recruited some mRNAs more actively than oocytes from the two parental strains (Table 5.7; 23 mRNAs in F1-UP >> Parental-UP and F1-UP & Parental-DOWN). Overall, in 45% of the genes in two major overdominance groups T23 and T24 B6 and D2 oocytes displayed an aberrant mRNA down-regulation. Moreover, B6 and D2 parental oocytes were not as efficient as F1 oocytes in recruiting 33% of the

mRNAs in T23 and T24 groups. This result clearly indicates that a large portion of mRNAs is differentially regulated in F1 and parental oocytes.

Among the genes for which mRNA abundance was only maintained in F1 oocytes, the biggest difference in the changes during the GV-to-MII transition was found in *Llph* and *Slco1a5* genes (Table 5.8). While the change in F1 *Llph* mRNA abundance was only about 8 %, it was decreased in B6 and D2 oocytes by 48% and 38% respectively. The *Slco1a5* mRNA abundance was decreased by 35% in B6 oocytes and 47% in D2 oocytes but declined by only 3% in F1 oocytes. The next biggest difference was shown in *Prpf19* and *Rps6ka3* mRNAs. The mRNA abundance of *Prpf19* gene, a pre-mRNA splicing factor and homolog of yeast *Pso4*, was maintained in F1 oocytes during the GV-to-MII transition while increased in B6 and D2 oocytes (37% and 28%). A similar pattern of transition was observed with *Rps6ka*: the mRNA abundance in F1 oocytes remain unaltered while there was about 30% increase in B6 and D2 oocytes.

Among the genes in T24 cluster B category (with mRNA abundance maintained in B6 and D2 oocytes but increased mRNA abundance in F1 oocytes), *Pla2g12b* showed the most significant amount of difference (Table 5.8). There was 60% increase in *Pla2g12b* mRNA abundance in F1 oocytes during the transition from GV to MII-stage while B6 and D2 mRNA abundance was increased only by less 7-9 %. The mRNA abundance of a putative RNA helicase *Dhx30* gene only increased in F1 oocytes by 37%. The protein product of the gene may be involved in translation initiation, nuclear and mitochondrial splicing, and ribosome and spliceosome assembly. Proteins in DEAD box protein family are believed to be involved in early embryonic development (Matsumoto *et al.*, 2005; Mouillet *et al.*, 2008; Sawada *et al.*, 2006).

Table 5.7: Comparison of gene expression changes in oocytes from F1 and parental strains during the GV-to-MII stage transition.

Type of mRNA regulation in F1 and parental oocytes	Number of genes		Percentage of genes with the pattern (%)
	[T23] from GV-equal to MII-ODL	[T24] from GV-equal to MII-ODH	
F1-UP << Parental-UP	39	0	20.6
F1-UP >> Parental-UP	0	23	12.2
F1-DOWN >> Parental-DOWN	43	0	22.8
F1-DOWN << Parental-DOWN	0	44	23.3
F1-UP & Parental-No change	0	1	0.5
F1-DOWN & Parental-No change	0	0	0.0
F1-No change & Parental-UP	2	0	1.1
F1-No change & Parental-DOWN	0	4	2.1
F1-DOWN & Parental-UP	10	0	5.3
F1-UP & Parental-DOWN	0	4	2.1
Others	10	9	10.1
Total # genes w/ distinct patterns	104	85	
	189 genes		

Table 5.8: Genes that showed the biggest difference in the mRNA expression changes among 3 strains during the GV-to-MII transition

	Gene Symbol	Gene Title	Ratio of Change			Average Array Raw Intensities					
			B6	F1	D2	B6-GV	F1-GV	D2-GV	B6-MII	F1-MII	D2-MII
T23 From GV- equal to MII- ODL	<i>Myst4</i>	MYST histone acetyltransferase monocytic leukemia 4	1.34	1.13	1.56	1598.99	1391.99	1400.04	2141.05	1577.43	2187.44
	<i>Rps6ka3</i>	Ribosomal protein S6 kinase polypeptide 3	1.31	1.02	1.32	1380.49	1269.20	1248.25	1801.97	1289.31	1651.84
	<i>Kif2a</i>	Kinesin family member 2A	1.21	0.90	1.73	1214.89	1262.44	1275.28	1465.06	1133.20	2207.40
	<i>Prpf19</i>	PRP19/PSO4 pre-mRNA Processing factor 19 homolog (<i>S. cerevisiae</i>)	1.33	0.96	1.24	610.48	510.27	620.01	810.43	488.82	765.83
	<i>Rab11fip4</i>	RAB11 family interacting protein 4 (class II)	1.20	0.92	1.25	627.83	627.08	702.36	751.46	576.64	875.53
T24 From GV- equal to MII- ODH	<i>Pla2g12b</i>	Phospholipase A2, group XIIB	1.07	1.60	1.09	481.84	476.07	528.71	517.95	760.36	577.27
	<i>Hspe1</i>	Heat shock protein 1 (chaperonin 10)	0.94	1.29	0.93	852.74	800.31	844.96	800.26	1030.77	781.77
	<i>Dhx30</i>	DEAH (Asp-Glu-Ala-His) box polypeptide 30	1.02	1.37	0.95	3831.25	3752.27	4084.72	3907.98	5127.98	3880.03
	<i>Llph</i>	LLP homolog, long-term synaptic facilitation (<i>Aplysia</i>)	0.52	1.08	0.62	2404.70	2440.03	2469.14	1242.38	2638.11	1538.47
	<i>Slco1a5</i>	Solute carrier organic anion transporter family, member 1a5	0.65	0.97	0.53	1628.24	1472.65	1610.64	1056.97	1426.87	859.33

The next two largest transition patterns were 34 genes that showed dominant high expression in F1 and B6 GV stage oocytes and then showed overdominant low expression in F1 MII oocytes (T14; Table 5.6), or reciprocally 14 that show dominant low expression in B6 and F1 GV stage oocytes and then show overdominant high expression at the MII stage (T17; Table 5.6). These genes thus display initial expression values that distinguish B6 and F1 oocytes from D2 oocytes, but then undergo dramatic shifts in expression with oocyte maturation that are more exaggerated in the F1 oocytes than in the B6 oocytes.

The transcriptome analysis of oocytes with F1 and parental inbred genetic backgrounds revealed that F1 genotype exerts its effects on how mRNA abundance is regulated during the oocyte maturation. Approximately 83% of overdominance genes show one of the four transition patterns out of total 32 possible patterns. Genes in these four major transition groups did not show overdominance at the GV stage but gained the overdominance expression pattern during the GV to MII stage transition. The evaluation of array raw intensities for each gene at GV and MII stages indicated that the overdominance at the MII stage was obtained through differential regulation of mRNA abundance in F1 and inbred oocytes.

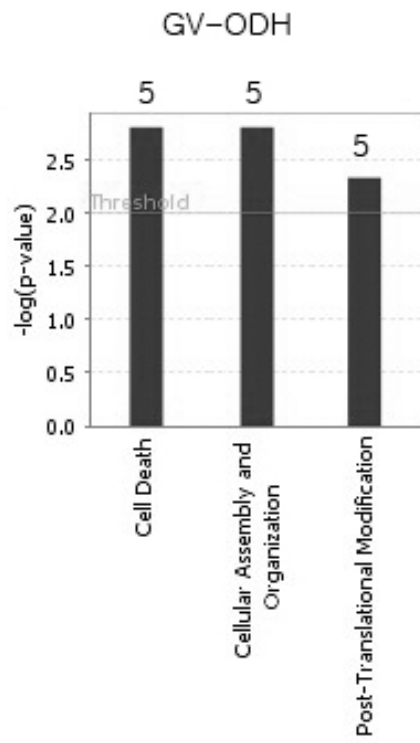
5.2.2 Biofunctional Analysis for Overdominance Genes

The identification of genes that show an overdominance effect in oocyte mRNA expression provides an opportunity to evaluate the biological functions and pathways in the oocyte that are most likely affected by hybrid vigor. Using IPA, I examined the potential functions of genes in the major groups shown in Table 5.4. For the 24 genes showing overdominant high expression at the GV stage (GV-ODH), the major affected functions were cell death, cellular assembly and organization, and post-translational modification (5 genes each, Table 5.9, Figure 5.5).

Table 5.9: Molecular and cellular functions over-represented in GV-ODH genes
 [Threshold = Fisher's exact test p-value <0.01 & #Molecules ≥5]

Category	p-value	Genes
Cell Death	1.52E-03- 4.11E-02	<i>Ppid, Trim32, Nras, Tardbp, Rtn4</i>
Cellular Assembly and Organization	1.52E-03- 4.48E-02	<i>Ppid, Tubgcp5, Nras, Rtn4, Stx18</i>
Post-Translational Modification	4.57E-03- 3.31E-02	<i>Ppid, Trim32, Nras, Uba3, Ppp1cb</i>

Figure 5.5: Molecular and Cellular Functions over-represented in GV-ODH genes [Threshold = Fisher's exact test p-value <0.01 & #Molecules ≥5]



For the 21 genes showing overdominant low expression at the GV stage (GV-ODL), the major affected functions represented were cell growth & proliferation (n=10 genes), cellular development (n=9), cellular function & maintenance (6 genes), and additional functional categories represented by smaller gene sets affecting cell cycle, DNA replication, gene expression, cell death, molecular transport, small molecular biochemistry, and cell-cell signaling (Table 5.10, Figure 5.6). Fourteen of the 21 GV-ODL had functional interactions in an IPA network related to lipid metabolism, molecular transport and small molecule biochemistry (Figure 5.7). The GV-ODL genes in this network related to lipid metabolism and steroidogenesis are *Lepr*, *Nr2e1*, *Pla2g4f* and *Gdpd3*, which interact with other regulators of lipid metabolism, steroidogenesis and small molecule biochemistry, e.g. beta-estradiol, arachidonic acid, *Ptgs1*, *Apod*, *Leprot*, *Tgfb1* and etc.

For the genes showing overdominant low expression at the MII stage (MII-ODL), there were 21 major affected functions identified with 6-93 genes each (Supplemental Table S14, Figure 5.8). The most highly ranked categories in terms of statistical significance and number of genes were again related to a variety of cellular processes such as cell structure, cell cycle & replication, cell signaling, carbohydrate metabolism, nucleic acid metabolism, and small molecule biochemistry. The categories with the largest numbers of affected genes were cell death (n=93), cell growth & proliferation (n=74), and gene expression (n=72). Carbohydrate metabolism and small molecule biochemistry were identified as the biological function most affected by the genes with overdominant high expression pattern at the MII stage (MII-ODH; Table 5.11, Figure 5.9). Compared to the MII-ODL group of genes, much fewer biological functional categories (21 vs. 4) were affected by the genes showing overdominant high expression at MII stage (MII-ODH) at the P-value threshold setting of <0.01. The number of genes

categorized in the biological functions of statistical significance were also much fewer in MII-ODH group than MII-ODL (200 MII-ODL genes vs. 48 MII-ODH genes).

In summary, the biofunction category most significantly over-represented in F1 GV oocytes was cell death, whereas the biofunction under-represented in F1 GV oocytes is cellular growth and proliferation. It was observed that there were overlaps in biofunction categories over-represented in MII-ODL and MII-ODH genes. Functions such as cellular assembly and organization, carbohydrate metabolism and small molecule biochemistry were identified to be significantly enriched among genes both higher and lower in F1 oocytes than in oocytes from inbred strains. The genes that make up these functional categories, however, were different for MII-ODL and MII-ODH groups. 'Protein synthesis' was the only biofunction category that was unique to the genes more highly expressed in F1 MII eggs. Genes with lower mRNA abundance in F1 MII eggs are involved in numerous biofunction categories, the top three of which are 'cellular movement', 'amino acid metabolism' and 'post-translational modification.'

Table 5.10: Molecular and cellular functions over-represented in GV-ODL genes
 [Threshold = Fisher's exact test p-value <0.01 & # Molecules ≥5]

Category	p-value	Genes
Cellular Growth and Proliferation	9.71E-06-4.03E-02	<i>Ceacam1,Nr2e1,Ftl,Gli2,Atf3,Lepr,Pnp,Lef1,Msi2,Icoslg</i>
Cellular Development	6.91E-05-4.57E-02	<i>Ceacam1,Ftl,Nr2e1,Gli2,Atf3,Lepr,Pnp,Lef1,Icoslg</i>
Cellular Function and Maintenance	6.91E-05-4.4E-02	<i>Ceacam1,Ftl,Nr2e1,Pnp,Lef1,Icoslg</i>
Cell Cycle	1.25E-04-4.84E-02	<i>Ceacam1,Nr2e1,Atf3,Gli2,Foxn3,Lef1</i>
Gene Expression	6.15E-04-3.79E-02	<i>Nr2e1,Atf3,Gli2,Lepr,Foxn3,Lef1</i>
Cell Death	1.28E-03-4.41E-02	<i>Ceacam1,Nr2e1,Atf3,Gli2,Lepr,Pnp,Slc1a1,Lef1,Icoslg</i>
DNA Replication, Recombination, and Repair	1.28E-03-3.29E-02	<i>Ceacam1,Atf3,Gli2,Foxn3,Lef1</i>
Molecular Transport	1.28E-03-4.65E-02	<i>Atf3,Lepr,Pnp,Slc1a1</i>
Small Molecule Biochemistry	1.28E-03-4.65E-02	<i>Ftl,Atf3,Lepr,Pnp,Slc1a1</i>
Cell-To-Cell Signaling and Interaction	5.13E-03-3.71E-02	<i>Ceacam1,Nr2e1,Lepr,Icoslg</i>

Figure 5.6: Molecular and Cellular Functions over-represented in GV-ODL genes [Threshold = Fisher's exact test p-value <0.01 & #Molecules ≥5]

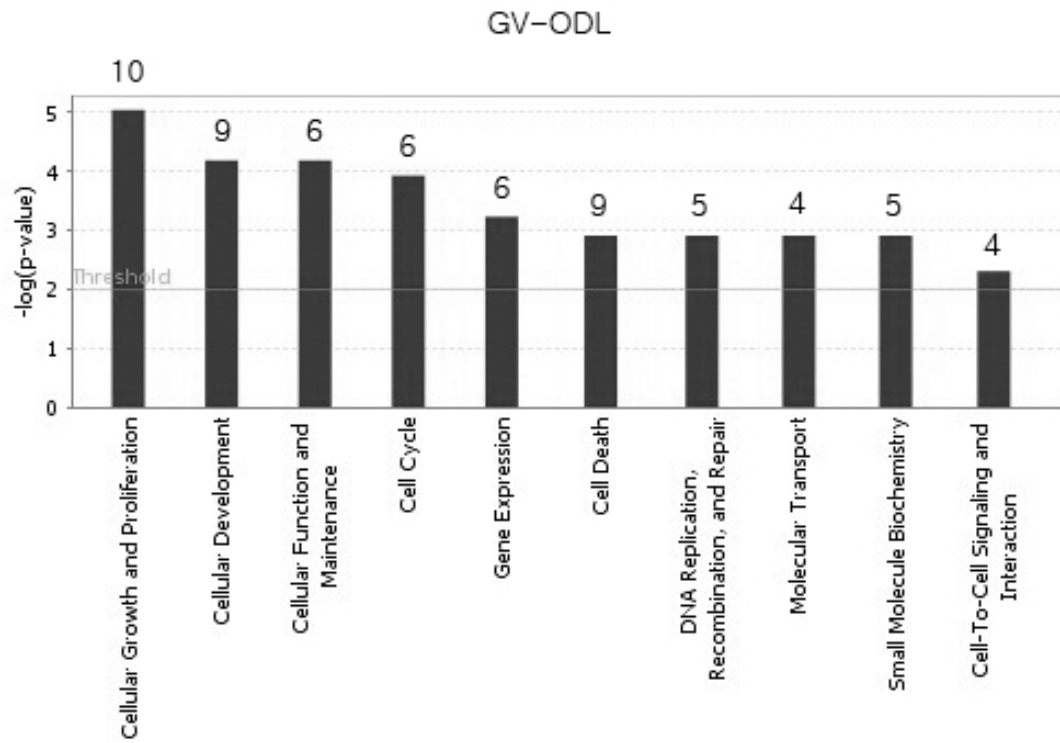


Figure 5.8: Molecular and Cellular Functions over-represented in MII-ODL genes [Threshold = Fisher's exact test p-value <0.01 & #Molecules ≥5]

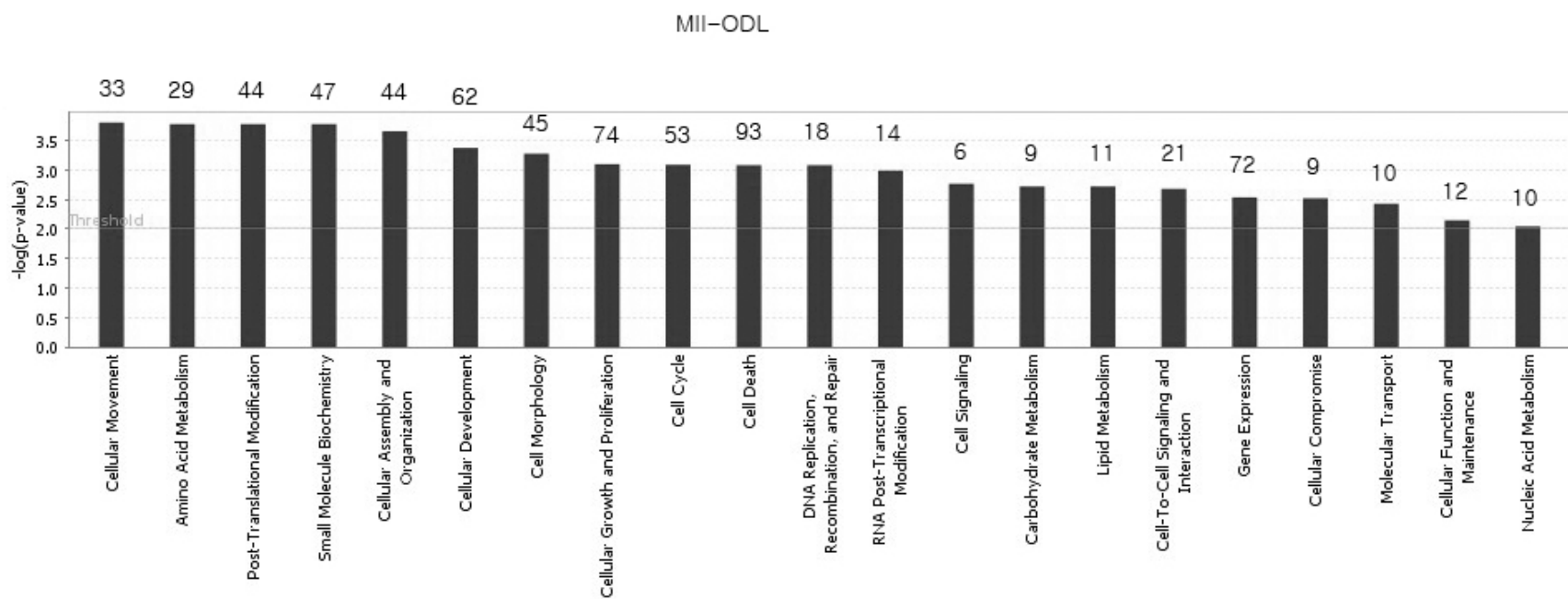
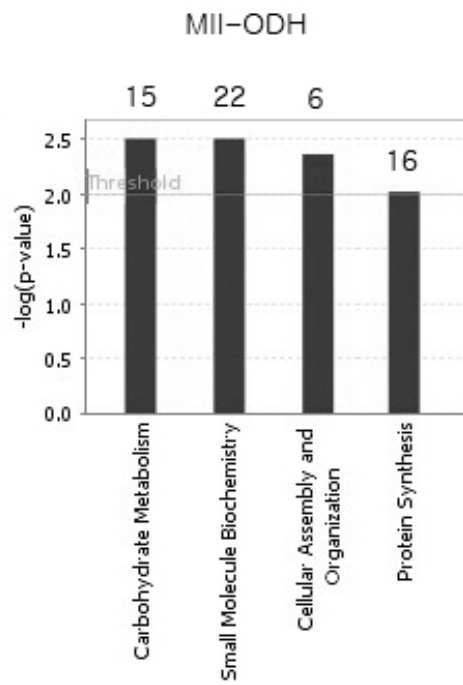


Table 5.11: Molecular and Cellular Functions over-represented in MII-ODH genes
 [Threshold = Fisher's exact test p-value <0.01 & #Molecules ≥5]

Category	p-value	Genes
Carbohydrate Metabolism	3.13E-03- 4.36E-02	<i>Gla, Tmem55b, Mfng, Hbegf, Rps6, Pigq, Glo1, Pgd, Lpcat2, Galt, Gale, Smarcb1, Impa2, Nans, Akr1b1</i>
Small Molecule Biochemistry	3.13E-03- 4.84E-02	<i>Gla, Slc1a4, Dbi, Tmem55b, Mfng, Mpg, Hbegf, Rps6, Coasy, Stx1a, Tgm2, Pgd, Lpcat2, Galt, Gale, Hspe1, Smarcb1, Phgdh, Naglu, Akr1b1, Nans, Acot8</i>
Cellular Assembly and Organization	4.34E-03- 4.36E-02	<i>Fis1, Ift20, Dnajc5, Arfgap1, Dvl1, Bet1l</i>
Protein Synthesis	9.56E-03- 4.27E-02	<i>Psmb3, Phlda1, Rpl27a, Psmb5, Ube2a, Rpl34, Rps6, Bace1, Pigq, Rpl23a, Rpl14, Eif2b2, Rps10, Rpl35, Htra2, Bace2</i>

Figure 5.9: Molecular and Cellular Functions over-represented in MII-ODH genes [Threshold = Fisher's exact test p-value <0.01 & #Molecules ≥5]



IPA analysis was performed on the genes showing equal expression at the GV stage transitioning to overdominant low and high expression in F1 oocytes at the MII stage (T23 and T24, Table 5.6). For the T23 category, the functions reaching the highest statistical significance related to RNA processing (9 genes), cell-cell signaling (4 genes) cell assembly and organization (18 genes), cell morphology (15 genes), post-translational modification (16 genes), and DNA recombination and repair (12 genes), cell cycle (7 genes), cellular function and maintenance (9 genes), gene expression (21 genes) and cell death (25 genes) (Table 5.12; Figure 5.10). For the T24 category of genes showing equal expression at the GV stage transitioning to overdominant high expression at the MII stage, the most highly ranked biofunctions were RNA processing (8 genes), protein synthesis (8 genes), carbohydrate metabolism (5 genes), cell cycle (2 genes), cell morphology (1 gene), cell-cell signaling (2 genes), cellular assembly and organization (3 genes), cellular function and maintenance (5 genes), and lipid metabolism (3 genes) (Table 5.13; Figure 5.11).

Therefore, many of the affected biofunction categories are shared between the genes that transition from equal or intermediate expression at the GV stage to either overdominant high or low expression at the MII stage, including cell cycle & DNA replication, cell structure and organization, small molecule biochemistry, metabolic processes, and cell signaling. The affected genes may thus exert F1 hybrid genotype effects on phenotype via these pathways and processes. Comparing individual genes between lists reveals that the array of genes within particular functional categories differs, and in some cases, reveals opposite directions of regulation for different genes within some categories.

Table 5.12: Molecular and Cellular Functions over-represented among genes in “from GV-Equal to MII-ODL” transition (T23)

Category	p-value	Genes
RNA Post-Transcriptional Modification	4.7E-06 -7.54E-03	<i>Srpk2, Sfrs1, Hcfc1, Nono, Srpk1, Cdk11a, Sf3a1, Papolg, Sfrs2ip</i>
Cellular Assembly and Organization	8.28E-04 -3.72E-02	<i>Hcfc1, Cctf, Srpk1, Tjp1, Stk11, Csk, Golga3, Ckap5, Myo1c, Sfrs2ip, Npc1, Srpk2, Kif2a, Diaph1, Smc2, Rab11fip4, Sorbs2, Gna13</i>
Cell Morphology	1.15E-03 -4.44E-02	<i>Col4a3, Stk11, Csk, Ckap5, Clic4, Lmnb1, Parvb, Npc1, Diaph1, Kif2a, Lyst, Sorbs2, Ncor1, Gna13, Dyrk1a</i>
Post-Translational Modification	1.76E-03 -4.16E-02	<i>Huwe1, Ick, Srpk1, Prpf19, Stk11, Cdk11a, Csk, Myst4, Col4a3, Ube4a, Srpk2, Ccdc88a, Diaph1, Hmgb111, Nrd1, Dyrk1a</i>
DNA Replication, Recombination, and Repair	2.96E-03 -3.72E-02	<i>Huwe1, Kif2a, Ccdc88a, Hcfc1, Tfam, Prpf19, Cctf, Srpk1, Smc2, Atf7ip, Golga3, Ckap5</i>
Cell Cycle	4.83E-03 -3.72E-02	<i>Srpk2, Kif2a, Hcfc1, Cctf, Srpk1, Smc2, Ckap5</i>
Cellular Function and Maintenance	6.31E-03 -3.99E-02	<i>Npc1, Kif2a, Mllt10, Stk11, Csk, Rps6ka3, Gna13, Myo1c, Bmp5</i>
Gene Expression	7.11E-03 -4.44E-02	<i>Hcfc1, Cctf, Tjp1, Gtf3c2, Myst4, Cct2, Gtf2f1, Sin3a, Hsbp1, Cux1, Nfx1, Parvb, Tfam, Smc2, Ldb1, Foxn3, Atf7ip, Ncor1, Topors, Gna13, Dyrk1a</i>
Cell Death	7.54E-03 -2.66E-02	<i>Prpf19, Cctf, Srpk1, Col4a3, Cct2, Clic4, Lmnb1, Srpk2, Parvb, Ccdc88a, Gna13, Huwe1, Nek1, Csk, Cdk11a, Stk11, Bmp5, Tub, Sin3a, Npc1, Tfam, Hmgb111, Fxr1, Sorbs2, Topors</i>
Cellular Development	7.54E-03 -4.44E-02	<i>Parvb, Cctf, Mllt10, Ldb1, Stk11, Ncor1, Gna13, Clic4</i>
Cellular Movement	7.54E-03 -4.7E-02	<i>Npc1, Ccdc88a, Hmgb111, Pik3c2a, Col4a3, Csk, Gna13</i>
Lipid Metabolism	7.54E-03 -4.44E-02	<i>Npc1, Mtmr4, Pik3c2a, Far1, Rps6ka3, Ncor1, Bmp5</i>
Small Molecule Biochemistry	7.54E-03 -4.44E-02	<i>Ick, Srpk1, Pik3c2a, Cdk11a, Csk, Stk11, Rps6ka3, Far1, Npc1, Srpk2, Mtmr4, Aldh18a1, Ncor1, Dyrk1a</i>

Figure 5.10: Molecular and Cellular Functions over-represented among genes in “from GV-Equal to MII-ODL” transition (T23)

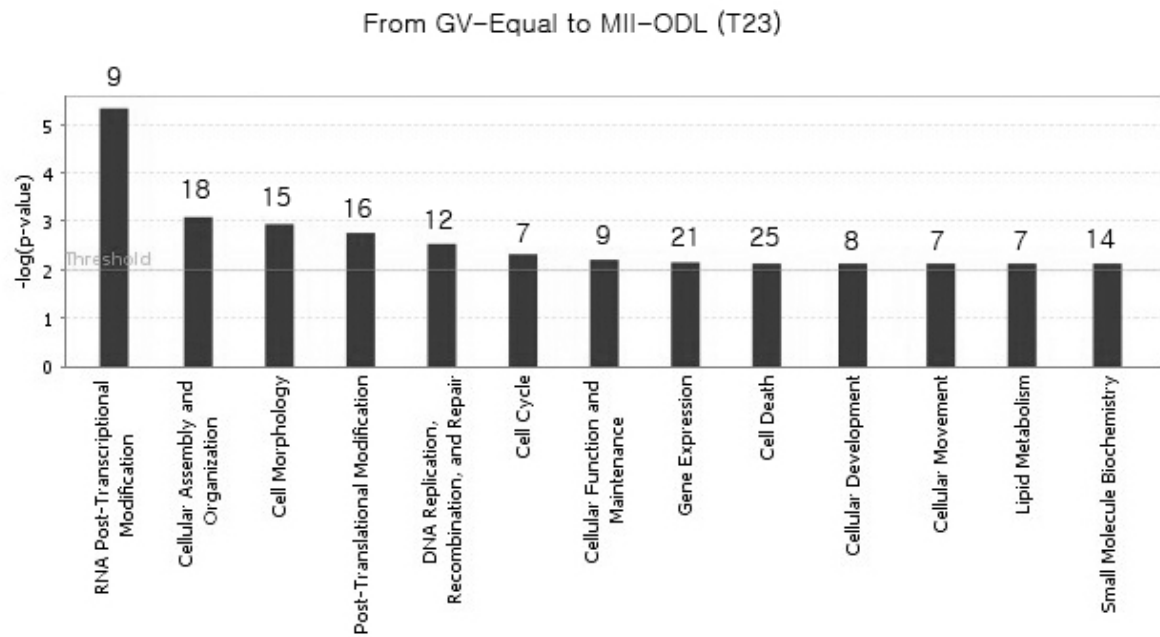
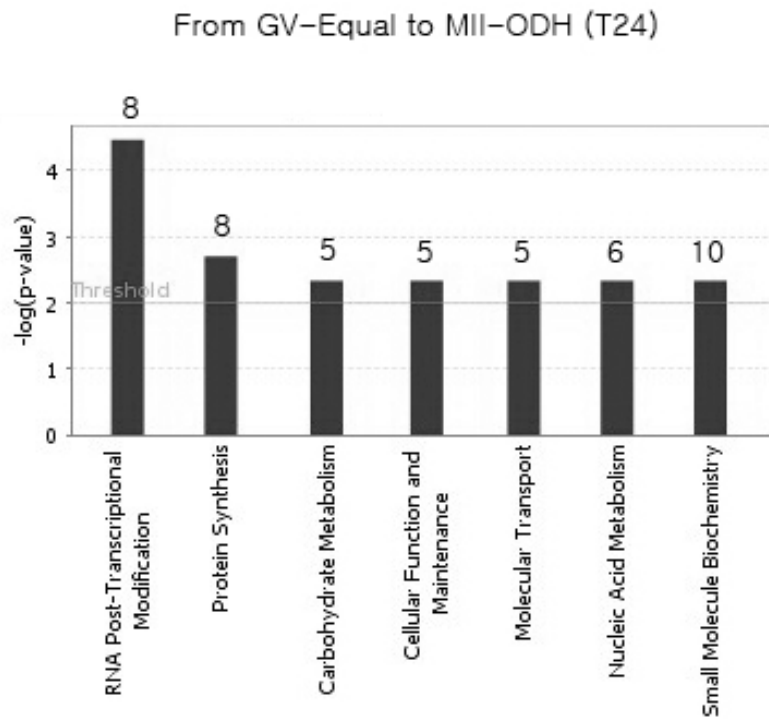


Table 5.13: Molecular and cellular functions over-represented among genes in “from GV-Equal to MII-ODH” transition (T24)

Category	p-value	Genes
RNA Post-Transcriptional Modification	3.41E-05-4.53E-02	<i>Ddx39, Wdr55, Snrpg, Rps16, Rps6, Safb, Rpl14, Usp39</i>
Protein Synthesis	1.99E-03-3.21E-02	<i>Phlda1, Rpl27a, Ube2a, Rps6, Rpl14, Htra2, Rpl23a, Eif2b2</i>
Carbohydrate Metabolism	4.65E-03-4.56E-02	<i>Hk1, Pgd, Galt, Rps6, Ganab</i>
Cellular Function and Maintenance	4.65E-03-4.11E-02	<i>Hk1, Ift20, Bap1, Rps6, Safb</i>
Molecular Transport	4.65E-03-4.56E-02	<i>Eif2s2, Gla, Slc1a4, Galt, Slco1a5</i>
Nucleic Acid Metabolism	4.65E-03-4.56E-02	<i>Eif2s2, Pgd, Dbi, Galt, Hspe1, Acot8</i>
Small Molecule Biochemistry	4.65E-03-4.56E-02	<i>Eif2s2, Gla, Pgd, Slc1a4, Dbi, Galt, Hspe1, Rps6, Ganab, Acot8</i>

Figure 5.11: Molecular and Cellular Functions over-represented among genes in “from GV-Equal to MII-ODH” transition (T24)



5.2.3 3'UTR Analysis of MII-stage Overdominance Genes

To investigate what may govern the differential regulation of mRNA abundance in F1 eggs, 3'UTR analysis was performed on MII-ODL (n=377) and MII-ODH (n=257) genes that are associated with known annotations and mRNA sequences. Motifs with significant differences of frequencies in 3'UTR sequences of MII-ODL and MII-ODH mRNAs were identified at a statistical significance threshold of BH-adjusted $P < 0.01$. Notably, all motifs with significant differences showed a higher frequency of detection in 3'UTR of MII-ODL genes than MII-ODH genes. Moreover, among the motifs with significant differences, 45 motifs were only detected in 3'UTR of MII-ODL genes but absent in MII-ODH 3'UTR sequences (Table 5.14). In summary, 45 motifs were significantly enriched in 3'UTR of MII-ODL mRNAs, whereas no motif enrichment was observed in 3'UTR of MII-ODH mRNAs. Also, all motifs that passed the statistical significance test were more frequently detected in MII-ODH 3'UTR sequences than in MII-ODL 3'UTR sequences. Due to the absence of motif enrichment in MII-ODH 3'UTR sequences, further motif analyses were only focused on MII-ODL 3'UTR motifs.

A set of motifs with the largest coverage over the MII-ODL 3'UTR sequences were identified using formulae described in chapter 2. Those 45 motifs only detected in 3'UTR of MII-ODL genes ($P < 0.01$) and 100 motifs with the biggest log ratio of differences ($P < 0.01$) were used in this analysis. The analysis result revealed that more than 94% of 3'UTR sequences of MII-ODL genes were covered by the 145 motifs analyzed, and as few as 31 motifs could cover 90% of the MII-ODL 3' UTR sequences (Supplemental Table S13).

To identify potential consensus sequences, a hierarchical clustering analysis was performed on the 45 motifs only detected in MII-ODL 3'UTR sequences and the top 50 motifs with significant differences. The HCL analysis displayed that the top 50 motifs

could be categorized into 16 clusters (Figure 5.12). The biggest subcluster is composed of 12 motifs out of total 95 motifs analyzed. Motifs in this cluster are 8-9 nt in length and 3 of the 12 motifs in the cluster contain AUUUA sequence, which is known to promote destabilization of the mRNA (Hennessy *et al.*, 1989; Raymond *et al.*, 1989). All 3 motifs containing the AUUUA motif are among 45 motifs only detected in MII-ODL 3'UTR sequences (AUUUAAAUG; UAUUUAAAU; AUUUAAAAC). A further motif analysis is needed to identify the MII-ODL mRNAs containing these 3 motifs in 3'UTR.

The destabilization of mRNAs containing 3'UTR AUUUA motifs (ARE; AU-Rich Element) is mediated by RNA binding proteins that recognize and bind to the ARE. It is interesting to note that *Hnrnpa3* mRNA, a member of the hnRNP family proteins, was more highly expressed in F1 GV oocytes than in the oocytes from parental strains (GV-ODH). The hnRNP proteins are involved in pre-mRNA processing and *Hnrnpa3*, in particular, is known to bind to the AU-rich element in the 3'-UTR region (Ma *et al.*, 2002; Rousseau *et al.*, 2002).

Table 5.14: 45 motifs that were only detected in 3'UTR sequences of MII-ODL genes.

Motif	 m 	$f(m)$	$f_H(m)$	$f_{lr}(m)$
CAUACUA	7	0.080	0	Inf
CCCAUAC	7	0.072	0	Inf
UAUUA AUG	8	0.086	0	Inf
UCUCAGUU	8	0.094	0	Inf
UACUGAAU	8	0.083	0	Inf
ACUUAAAA	8	0.123	0	Inf
GAA AUGUU	8	0.097	0	Inf
UAAACAUA	8	0.083	0	Inf
CUUGUGAU	8	0.08	0	Inf
UAAAAUCA	8	0.078	0	Inf
UGUUGAGU	8	0.075	0	Inf
CUGUUCAA	8	0.072	0	Inf
CUUAAAAU	8	0.129	0	Inf
AUAAUUG	8	0.094	0	Inf
GUAUUGUU	8	0.086	0	Inf
UUGGUUAU	8	0.078	0	Inf
GUUUAAAU	8	0.102	0	Inf
AUUCUUGU	8	0.094	0	Inf
GAAAAAAG	8	0.088	0	Inf
UUGUUUAG	8	0.088	0	Inf
ACAAAUAU	8	0.083	0	Inf
UUGUAAGA	8	0.08	0	Inf
UAUUGCUU	8	0.08	0	Inf
UACAUGUA	8	0.078	0	Inf
ACUGCAUU	8	0.078	0	Inf
UUGUUGAA	8	0.075	0	Inf
UCAAAUUG	8	0.075	0	Inf
AUAGAAUU	8	0.075	0	Inf
UAUUCAGA	8	0.072	0	Inf
AAUUUCUA	8	0.072	0	Inf
UAUUUUAG	8	0.072	0	Inf
UUUUUUCCU	9	0.131	0	Inf
AUUUAAAUG	9	0.075	0	Inf
UUGUUGUUG	9	0.094	0	Inf
AAUAUUUUA	9	0.083	0	Inf
UAUUUAAAU	9	0.08	0	Inf
AUAUUUUA	9	0.078	0	Inf
AUGUUUUUA	9	0.078	0	Inf
UUUUUCUUA	9	0.075	0	Inf
AUUUAAAAC	9	0.075	0	Inf
UUUAAAGAA	9	0.072	0	Inf
UUUUUUUCCU	10	0.078	0	Inf
UUUGUUGUUG	10	0.075	0	Inf
UUUUUUCCUU	10	0.072	0	Inf
UUUUUUUUUUUU	11	0.072	0	Inf

5.3 Dominance Effects in Gene Expression

5.3.1 Identification of Dominance Genes

Hybrid vigor effects may arise not only from overdominance but also arise due to the combination of dominant traits. Genes displaying dominance effects in expression were defined as those for which expression was similar between the F1 oocytes and one parental strain, but different compared to the other parental strain (Table 5.4; Supplemental Tables S15a,b-S18a,b). It was revealed from my array data that there were many more genes displaying a dominant B6 phenotype than a dominant D2 phenotype (1792 genes versus 368) in the GV stage, indicating that the similarity observed between B6 and F1 oocytes by hierarchical clustering analysis (Figure 5.1) was largely attributable to genes that display dominant B6-like expression values. The number of genes showing B6 dominance increased to a lesser degree from the GV to MII stage as compared to the changes occurred in the overdominance set (1.39-fold versus 14-fold increase), indicating that the genes showing dominance effects likely affect GV stage phenotype to nearly the same degree as MII stage phenotype. The change in fraction D2 dominance genes between stages was slightly larger (3-fold) than for B6 dominance, and fewer genes overall displayed D2 dominance versus B6 dominance (1,116 versus 2,488). Thus, in terms of mRNA expression levels, the B6 genotype appears to make a disproportionate contribution to the expression profile of F1 oocytes.

5.3.2 Biofunctional Analysis for Dominance Genes

Biological functions and pathways affected by dominance were identified using IPA. The lists of genes showing dominance effects were filtered by a parental-to-F1 expression ratio of 2 or greater and the maximum average array intensity values of 100

or higher. Only those biofunctional categories containing five molecules or more at Fisher's exact test p -value < 0.01 were accepted as significantly over-represented functional categories.

5.3.2.1 Biofunctional Analysis for the GV-stage Dominance Genes

Among 2,069 probe sets showing B6 dominance expression pattern at GV stage, 1,954 were filtered by the criteria mentioned above. Cell cycle regulation was identified as the most highly over-represented biofunction among the B6-dominance genes in GV stage (26 genes). Included in the cell cycle category were genes involved in cytokinesis or meiosis I such as *Cdc25b*, *Rad51c*, *Brd4*, *Kif23*, *Anln* and etc (Table 5.15; Figure 5.13). Five of the 7 genes in the next most significant biofunctional category 'cellular movement' overlap in their function in cytokinesis (*Anln*, *Brd4*, *Ivns1abp*, *Kif23* and *Kif20b*), and thus the two most significant biological functions affected by B6 dominance are related to the cell cycle. Other biological functions over-represented among B6-dominance genes in GV oocytes are lipid metabolism (9 genes), small molecule biochemistry (16 genes), cell death (21 genes), drug metabolism (7 genes) and molecular transport (10 genes). Two genes, *Stc1* and *Cyp19a1*, are members in all five of these other biofunction categories significantly over-represented in B6 dominance genes at GV stage, *Stc1* belongs to GV-FBL while *Cyp19a1* to GV-FBH. These two genes were also identified as differentially regulated in rhesus monkey IVM and VVM oocytes and cumulus cells, and were implicated as makers for oocyte quality. Small molecule biochemistry was also significantly over-represented among D2-dominance genes in GV-stage oocytes (5 genes). Cellular assembly and organization was also identified as a significant biofunctional category for D2-dominance genes at the GV stage (5 genes) (Table 5.16; Figure 5.14).

Table 5.15: Molecular and cellular functions over-represented in GV-B6-dominance genes (GV-FBL & GV-FBH) [Threshold = Fold change ≥ 2 ; Fisher's exact test p -value < 0.01 ; # Molecules ≥ 5]

Category	p-value	Genes
Cell Cycle	2.59E-04- 3.89E-02	<i>Kif23, Cul5, Itsn1, Btg3, Tpr, Cdc25b, Nek2, Fancd2, Fshr, Gfra1, Hus1, Rhou, Brd4, Rad51c, Ctnnb1, Cited2, Cdk13, Ep400, Hdac2, Anln, Ivns1abp, Arhgap32, Smarca2, Kif20b, Bcl2l11, Chn2</i>
Cellular Movement	2.59E-04- 3.31E-02	<i>Kif23, Ivns1abp, Kif20b, Gfra1, Brd4, Anln, Ctnnb1</i>
Lipid Metabolism	7.19E-04- 3.87E-02	<i>Stc1, Sepp1, Brd2, Cyp19a1, Fshr, Far1, Bmpr2, Sgms1, Prdx2</i>
Small Molecule Biochemistry	7.19E-04- 3.87E-02	<i>Brd2, Slc35a1, Slc7a11, Pbx1, Far1, Bmpr2, Slc18a2, Sgms1, Pld1, Stc1, Sepp1, Cyp19a1, Fshr, Tktl1, Ctnnb1, Prdx2</i>
Cell Death	2.46E-03- 4.82E-02	<i>Clns1a, Tnfaip8, Serpini1, Itsn1, Pbx1, Anln, Hspa5, Cct8, Pld1, Cdc25b, Ndn12, Stc1, Dnajc5, Cyp19a1, Fshr, Gfra1, Exoc2, Ctnnb1, Bcl2l11, Hspb1, Prdx2</i>
Drug Metabolism	4.09E-03- 3.87E-02	<i>Stc1, Brd2, Slc7a11, Cyp19a1, Fshr, Bmpr2, Slc18a2</i>
Molecular Transport	4.09E-03- 3.87E-02	<i>Stc1, Brd2, Slc35a1, Slc7a11, Dnajc5, Cyp19a1, Fshr, Slc18a2, Inpp5a, Pld1</i>

Figure 5.13: Molecular and Cellular Functions over-represented in GV-B6-dominance genes (GV-FBL & GV-FBH) [Threshold = Fold change ≥ 2 ; Fisher's exact test p-value < 0.01 ; #Molecules ≥ 5]

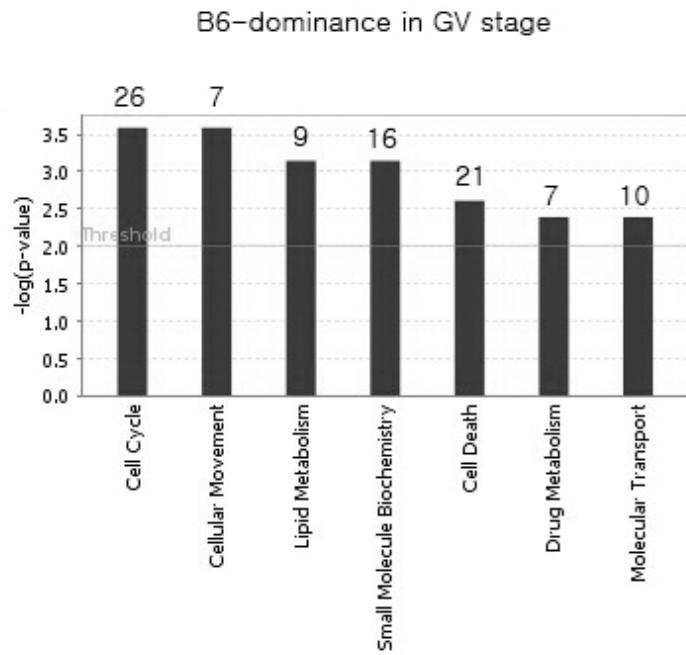
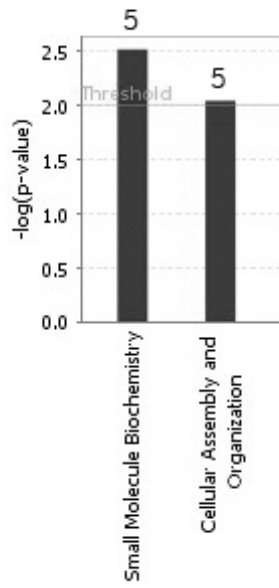


Table 5.16: Molecular and cellular functions over-represented in GV-D2-dominance genes (GV-FDL & GV-FDH) [Threshold = Fold change ≥ 2 ; Fisher's exact test p-value < 0.01 ; #Molecules ≥ 5]

Category	p-value	Genes
Small Molecule Biochemistry	2.97E-03- 4.65E-02	<i>Inpp5f, Cyth1, Cadps, Ugcg, Txnrd1</i>
Cellular Assembly and Organization	8.88E-03- 3.51E-02	<i>Krt25, Cadps, Hck, Ugcg, Myo10</i>

Figure 5.14: Molecular and Cellular Functions over-represented in GV-D2-dominance genes (GV-FDL & GV-FDH) [Threshold = Fold change ≥ 2 ; Fisher's exact test p-value < 0.01 ; # Molecules ≥ 5]

D2-dominance in GV stage



5.3.2.2 Biofunctional Analysis for the B6 Dominance Genes at the MII-stage

There was a large number of biofunction categories over-represented in the genes showing B6 dominant expression patterns in MII-stage eggs (Figure 5.15; Supplemental Table S19). This suggests that the majority of major biological functions were differentially regulated in D2 oocytes compared to B6 and F1 oocytes. The biofunction category of the highest statistical significance is 'cell morphology.' Genes in this category were further classified into eight different subcategories based on the functional annotations in the IPA database (Supplemental Table S20). The top subfunctions within the cell morphology function affected by B6 dominance genes at MII stage are 'contraction' and 'blebbing' and include genes such as *Rock1*, *Taok1* and *Cttn*.

The biological functions impacted in B6 dominance genes at the GV-stage continue to be of a significant importance in B6 dominance genes at the MII-stage. Cell cycle, cellular movement, lipid metabolism, small molecule biochemistry and cell death are among the biofunction categories over-represented in genes showing B6-dominant expression patterns in MII eggs. Biological functions such as RNA post-transcriptional modification, protein synthesis, amino acid metabolism, post-translational modification are unique to B6 dominance genes at the MII-stage. There are 26 genes shared in the three categories, 'amino acid metabolism', 'post-translational modification' and 'small molecule biochemistry.' These genes are involved in phosphorylation, moiety attachment or modification.

5.3.2.3 Biofunctional Analysis for the D2 Dominance Genes at the MII-stage

Among D2-dominance genes at the MII-stage, cellular growth and proliferation (10 genes) was the most significantly affected biological function followed by cellular development (9 genes) and lipid metabolism (9 genes) (Table 5.17, Figure 5.16).

Functional categories identified in D2 dominance genes at the GV-stage, small molecule biochemistry and cellular assembly and organization, are also significantly over-represented in the MII-stage D2 dominance genes. The 'small molecule biochemistry' function, in particular, was identified as significantly over-represented in both B6 and D2 dominance groups at both GV and MII stages. Although the biological function is shared between B6 and D2 dominance groups, the genes included in the category differ between groups.

Genes involved in embryonic development, *Bmp7* and *Pdgf1*, were identified as having D2 dominant high expression (MII-FDH) while growth suppressor genes such as *Rbl1*, *Foxp2* and *Plagl1* showed D2 dominant low expression at the MII stage (MII- FDL) (Supplemental Table S21). The array values for the paternally imprinted *Plagl1* gene were two-fold greater in B6 eggs than in F1 or D2 eggs with raw intensity values of around 3,500 in B6 eggs, and 1,500 in F1 and D2. The *Plagl1* was also differentially expressed between rhesus monkey IVM and VVM MII eggs: it was expressed 4-fold higher in rhesus monkey IVM eggs (Table 3.3).

Figure 5.15: Molecular and Cellular Functions over-represented in MII-B6-dominance genes (MII-FBL & MIIV-FBH) [Threshold = Fold change ≥ 2 ; Fisher's exact test p-value < 0.01 ; #Molecules ≥ 5]

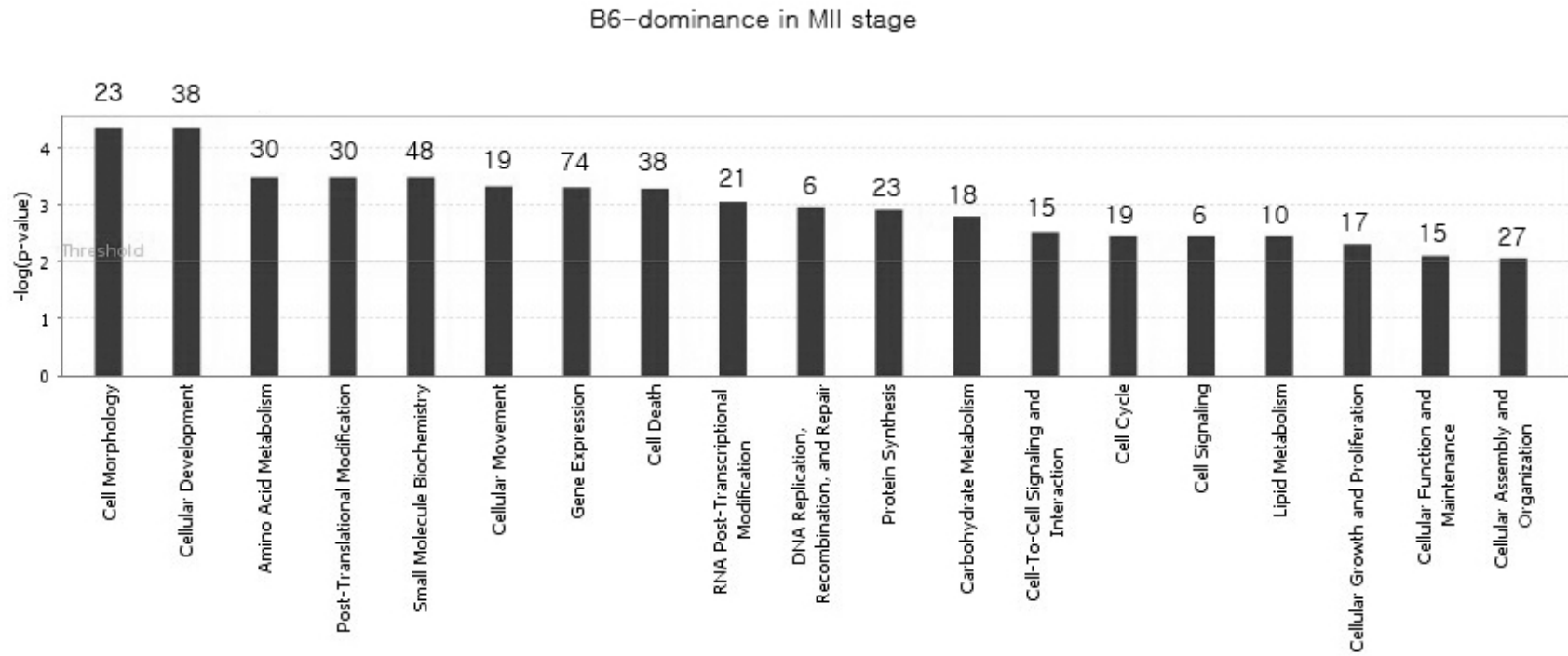
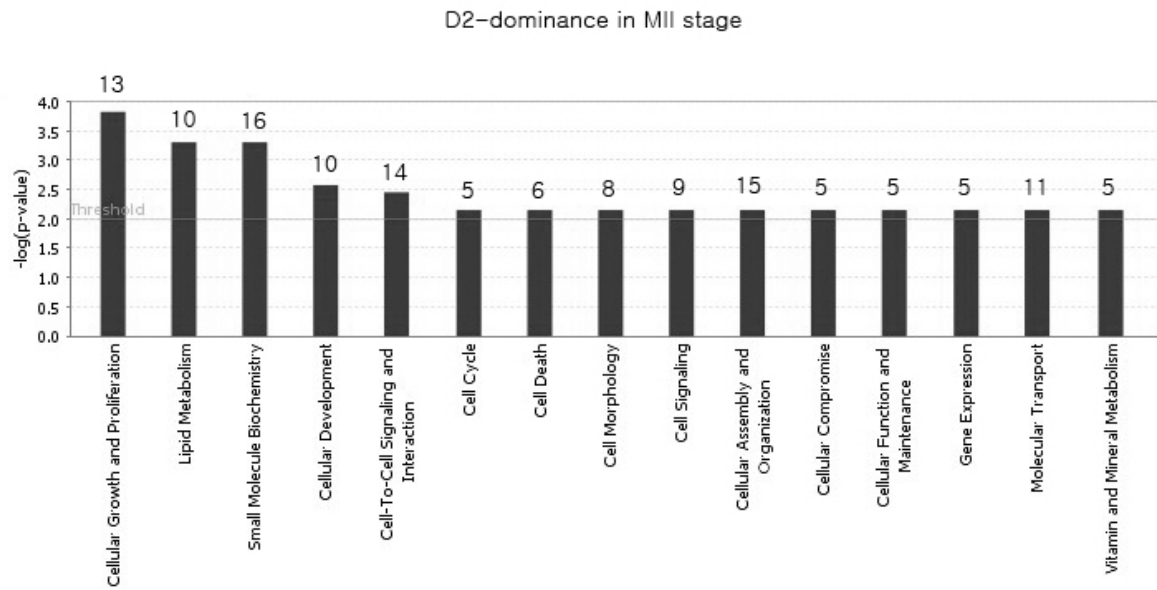


Table 5.17: Molecular and cellular functions over-represented in MII-D2-dominance genes (MII-FDL & MII-FDH) [Threshold = Fold change ≥ 2 ; Fisher's exact test p-value < 0.01 ; # Molecules ≥ 5] (Supplemental Table S20)

Category	p-value	Genes
Cellular Growth and Proliferation	1.41E-04-4.73E-02	<i>Foxp2, Plagl1, Nr2e1, Mapk1, Kif13a, Pdgfa, Bmp7, Rbl1, Ndn, Ocln</i>
Cellular Development	2.42E-03-4.73E-02	<i>Plagl1, Vwc2, Mapk1, Kif13a, Pdgfa, Bmp7, Rbl1, Ndn, Ocln</i>
Lipid Metabolism	3.49E-03-4.73E-02	<i>Myo5a, Mapk1, Pnpla3, Pitpnc1, Bmp7, Dgat1, Pip4k2a, Tek, Adrb3</i>
Small Molecule Biochemistry	3.49E-03-4.73E-02	<i>Mapk1, Pnpla3, Pkd2, Slc1a1, Ruvbl1, Ndn, Adrb3, Gsto1, Myo5a, Cyth1, Pitpnc1, Bmp7, Dgat1, Pip4k2a, Tek</i>
Cell Cycle	6.7E-03-4.73E-02	<i>Nr2e1, Plagl1, Mapk1, Bmp7, Rbl1</i>
Cell Death	6.9E-03-5E-02	<i>Plagl1, Mapk1, Bmp7, Cflar, Rbl1, Ndn</i>
Cell Morphology	6.9E-03-3.4E-02	<i>Myo5a, Plagl1, Bmp7, Rbl1, Myo10, Tek, Ocln</i>
Cell Signaling	6.9E-03-4.73E-02	<i>Myo5a, Cyth1, Pkd2, Cox10, Bmp7, Ndn, Tek, Ocln, Cox15</i>
Cellular Assembly and Organization	6.9E-03-4.73E-02	<i>Agfg1, Pdgfa, Cox10, Stk25, Pcdh15, Tgoln2, Rpl14, Adrb3, Ocln, Myo5a, Nsf, Pak7, Bmp7, Il22, Myo10</i>
Cellular Compromise	6.9E-03-3.4E-02	<i>Mapk1, Slc1a1, Pak7, Adrb3, Ocln</i>
Cellular Function and Maintenance	6.9E-03-4.07E-02	<i>M6pr, Nsf, Stk25, Cox10, Cflar</i>
Gene Expression	6.9E-03-4.73E-02	<i>Plagl1, Mapk1, Ehf, Bmp7, Rbl1</i>
Molecular Transport	6.9E-03-4.07E-02	<i>Myo5a, Mapk1, Cyth1, Pkd2, Pitpnc1, Slc1a1, Dgat1, Pip4k2a, Ndn, Gsto1, Tek</i>
Vitamin and Mineral Metabolism	6.9E-03-4.07E-02	<i>Myo5a, Pkd2, Bmp7, Ndn, Gsto1</i>

Figure 5.16: Molecular and Cellular Functions over-represented in MII-D2-dominance genes (MII-FDL & MIIV-FDH) [Threshold = Fold change ≥ 2 ; Fisher's exact test p-value < 0.01 ; # Molecules ≥ 5]



5.4 Discussion

Genetic effects on oocyte quality were explored by comparing transcriptomes of oocytes with different genetic backgrounds, namely B6 and D2 inbred strains vs. F1 hybrid. This array analysis yielded several novel findings related to the genetic basis underlying oocyte quality. The analysis results revealed that the overdominance effect in the oocyte increases during oocyte maturation. The number of mRNAs with overdominant expression pattern at the GV stage is much smaller than those at the MII stage. During the transition from GV to MII stage, overdominance genes increase by almost 15 fold, from 45 genes to 656 genes. Consistent with this finding, the analysis on transition patterns revealed that the majority of overdominance genes at MII stage showed either an intermediate expression pattern or equal expression of F1 and inbred parental strain oocytes at the GV stage. Most of the GV-stage overdominance genes were also shown to have either intermediate or equal expression pattern at the MII stage. Only five genes were overdominant at both GV and MII stages, and a small fraction of (about 10%) of overdominance genes were overdominant in one stage and dominant in the other. These changes in mRNA abundance in oocytes occur during the period of transcriptional silence and, therefore, result from either stabilization/polyadenylation or destabilization/deadenylation of maternal transcripts. These results indicate that the overdominance effects may be acquired via differential regulation of maternal mRNAs in F1 oocytes during the GV-to-MII transition.

In fully grown oocytes, stable and untranslated maternal mRNAs are stored in cytoplasm, and become recruited for translation during meiotic maturation or after fertilization (Huarte *et al.*, 1992). Other mRNAs are translated at one stage and then become deadenylated or silenced with the resumption of meiosis (Bachvarova, *et al.*, 1985; Fox & Wickens, 1990) or after fertilization. This translational control of maternal

mRNAs is thought to be largely associated with sequences in 3'UTR, such as the AAUAAA hexanucleotides or CPEs, which are involved in polyadenylation and translational activation of maternal mRNAs. It was demonstrated that the same 3'UTR region is also required for both deadenylation and silencing (Huarte, *et al.*, 1992). It was also shown that translational regulation may be mediated by an interaction between 3'UTR sequence and a RNA binding protein, independent of the length of poly(A) tails (Decker & Parker, 1995; Yu *et al.*, 2002).

An increase in the number of mRNAs showing overdominance after oocyte maturation indicates that F1 oocytes are post-transcriptionally regulating their maternal transcripts at different rates than the two parental strains. Considering the roles of 3'UTR sequences in activation and silencing of oocyte mRNAs, this difference in mRNA regulation may be due to the differential regulation of the 3'UTR CPEs by cis-acting elements and/or trans-acting factors that have different activities in F1 and parental oocytes. The 3'UTR sequence analysis of MII-ODL and MII-ODH mRNAs identified a significant enrichment of short motifs in 3'UTR region of MII-ODL mRNAs but no enrichment of motifs in MII-ODH 3'UTR sequences. This result indicates that there may be 3'UTR motif sequence(s) that direct deadenylation or degradation of mRNAs at a greater rate in F1 oocytes. Alternatively, it is also possible that these 3'UTR sequences may function in preventing F1 mRNAs from being recruited for polyadenylation. Evaluation of mRNA expression changes in MII-ODL genes from GV to MII stage revealed that the MII-ODL pattern could be acquired not only through a greater reduction of F1 mRNA but also through less efficient up-regulation of F1 mRNA than the parental strains (Table 5.7). A more detailed 3'UTR sequence analysis of MII-ODL genes is needed to uncover the mRNA regulatory mechanism that directs hybrid vigor effects in mouse oocytes. IPA biofunction analysis of major transition groups, T23 and T24, among MII stage overdominance genes also identified the 'RNA post-transcriptional

modification' as the most significantly over-represented in both T23 (MII-ODL) and T24 (MII-ODH) genes (Tables 5.12 and 5.13). This result further indicates the potential importance of mRNA regulation in establishing overdominance or hybrid vigor effects in the oocyte.

This array study also provided insight into the dominance effects in the oocyte. First, I found that there are more mRNAs with B6 dominant expression pattern than those with D2 dominant expression pattern at both GV and MII stages. This finding is consistent with the results from SAM and hierarchical clustering analysis that B6 and F1 oocyte transcriptomes were similar to each other than to the D2 oocyte transcriptome. As with the overdominance genes, the number of dominance genes also increased from GV to MII stage. B6 dominance genes increased by 1.4 fold while D2 dominance genes increased by 3 folds from GV stage to MII stage (Table 5.4). Additionally, the greater degree of similarity between B6 and F1 oocyte transcriptomes is reminiscent of phenotypic similarities in phenotype, such as cloning ability, androgenone development, parthenogenone development, and embryo culture (Gao *et al.*, 2004; Latham & Solter, 1991; Liang *et al.*, 2009)..

The SAM results showed that the number of genes differentially expressed between F1 and B6 or D2 became much larger at the MII stage (Table 5.2). On the other hand, the genes differentially expressed between the two parental strains, B6 and D2, at the MII stage remained very similar to the number of differentially expressed genes at GV stage. This indicates that the F1 transcriptome became progressively more distinct from the two parental transcriptomes. As mentioned above, this change occurs during the period of transcriptional silence, which means the up or down-regulation of mRNAs must occur by the differential mRNA regulation. Therefore, it appears that both overdominance and dominance patterns in MII stage eggs are obtained during oocyte maturation via differential regulation of mRNAs in F1 oocytes.

Both B6 and D2 dominance genes are enriched in numerous biofunctions and pathways and thus most biofunctions are shared between B6 and D2 dominance genes. However, when the dominance genes were categorized into smaller groups according to functional annotations of individual genes, 'blebbing' was identified as a biofunction most significantly enriched among B6 dominance genes. Blebbing is commonly observed during apoptosis or cytokinesis. In caspase-dependent apoptosis, ROCK1 is a key mediator of blebbing and consequent apoptosis (Sebbagh *et al.*, 2005). A more recent study, however, showed that blebbing activated by plasma membrane injury may be used as a protective mechanism to prevent cellular lysis (Babiychuk *et al.*, 2011) rather than promoting cell death. Bleb formation also occurs during cell spreading or virus infection (Erickson & Trinkaus, 1976; Mercer & Helenius, 2008). It was reported that bleb formation in mouse was only observed in eggs activated by sperm or parthenogenetically, and specifically during cell division (Szollosi & Szollosi, 1988). Nuclear blebs form during the early cleavage stages of embryo and may function as a means to transport material from nucleus to cytoplasm (Szollosi & Szollosi, 1988).

A recent study showed that blebs do form in *C. elegans* oocytes and blebbing is involved in the assembly of ribonucleoproteins (RNPs) particles. In *C. elegans* oocytes, blebbing mediates the transport of nucleoporins to the cell cortex and the recruitment of RNA and proteins into RNPs during the extended meiotic arrest or after environmental stress (Jud *et al.*, 2008; Patterson *et al.*, 2011). Although it is yet unclear whether there is an association with blebbing, RNP particles containing maternal mRNAs were recently identified in mouse oocytes. P bodies involved in maternal mRNA storage disappear during the oocyte growth, and in fully grown oocytes P-body components are relocated into subcortical ribonucleoprotein particle (RNP) domain (SCRD) that serves as a storage for maternal mRNAs and RNA processing proteins (Flemer *et al.*, 2010). A previously identified subcortical complex, SCMC, is also assembled during oocyte

growth and essential for the first cleavage cycle of the embryo. However, the function of SCMC seems to be more involved in the storage of stable maternal proteins and its function in RNA storage or metabolism has not been described (L. Li *et al.*, 2008).

Those B6 dominance genes involved in 'blebbing' showed B6-dominance low expression pattern (MII-FBL), which means the mRNA abundance of genes involved in blebbing is greater in D2 eggs than in B6 or F1 eggs (Supplemental Table S20). Therefore, my array data showed that 'blebbing' function was significantly under-represented in B6 and F1 MII stage eggs, or in another word 'blebbing' was over-represented in D2 eggs. The mRNA abundance of genes involved in blebbing, such as *Cttn*, *Rock1*, *Taok1* and *Mapk8*, were up-regulated from GV stage to MII stage more highly in D2 eggs (Supplemental Table S16a). This means that the mRNAs of blebbing genes were actively recruited for polyadenylation in D2 eggs but the recruitment of those mRNAs either did not occur or was less efficient in F1 and B6 oocytes. However, the significance or consequence of this mRNA recruitment of blebbing genes in D2 eggs is unknown at this time. According to the study discussed previously (Szollosi & Szollosi, 1988), blebbing normally occurs only during the first two cell cycles in mouse embryo and should not occur in GV or unfertilized eggs. If this is the case, the mRNAs of genes involved in blebbing must be silenced and kept in dormant forms in the oocyte until the egg becomes fertilized and undergoes the first cleavage. Even in the case where blebbing function is associated with the assembly of subcortical complexes, SCMC or SCRD, mRNA recruitment of blebbing genes were not done in a timely manner. The assembly of those subcortical complexes is achieved during oocyte growth prior before the oocyte maturation begins (Flemr, *et al.*, 2010; L. Li, *et al.*, 2008) and thus the up-regulation of the blebbing genes in MII stage is likely an abnormal regulation of the blebbing genes in D2 eggs. The abnormal recruitment of mRNAs of blebbing genes in D2 eggs indicate that D2 eggs may be compromised in mRNA regulation of blebbing

genes, which may explain the lower developmental competence of embryos originating from D2 eggs.

The transcriptome analyses of oocytes with different genetic backgrounds provided insights into how the overdominance and dominance phenotypes become established in mouse oocytes. The data from this array study revealed that the maternal mRNA regulation was the most critical mechanism that determined the direction and/or the degree of mRNA abundance changes in oocytes of different genetic backgrounds. The differential regulation of maternal mRNAs in three strains resulted in the increased number of overdominance and dominance effect genes from the GV-to-MII transition period as well as the abnormal regulation of various cellular processes. IPA analysis results showed that 'RNA post-transcriptional modification' was affected by the overdominance and the blebbing was most significantly affected by the B6 dominance. Further analysis of 3'UTR sequences of overdominance and dominance genes and identification of trans-acting proteins regulating those 3'UTR sequences may provide a better understanding of how the genetic background impacts the maternal mRNA regulation mechanisms and the developmental competence of oocyte.

CHAPTER 6

DISCUSSION

Transcriptome analyses of rhesus monkey eggs, cumulus cells and mouse oocytes of different genetic backgrounds provided insight into the potential mechanisms governing the oocyte maturation process as well as their implications in the establishment of oocyte quality. In this study, three different approaches were taken to investigate the molecular basis of oocyte quality. The first array analysis was focused on enumeration of molecular differences between rhesus monkey oocytes of different qualities. The findings from this analysis lead to an identification of genes and pathways that may be compromised in low quality oocytes. The results from this study indicated that an improvement in IVM conditions could increase the quality of oocyte and also the clinical outcomes of ART treatments. In my second array analysis, I investigated how the mRNA expression in companion cumulus cells relates to the quality of oocyte. Based on the results from the second array analysis, cumulus cell markers were designed and tested for a noninvasive assay for a clinical evaluation of oocyte quality. The third array analysis was performed to compare transcriptomes from mouse oocytes from two inbred strains and their F1 hybrid. In that array analysis, I investigated how the genetic background may affect the developmental competence of oocyte and embryo. The analysis revealed that the hybrid vigor effects in oocyte quality may be further acquired during oocyte maturation via differential mRNA regulations in F1 hybrid oocytes.

A collective inspection of results from all three array analyses showed that there were some similarities and differences among the oocyte quality determinants identified by the three arrays studies. A comparison of differentially expressed mRNAs from the three array studies revealed the mRNA abundance of 8 genes was significantly altered by the changes in oocyte quality in all three studies (Table 6.1). There were also 9

mRNAs shared between the rhesus monkey oocyte and cumulus cell arrays and 6 mRNAs shared between the rhesus monkey oocyte and mouse oocyte arrays (Table 6.2). All 23 mRNAs shared between different array studies were more highly expressed in rhesus monkey IVM eggs than VVM eggs. However, the mRNA expression regulation of 8 out of those 23 genes was not necessarily in the same direction in the other two array studies. For example, two genes involved in steroid metabolism, *CYP19A1* and *LDLR*, were both more highly expressed in rhesus monkey IVM eggs but the mRNA regulation of these two genes occurred in the opposite directions in cumulus cells during IVM and VVM. The *CYP19A1* mRNA was down-regulated only during VVM and was significantly higher in IVM-CC than VVM-CC at the end of the maturation period. The *LDLR* mRNA, on the other hand, was significantly up-regulated only in VVM-CC.

Among 17 mRNAs shared between the rhesus monkey oocyte and cumulus cells array studies (Tables 6.1 and 6.2), almost half of the mRNAs were regulated in the same pattern in rhesus monkey oocyte and cumulus cells. Eight mRNAs (*LDLR*, *PGAP1*, *SND1*, *STC1*, *MITD1*, *NPTX2*, *OSMR* and *STAR*) were more highly expressed in rhesus monkey IVM oocytes and significantly up-regulated in cumulus cell mRNA expression only during VVM, which appears to be the only apparent pattern among these genes. Moreover, there seems to be no apparent correlation of rhesus monkey cumulus cell mRNA expression patterns to the mRNA expression pattern in mouse oocytes. Although 6 out of 8 mRNAs showed a B6-dominance in mouse, the directionality and the stage of the B6 dominance were variable without any specific trend. A similar finding was observed among mRNAs shared between rhesus monkey and mouse oocytes array studies: 5 of the 6 mRNAs in the list showed B6 dominance at either GV or MII stage but with a different directionality (Table 6.2).

In summary, there was no specific pattern of mRNA expression observed among the genes commonly shared by all three array studies. There was only a pattern that

affected 8 out of 17 mRNAs analyzed, in which the mRNAs more highly expressed in rhesus monkey IVM eggs become up-regulated only in VVM-CCs. For those differentially expressed between rhesus monkey and mouse oocytes, 11 of 14 mRNAs were B6 dominance genes. However, the directionality and stage in which B6 dominance was observed for the 11 mRNAs were variable. There was no correlation observed between the mRNA expression differences in rhesus monkey cumulus cells and mouse oocytes. These results indicate that it may not be feasible to make a prediction with high confidence on the mRNA expression pattern of an individual oocyte quality factor candidate in different species and/or cell types.

To determine whether there are any specific biofunctions governing the quality of oocytes, IPA biofunction analysis results for the three array studies were compared (Tables 3.4, 4.4, 5.9–5.11 and S14). The comparison of biofunctions showed that there were several biofunctions shared by all three array studies; e.g., cell growth and maintenance, small molecule biochemistry, lipid metabolism, cellular process/maintenance. However, the comparison result revealed that individual genes affected in those shared biofunctions were different for each array study.

Different aspects of oocyte quality were investigated in each of the three studies using cDNA-based arrays. The results from the rhesus monkey oocyte and cumulus cells arrays showed that an exogenous factor such as IVM caused a much larger change in gene expression of companion cumulus cells than in the oocyte. In IVM-CC, remarkable compensatory changes in gene expression were observed, especially in lipid/steroid metabolism, steroid biogenesis and cell-cell interactions. IVM oocytes were also affected the changes in mRNA abundance of the genes involved in cell-cell interactions and steroid metabolism. A disrupted dialog between the oocyte and surrounding cumulus cells seems to be responsible for the gene expression changes in both the oocyte and cumulus cells.

Genetic factors, on the other hand, caused a wide range of changes in the oocyte transcriptome. The array results indicated that there may be a genetic factor that drives the differential regulation of maternal mRNAs. The fact that all three strains of mice are capable of producing viable offspring, along with the observation of large changes in oocyte transcriptome, suggests that those differences may reflect compensatory changes to balance the genetic differences governing the oogenesis. Further investigations on oocyte quality determinants in various species and conditions may provide a better understanding of how various cellular mechanisms work together to maintain the balance necessary for the development.

Table 6.1: Genes that showed significant differential expression in all three array studies.

Gene symbol	Gene name	Rhesus monkey MII oocytes	Rhesus monkey cumulus cells	Mouse oocytes
<i>CYP19A1</i>	cytochrome P450, family 19, subfamily a, polypeptide 1	higher in IVM-MII	Higher in IVM-CC & VVM-DOWN	GV-FBH
<i>LDLR</i>	low density lipoprotein receptor	higher in IVM-MII	VVM-UP	MII-FBL
<i>PGAP1</i>	post-GPI attachment to proteins 1 (GPI deacylase)	higher in IVM-MII	VVM-UP	GV-FDH
<i>PLAGL1</i>	pleiomorphic adenoma gene-like 1	higher in IVM-MII	IVM-UP	MII-FDL
<i>RPS6KA5</i>	ribosomal protein S6 kinase, polypeptide 5	higher in IVM-MII	VVM-DOWM	MII-FBL
<i>SLC6A6</i>	solute carrier family 6 (neurotransmitter transporter, taurine), member 6	higher in IVM-MII	IVM-UP and VVM-UP	GV-FBH
<i>SND1</i>	staphylococcal nuclease and tudor domain containing 1	higher in IVM-MII	VVM-UP	MII-FBH
<i>STC1</i>	stanniocalcin 1	higher in IVM-MII	VVM-UP	GV-FBL

Table 6.2: Genes that showed significant differential expression in two of the three array studies.

Gene symbol	Gene name	Rhesus monkey MII oocytes	Rhesus monkey cumulus cells	Mouse oocytes
<i>EFNA1</i>	ephrin A1	higher in IVM-MII	IVM-UP and VVM-UP	--
<i>HSD11B2</i>	hydroxysteroid (11-beta) dehydrogenase 2	higher in IVM-MII	Higher in IVM-CC & VVM-DOWN	--
<i>KCNK3</i>	Potassium channel, subfamily K, member 3	higher in IVM-MII	Higher in IVM-CC & IVM-UP	--
<i>MITD1</i>	MIT, microtubule interacting and transport, domain containing 1	higher in IVM-MII	VVM-UP	--
<i>NPTX2</i>	neuronal pentraxin II	higher in IVM-MII	VVM-UP	--
<i>OSMR</i>	oncostatin M receptor	higher in IVM-MII	VVM-UP	--
<i>RPL13</i>	ribosomal protein L13	higher in IVM-MII	VVM-DOWN	--
<i>STAR</i>	steroidogenic acute regulatory protein	higher in IVM-MII	VVM-UP	--
<i>USP54</i>	ubiquitin specific peptidase 54	higher in IVM-MII	IVM-DOWN and VVM-DOWN	--
<i>CUGBP2</i>	CUG triplet repeat, RNA binding protein 2	higher in IVM-MII	--	MII-FBL
<i>IL6ST</i>	Interleukin 6 signal transducer (gp130, oncostatin M receptor)	higher in IVM-MII	--	MII-ODL
<i>MDM4</i>	Mdm4, transformed 3T3 cell double minute 4, p53 binding protein homolog (mouse)	higher in IVM-MII	--	MII-FBL
<i>NBEAL1</i>	neurobeachin like 1	higher in IVM-MII	--	MII-FBL
<i>SLC12A5</i>	solute carrier family 12, (potassium-chloride transporter) member 5	higher in IVM-MII	--	GV-FBH
<i>TDRD1</i>	tudor domain containing 1	higher in IVM-MII	--	GV-FBH

REFERENCES CITED

- Adriaenssens, T., Segers, I., Wathlet, S., & Smitz, J. (2011). The cumulus cell gene expression profile of oocytes with different nuclear maturity and potential for blastocyst formation. *J Assist Reprod Genet*, 28(1), 31-40.
- Affymetrix. (2002). Data Analysis Fundamentals. Retrieved from http://media.affymetrix.com/support/downloads/manuals/data_analysis_fundamentals_manual.pdf
- Affymetrix. (2005). Guide to Probe Logarithmic Intensity Error (PLIER) Estimation. Retrieved from http://media.affymetrix.com/support/technical/technotes/plier_technote.pdf
- Affymetrix. (2006). Affymetrix Expression Console Software Version 1.0 - User Guide. Retrieved from http://media.affymetrix.com/support/downloads/manuals/expression_console_userguide.pdf
- AgilentTechnologies. (2008). GeneSpring GX Manual. Retrieved from <http://www.chem.agilent.com/Library/usermanuals/Public/GeneSpring-manual.pdf>
- Albertini, D. F., & Anderson, E. (1974). The appearance and structure of intercellular connections during the ontogeny of the rabbit ovarian follicle with particular reference to gap junctions. *J Cell Biol*, 63(1), 234-250.
- Albertini, D. F., Combelles, C. M., Benecchi, E., & Carabatsos, M. J. (2001). Cellular basis for paracrine regulation of ovarian follicle development. *Reproduction*, 121(5), 647-653.
- Amleh, A., & Dean, J. (2002). Mouse genetics provides insight into folliculogenesis, fertilization and early embryonic development. *Hum Reprod Update*, 8(5), 395-403.
- Anderson, R. A., Sciorio, R., Kinnell, H., Bayne, R. A., Thong, K. J., de Sousa, P. A., et al. (2009). Cumulus gene expression as a predictor of human oocyte fertilisation, embryo development and competence to establish a pregnancy. *Reproduction*, 138(4), 629-637.
- Andric, N., Thomas, M., & Ascoli, M. (2010). Transactivation of the epidermal growth factor receptor is involved in the lutropin receptor-mediated down-regulation of ovarian aromatase expression in vivo. *Mol Endocrinol*, 24(3), 552-560.
- Assidi, M., Dieleman, S. J., & Sirard, M. A. (2010). Cumulus cell gene expression following the LH surge in bovine preovulatory follicles: potential early markers of oocyte competence. *Reproduction*, 140(6), 835-852.

- Assidi, M., Montag, M., Van Der Ven, K., & Sirard, M. A. (2011). Biomarkers of human oocyte developmental competence expressed in cumulus cells before ICSI: a preliminary study. *J Assist Reprod Genet*, 28(2), 173-188.
- Assou, S., Haouzi, D., De Vos, J., & Hamamah, S. (2010). Human cumulus cells as biomarkers for embryo and pregnancy outcomes. *Mol Hum Reprod*, 16(8), 531-538.
- Assou, S., Haouzi, D., Mahmoud, K., Aouacheria, A., Guillemin, Y., Pantesco, V., et al. (2008). A non-invasive test for assessing embryo potential by gene expression profiles of human cumulus cells: a proof of concept study. *Mol Hum Reprod*, 14(12), 711-719.
- Ata, B., Shalom-Paz, E., Chian, R. C., & Tan, S. L. (2010). In vitro maturation of oocytes as a strategy for fertility preservation. *Clin Obstet Gynecol*, 53(4), 775-786.
- Babiychuk, E. B., Monastyrskaya, K., Potez, S., & Draeger, A. (2011). Blebbing confers resistance against cell lysis. *Cell Death Differ*, 18(1), 80-89.
- Bachvarova, R., & De Leon, V. (1980). Polyadenylated RNA of mouse ova and loss of maternal RNA in early development. *Dev Biol*, 74(1), 1-8.
- Bachvarova, R., De Leon, V., Johnson, A., Kaplan, G., & Paynton, B. V. (1985). Changes in total RNA, polyadenylated RNA, and actin mRNA during meiotic maturation of mouse oocytes. *Dev Biol*, 108(2), 325-331.
- Bao, S., Obata, Y., Carroll, J., Domeki, I., & Kono, T. (2000). Epigenetic modifications necessary for normal development are established during oocyte growth in mice. *Biol Reprod*, 62(3), 616-621.
- Barnard, D. C., Cao, Q., & Richter, J. D. (2005). Differential phosphorylation controls Maskin association with eukaryotic translation initiation factor 4E and localization on the mitotic apparatus. *Mol Cell Biol*, 25(17), 7605-7615.
- Bavister, B. D., Boatman, D. E., Collins, K., Dierschke, D. J., & Eisele, S. G. (1984). Birth of rhesus monkey infant after in vitro fertilization and nonsurgical embryo transfer. *Proc Natl Acad Sci U S A*, 81(7), 2218-2222.
- Bettegowda, A., & Smith, G. W. (2007). Mechanisms of maternal mRNA regulation: implications for mammalian early embryonic development. *Front Biosci*, 12, 3713-3726.
- Bieche, I., Narjoz, C., Asselah, T., Vacher, S., Marcellin, P., Lidereau, R., et al. (2007). Reverse transcriptase-PCR quantification of mRNA levels from cytochrome (CYP)1, CYP2 and CYP3 families in 22 different human tissues. *Pharmacogenet Genomics*, 17(9), 731-742.
- Boatman, D. E., & Bavister, B. D. (1984). Stimulation of rhesus monkey sperm capacitation by cyclic nucleotide mediators. *J Reprod Fertil*, 71(2), 357-366.

- Bolstad, B. M., Irizarry, R. A., Astrand, M., & Speed, T. P. (2003). A comparison of normalization methods for high density oligonucleotide array data based on variance and bias. *Bioinformatics*, 19(2), 185-193.
- Borghol, N., Lornage, J., Blachere, T., Sophie Garret, A., & Lefevre, A. (2006). Epigenetic status of the H19 locus in human oocytes following in vitro maturation. *Genomics*, 87(3), 417-426.
- Brady, G., & Iscove, N. N. (1993). Construction of cDNA libraries from single cells. *Methods Enzymol*, 225, 611-623.
- Brevini, T. A., Cillo, F., Antonini, S., & Gandolfi, F. (2007). Cytoplasmic remodelling and the acquisition of developmental competence in pig oocytes. *Anim Reprod Sci*, 98(1-2), 23-38.
- Brown, M. S., & Goldstein, J. L. (1979). Receptor-mediated endocytosis: insights from the lipoprotein receptor system. *Proc Natl Acad Sci U S A*, 76(7), 3330-3337.
- Brown, M. S., & Goldstein, J. L. (1986). A receptor-mediated pathway for cholesterol homeostasis. *Science*, 232(4746), 34-47.
- Burton, P. J., Krozowski, Z. S., & Waddell, B. J. (1998). Immunolocalization of 11beta-hydroxysteroid dehydrogenase types 1 and 2 in rat uterus: variation across the estrous cycle and regulation by estrogen and progesterone. *Endocrinology*, 139(1), 376-382.
- Cai, C., Tamai, K., & Molyneaux, K. (2010). KHDC1B is a novel CPEB binding partner specifically expressed in mouse oocytes and early embryos. *Mol Biol Cell*, 21(18), 3137-3148.
- Cai, Z., Kwintkiewicz, J., Young, M. E., & Stocco, C. (2007). Prostaglandin E2 increases cyp19 expression in rat granulosa cells: implication of GATA-4. *Mol Cell Endocrinol*, 263(1-2), 181-189.
- Caixeta, E. S., Ripamonte, P., Franco, M. M., Junior, J. B., & Dode, M. A. (2009). Effect of follicle size on mRNA expression in cumulus cells and oocytes of *Bos indicus*: an approach to identify marker genes for developmental competence. *Reprod Fertil Dev*, 21(5), 655-664.
- Cao, Q., & Richter, J. D. (2002). Dissolution of the maskin-eIF4E complex by cytoplasmic polyadenylation and poly(A)-binding protein controls cyclin B1 mRNA translation and oocyte maturation. *EMBO J*, 21(14), 3852-3862.
- Carabatsos, M. J., Sellitto, C., Goodenough, D. A., & Albertini, D. F. (2000). Oocyte-granulosa cell heterologous gap junctions are required for the coordination of nuclear and cytoplasmic meiotic competence. *Dev Biol*, 226(2), 167-179.
- Cha, K. Y., Koo, J. J., Ko, J. J., Choi, D. H., Han, S. Y., & Yoon, T. K. (1991). Pregnancy after in vitro fertilization of human follicular oocytes collected from nonstimulated cycles, their culture in vitro and their transfer in a donor oocyte program. *Fertil Steril*, 55(1), 109-113.

- Chesnel, F., Wigglesworth, K., & Eppig, J. J. (1994). Acquisition of meiotic competence by denuded mouse oocytes: participation of somatic-cell product(s) and cAMP. *Dev Biol*, 161(1), 285-295.
- Chian, R. C., Gilbert, L., Huang, J. Y., Demirtas, E., Holzer, H., Benjamin, A., et al. (2009). Live birth after vitrification of in vitro matured human oocytes. *Fertil Steril*, 91(2), 372-376.
- Chuma, S., Hosokawa, M., Kitamura, K., Kasai, S., Fujioka, M., Hiyoshi, M., et al. (2006). Tdrd1/Mtr-1, a tudor-related gene, is essential for male germ-cell differentiation and nuage/germinal granule formation in mice. *Proc Natl Acad Sci U S A*, 103(43), 15894-15899.
- Clegg, K. B., & Piko, L. (1983). Quantitative aspects of RNA synthesis and polyadenylation in 1-cell and 2-cell mouse embryos. *J Embryol Exp Morphol*, 74, 169-182.
- Conti, M., Andersen, C. B., Richard, F., Mehats, C., Chun, S. Y., Horner, K., et al. (2002). Role of cyclic nucleotide signaling in oocyte maturation. *Mol Cell Endocrinol*, 187(1-2), 153-159.
- Coskun, S., Uzumcu, M., Lin, Y. C., Friedman, C. I., & Alak, B. M. (1995). Regulation of cumulus cell steroidogenesis by the porcine oocyte and preliminary characterization of oocyte-produced factor(s). *Biol Reprod*, 53(3), 670-675.
- Cox, G. F., Burger, J., Lip, V., Mau, U. A., Sperling, K., Wu, B. L., et al. (2002). Intracytoplasmic sperm injection may increase the risk of imprinting defects. *Am J Hum Genet*, 71(1), 162-164.
- Cui, X., & Loraine, A. (2006). Global correlation analysis between redundant probe sets using a large collection of Arabidopsis ath1 expression profiling data. *Comput Syst Bioinformatics Conf*, 223-226.
- D'Souza, S. W., Rivlin, E., Cadman, J., Richards, B., Buck, P., & Lieberman, B. A. (1997). Children conceived by in vitro fertilisation after fresh embryo transfer. *Arch Dis Child Fetal Neonatal Ed*, 76(2), F70-74.
- De La Fuente, R. (2006). Chromatin modifications in the germinal vesicle (GV) of mammalian oocytes. *Dev Biol*, 292(1), 1-12.
- De La Fuente, R., & Eppig, J. J. (2001). Transcriptional activity of the mouse oocyte genome: companion granulosa cells modulate transcription and chromatin remodeling. *Dev Biol*, 229(1), 224-236.
- De Leon, V., Johnson, A., & Bachvarova, R. (1983). Half-lives and relative amounts of stored and polysomal ribosomes and poly(A) + RNA in mouse oocytes. *Dev Biol*, 98(2), 400-408.
- de Moor, C. H., Meijer, H., & Lissenden, S. (2005). Mechanisms of translational control by the 3' UTR in development and differentiation. *Semin Cell Dev Biol*, 16(1), 49-58.

- de Moor, C. H., & Richter, J. D. (1999). Cytoplasmic polyadenylation elements mediate masking and unmasking of cyclin B1 mRNA. *EMBO J*, 18(8), 2294-2303.
- de Vantery, C., Stutz, A., Vassalli, J. D., & Schorderet-Slatkine, S. (1997). Acquisition of meiotic competence in growing mouse oocytes is controlled at both translational and posttranslational levels. *Dev Biol*, 187(1), 43-54.
- DeBaun, M. R., Niemitz, E. L., & Feinberg, A. P. (2003). Association of in vitro fertilization with Beckwith-Wiedemann syndrome and epigenetic alterations of LIT1 and H19. *Am J Hum Genet*, 72(1), 156-160.
- Decker, C. J., & Parker, R. (1995). Diversity of cytoplasmic functions for the 3' untranslated region of eukaryotic transcripts. *Curr Opin Cell Biol*, 7(3), 386-392.
- DeRenzo, C., & Seydoux, G. (2004). A clean start: degradation of maternal proteins at the oocyte-to-embryo transition. *Trends Cell Biol*, 14(8), 420-426.
- Donahue, R. P., & Stern, S. (1968). Follicular cell support of oocyte maturation: production of pyruvate in vitro. *J Reprod Fertil*, 17(2), 395-398.
- Ducibella, T., Anderson, E., Albertini, D. F., Aalberg, J., & Rangarajan, S. (1988). Quantitative studies of changes in cortical granule number and distribution in the mouse oocyte during meiotic maturation. *Dev Biol*, 130(1), 184-197.
- Dunphy, W. G., & Newport, J. W. (1989). Fission yeast p13 blocks mitotic activation and tyrosine dephosphorylation of the *Xenopus* cdc2 protein kinase. *Cell*, 58(1), 181-191.
- Edgar, R., Domrachev, M., & Lash, A. E. (2002). Gene Expression Omnibus: NCBI gene expression and hybridization array data repository. *Nucleic Acids Res*, 30(1), 207-210.
- Elvin, J. A., Clark, A. T., Wang, P., Wolfman, N. M., & Matzuk, M. M. (1999). Paracrine actions of growth differentiation factor-9 in the mammalian ovary. *Mol Endocrinol*, 13(6), 1035-1048.
- Elvin, J. A., Yan, C., & Matzuk, M. M. (2000). Oocyte-expressed TGF-beta superfamily members in female fertility. *Mol Cell Endocrinol*, 159(1-2), 1-5.
- Eppig, J. J. (1996). Coordination of nuclear and cytoplasmic oocyte maturation in eutherian mammals. *Reprod Fertil Dev*, 8(4), 485-489.
- Eppig, J. J., & O'Brien, M. J. (1996). Development in vitro of mouse oocytes from primordial follicles. *Biol Reprod*, 54(1), 197-207.
- Eppig, J. J., Schultz, R. M., O'Brien, M., & Chesnel, F. (1994). Relationship between the developmental programs controlling nuclear and cytoplasmic maturation of mouse oocytes. *Dev Biol*, 164(1), 1-9.

- Eppig, J. J., Wigglesworth, K., & Pendola, F. L. (2002). The mammalian oocyte orchestrates the rate of ovarian follicular development. *Proc Natl Acad Sci U S A*, 99(5), 2890-2894.
- Erickson, C. A., & Trinkaus, J. P. (1976). Microvilli and blebs as sources of reserve surface membrane during cell spreading. *Exp Cell Res*, 99(2), 375-384.
- Ernst, H., Zanin, M. K., Everman, D., & Hoffman, S. (1995). Receptor-mediated adhesive and anti-adhesive functions of chondroitin sulfate proteoglycan preparations from embryonic chicken brain. *J Cell Sci*, 108 (Pt 12), 3807-3816.
- Flemr, M., Ma, J., Schultz, R. M., & Svoboda, P. (2010). P-body loss is concomitant with formation of a messenger RNA storage domain in mouse oocytes. *Biol Reprod*, 82(5), 1008-1017.
- Fortier, A. L., Lopes, F. L., Darricarrere, N., Martel, J., & Trasler, J. M. (2008). Superovulation alters the expression of imprinted genes in the midgestation mouse placenta. *Hum Mol Genet*, 17(11), 1653-1665.
- Fox, C. A., Sheets, M. D., Wahle, E., & Wickens, M. (1992). Polyadenylation of maternal mRNA during oocyte maturation: poly(A) addition in vitro requires a regulated RNA binding activity and a poly(A) polymerase. *EMBO J*, 11(13), 5021-5032.
- Fox, C. A., & Wickens, M. (1990). Poly(A) removal during oocyte maturation: a default reaction selectively prevented by specific sequences in the 3' UTR of certain maternal mRNAs. *Genes Dev*, 4(12B), 2287-2298.
- Gao, S., Czirr, E., Chung, Y. G., Han, Z., & Latham, K. E. (2004). Genetic variation in oocyte phenotype revealed through parthenogenesis and cloning: correlation with differences in pronuclear epigenetic modification. *Biol Reprod*, 70(4), 1162-1170.
- Garrido, N., Navarro, J., Remohi, J., Simon, C., & Pellicer, A. (2000). Follicular hormonal environment and embryo quality in women with endometriosis. *Hum Reprod Update*, 6(1), 67-74.
- Garrido, N., Pellicer, A., Remohi, J., & Simon, C. (2003). Uterine and ovarian function in endometriosis. *Semin Reprod Med*, 21(2), 183-192.
- Gautier, J., Norbury, C., Lohka, M., Nurse, P., & Maller, J. (1988). Purified maturation-promoting factor contains the product of a *Xenopus* homolog of the fission yeast cell cycle control gene *cdc2+*. *Cell*, 54(3), 433-439.
- Gebauer, F., Xu, W., Cooper, G. M., & Richter, J. D. (1994). Translational control by cytoplasmic polyadenylation of *c-mos* mRNA is necessary for oocyte maturation in the mouse. *EMBO J*, 13(23), 5712-5720.
- Gicquel, C., Gaston, V., Mandelbaum, J., Siffroi, J. P., Flahault, A., & Le Bouc, Y. (2003). In vitro fertilization may increase the risk of Beckwith-Wiedemann syndrome related to the abnormal imprinting of the *KCN10T* gene. *Am J Hum Genet*, 72(5), 1338-1341.

- Gilchrist, R. B., Lane, M., & Thompson, J. G. (2008). Oocyte-secreted factors: regulators of cumulus cell function and oocyte quality. *Hum Reprod Update*, 14(2), 159-177.
- Gilchrist, R. B., Morrissey, M. P., Ritter, L. J., & Armstrong, D. T. (2003). Comparison of oocyte factors and transforming growth factor-beta in the regulation of DNA synthesis in bovine granulosa cells. *Mol Cell Endocrinol*, 201(1-2), 87-95.
- Gosden, R., & Lee, B. (2010). Portrait of an oocyte: our obscure origin. *J Clin Invest*, 120(4), 973-983.
- Gougeon, A. (1996). Regulation of ovarian follicular development in primates: facts and hypotheses. *Endocr Rev*, 17(2), 121-155.
- Grant, B., & Hirsh, D. (1999). Receptor-mediated endocytosis in the *Caenorhabditis elegans* oocyte. *Mol Biol Cell*, 10(12), 4311-4326.
- Grice, D. E., Reenila, I., Mannisto, P. T., Brooks, A. I., Smith, G. G., Golden, G. T., et al. (2007). Transcriptional profiling of C57 and DBA strains of mice in the absence and presence of morphine. *BMC Genomics*, 8, 76.
- Grondahl, C. (2008). Oocyte maturation. Basic and clinical aspects of in vitro maturation (IVM) with special emphasis of the role of FF-MAS. *Dan Med Bull*, 55(1), 1-16.
- Grondahl, M. L., Borup, R., Lee, Y. B., Myrholm, V., Meinertz, H., & Sorensen, S. (2008). Differences in gene expression of granulosa cells from women undergoing controlled ovarian hyperstimulation with either recombinant follicle-stimulating hormone or highly purified human menopausal gonadotropin. *Fertil Steril*.
- Groves, T. C., Wagner, G. F., & DiMattia, G. E. (2001). cAMP signaling can antagonize potent glucocorticoid post-transcriptional inhibition of stanniocalcin gene expression. *J Endocrinol*, 171(3), 499-516.
- Hansen, M., Kurinczuk, J. J., Bower, C., & Webb, S. (2002). The risk of major birth defects after intracytoplasmic sperm injection and in vitro fertilization. *N Engl J Med*, 346(10), 725-730.
- Hasegawa, J., Yanaihara, A., Iwasaki, S., Otsuka, Y., Negishi, M., Akahane, T., et al. (2005). Reduction of progesterone receptor expression in human cumulus cells at the time of oocyte collection during IVF is associated with good embryo quality. *Hum Reprod*, 20(8), 2194-2200.
- Hattori, M., Takesue, K., Nishida, N., Kato, Y., & Fujihara, N. (2000). Inhibitory effect of retinoic acid on the development of immature porcine granulosa cells to mature cells. *J Mol Endocrinol*, 25(1), 53-61.
- Hennessy, S. W., Frazier, B. A., Kim, D. D., Deckwerth, T. L., Baumgartel, D. M., Rotwein, P., et al. (1989). Complete thrombospondin mRNA sequence includes potential regulatory sites in the 3' untranslated region. *J Cell Biol*, 108(2), 729-736.

- Herman, B., & Albertini, D. F. (1982). The intracellular movement of endocytic vesicles in cultured granulosa cells. *Cell Motil*, 2(6), 583-597.
- Ho Sui, S. J., Mortimer, J. R., Arenillas, D. J., Brumm, J., Walsh, C. J., Kennedy, B. P., et al. (2005). oPOSSUM: identification of over-represented transcription factor binding sites in co-expressed genes. *Nucleic Acids Res*, 33(10), 3154-3164.
- Hodgman, R., Tay, J., Mendez, R., & Richter, J. D. (2001). CPEB phosphorylation and cytoplasmic polyadenylation are catalyzed by the kinase IAK1/Eg2 in maturing mouse oocytes. *Development*, 128(14), 2815-2822.
- Hogan, B. (1994). *Manipulating the mouse embryo : a laboratory manual* (2nd ed.). Plainview, N.Y.: Cold Spring Harbor Laboratory Press.
- Horner, K., Livera, G., Hinckley, M., Trinh, K., Storm, D., & Conti, M. (2003). Rodent oocytes express an active adenylyl cyclase required for meiotic arrest. *Dev Biol*, 258(2), 385-396.
- Horseley, K. (2006). Three million IVF babies born worldwide. *Bionews*. Retrieved from <http://www.bionews.org.uk/new.lasso?storyid=3086>
- Hosack, D. A., Dennis, G., Jr., Sherman, B. T., Lane, H. C., & Lempicki, R. A. (2003). Identifying biological themes within lists of genes with EASE. *Genome Biol*, 4(10), R70.
- Huang, F. J., Huang, H. W., Lan, K. C., Kung, F. T., Lin, Y. C., Chang, H. W., et al. (2002). The maturity of human cumulus-free oocytes is positively related to blastocyst development and viability. *J Assist Reprod Genet*, 19(12), 555-560.
- Huarte, J., Belin, D., Vassalli, A., Strickland, S., & Vassalli, J. D. (1987). Meiotic maturation of mouse oocytes triggers the translation and polyadenylation of dormant tissue-type plasminogen activator mRNA. *Genes Dev*, 1(10), 1201-1211.
- Huarte, J., Stutz, A., O'Connell, M. L., Gubler, P., Belin, D., Darrow, A. L., et al. (1992). Transient translational silencing by reversible mRNA deadenylation. *Cell*, 69(6), 1021-1030.
- Imamura, T., Kerjean, A., Heams, T., Kupiec, J. J., Thenevin, C., & Paldi, A. (2005). Dynamic CpG and non-CpG methylation of the Peg1/Mest gene in the mouse oocyte and preimplantation embryo. *J Biol Chem*, 280(20), 20171-20175.
- Irizarry, R. A., Bolstad, B. M., Collin, F., Cope, L. M., Hobbs, B., & Speed, T. P. (2003). Summaries of Affymetrix GeneChip probe level data. *Nucleic Acids Res*, 31(4), e15.
- Iscove, N. N., Barbara, M., Gu, M., Gibson, M., Modi, C., & Winegarden, N. (2002). Representation is faithfully preserved in global cDNA amplified exponentially from sub-picogram quantities of mRNA. *Nat Biotechnol*, 20(9), 940-943.

- Johnson, J. E., Higdon Iii, H. L., & Boone, W. R. (2007). Effect of human granulosa cell co-culture using standard culture media on the maturation and fertilization potential of immature human oocytes. *Fertil Steril*.
- Joyce, I. M., Pendola, F. L., O'Brien, M., & Eppig, J. J. (2001). Regulation of prostaglandin-endoperoxide synthase 2 messenger ribonucleic acid expression in mouse granulosa cells during ovulation. *Endocrinology*, *142*(7), 3187-3197.
- Jud, M. C., Czerwinski, M. J., Wood, M. P., Young, R. A., Gallo, C. M., Bickel, J. S., et al. (2008). Large P body-like RNPs form in *C. elegans* oocytes in response to arrested ovulation, heat shock, osmotic stress, and anoxia and are regulated by the major sperm protein pathway. *Dev Biol*, *318*(1), 38-51.
- Juneja, S. C., Barr, K. J., Enders, G. C., & Kidder, G. M. (1999). Defects in the germ line and gonads of mice lacking connexin43. *Biol Reprod*, *60*(5), 1263-1270.
- Jurema, M. W., & Nogueira, D. (2006). In vitro maturation of human oocytes for assisted reproduction. *Fertil Steril*, *86*(5), 1277-1291.
- Kalinowski, R. R., Berlot, C. H., Jones, T. L., Ross, L. F., Jaffe, L. A., & Mehlmann, L. M. (2004). Maintenance of meiotic prophase arrest in vertebrate oocytes by a Gs protein-mediated pathway. *Dev Biol*, *267*(1), 1-13.
- Khosla, S., Dean, W., Reik, W., & Feil, R. (2001). Culture of preimplantation embryos and its long-term effects on gene expression and phenotype. *Hum Reprod Update*, *7*(4), 419-427.
- Knowles, B. B., Evsikov, A. V., de Vries, W. N., Peaston, A. E., & Solter, D. (2003). Molecular control of the oocyte to embryo transition. *Philos Trans R Soc Lond B Biol Sci*, *358*(1436), 1381-1387.
- Koudstaal, J., Braat, D. D., Bruinse, H. W., Naaktgeboren, N., Vermeiden, J. P., & Visser, G. H. (2000). Obstetric outcome of singleton pregnancies after IVF: a matched control study in four Dutch university hospitals. *Hum Reprod*, *15*(8), 1819-1825.
- Kozak, M. (2008). Faulty old ideas about translational regulation paved the way for current confusion about how microRNAs function. *Gene*, *423*(2), 108-115.
- Krey, L. C., & Grifo, J. A. (2001). Poor embryo quality: The answer lies (mostly) in the egg. *Fertil Steril*, *75*(3), 466-468.
- Latham, K. E. (1999). Mechanisms and control of embryonic genome activation in mammalian embryos. *Int Rev Cytol*, *193*, 71-124.
- Latham, K. E., & Schultz, R. M. (2001). Embryonic genome activation. *Front Biosci*, *6*, D748-759.
- Latham, K. E., & Solter, D. (1991). Effect of egg composition on the developmental capacity of androgenetic mouse embryos. *Development*, *113*(2), 561-568.

- Lee, A. J., Cai, M. X., Thomas, P. E., Conney, A. H., & Zhu, B. T. (2003). Characterization of the oxidative metabolites of 17beta-estradiol and estrone formed by 15 selectively expressed human cytochrome p450 isoforms. *Endocrinology*, *144*(8), 3382-3398.
- Lee, Y. S., Latham, K. E., & Vandervoort, C. A. (2008). Effects of in vitro maturation on gene expression in rhesus monkey oocytes. *Physiol Genomics*, *35*(2), 145-158.
- Leese, H. J., & Barton, A. M. (1985). Production of pyruvate by isolated mouse cumulus cells. *J Exp Zool*, *234*(2), 231-236.
- Levesque, J. T., & Sirard, M. A. (1995). Effects of different kinases and phosphatases on nuclear and cytoplasmic maturation of bovine oocytes. *Mol Reprod Dev*, *42*(1), 114-121.
- Levey, I. L., Stull, G. B., & Brinster, R. L. (1978). Poly(A) and synthesis of polyadenylated RNA in the preimplantation mouse embryo. *Dev Biol*, *64*(1), 140-148.
- Li, L., Baibakov, B., & Dean, J. (2008). A subcortical maternal complex essential for preimplantation mouse embryogenesis. *Dev Cell*, *15*(3), 416-425.
- Li, T., Vu, T. H., Ulaner, G. A., Littman, E., Ling, J. Q., Chen, H. L., et al. (2005). IVF results in de novo DNA methylation and histone methylation at an Igf2-H19 imprinting epigenetic switch. *Mol Hum Reprod*, *11*(9), 631-640.
- Li, X., Nokkala, E., Yan, W., Streng, T., Saarinen, N., Warri, A., et al. (2001). Altered structure and function of reproductive organs in transgenic male mice overexpressing human aromatase. *Endocrinology*, *142*(6), 2435-2442.
- Li, X., Warri, A., Makela, S., Ahonen, T., Streng, T., Santti, R., et al. (2002). Mammary gland development in transgenic male mice expressing human P450 aromatase. *Endocrinology*, *143*(10), 4074-4083.
- Liang, C. G., Han, Z., Cheng, Y., Zhong, Z., & Latham, K. E. (2009). Effects of ooplasm transfer on paternal genome function in mice. *Hum Reprod*, *24*(11), 2718-2728.
- Livak, K. J., & Schmittgen, T. D. (2001). Analysis of relative gene expression data using real-time quantitative PCR and the 2(-Delta Delta C(T)) Method. *Methods*, *25*(4), 402-408.
- Lohka, M. J., Hayes, M. K., & Maller, J. L. (1988). Purification of maturation-promoting factor, an intracellular regulator of early mitotic events. *Proc Natl Acad Sci U S A*, *85*(9), 3009-3013.
- Lucifero, D., Mertineit, C., Clarke, H. J., Bestor, T. H., & Trasler, J. M. (2002). Methylation dynamics of imprinted genes in mouse germ cells. *Genomics*, *79*(4), 530-538.
- Lund, E. G., Kerr, T. A., Sakai, J., Li, W. P., & Russell, D. W. (1998). cDNA cloning of mouse and human cholesterol 25-hydroxylases, polytopic membrane proteins

- that synthesize a potent oxysterol regulator of lipid metabolism. *J Biol Chem*, 273(51), 34316-34327.
- Ma, A. S., Moran-Jones, K., Shan, J., Munro, T. P., Snee, M. J., Hoek, K. S., et al. (2002). Heterogeneous nuclear ribonucleoprotein A3, a novel RNA trafficking response element-binding protein. *J Biol Chem*, 277(20), 18010-18020.
- Madgwick, S., & Jones, K. T. (2007). How eggs arrest at metaphase II: MPF stabilisation plus APC/C inhibition equals Cytostatic Factor. *Cell Div*, 2, 4.
- Matsumoto, K., Kwon, O. Y., Kim, H., & Akao, Y. (2005). Expression of rck/p54, a DEAD-box RNA helicase, in gametogenesis and early embryogenesis of mice. *Dev Dyn*, 233(3), 1149-1156.
- Matzuk, M. M., Burns, K. H., Viveiros, M. M., & Eppig, J. J. (2002). Intercellular communication in the mammalian ovary: oocytes carry the conversation. *Science*, 296(5576), 2178-2180.
- McGrew, L. L., & Richter, J. D. (1990). Translational control by cytoplasmic polyadenylation during *Xenopus* oocyte maturation: characterization of cis and trans elements and regulation by cyclin/MPF. *EMBO J*, 9(11), 3743-3751.
- McKenzie, L. J., Pangas, S. A., Carson, S. A., Kovanci, E., Cisneros, P., Buster, J. E., et al. (2004). Human cumulus granulosa cell gene expression: a predictor of fertilization and embryo selection in women undergoing IVF. *Hum Reprod*, 19(12), 2869-2874.
- Mehlmann, L. M., Jones, T. L., & Jaffe, L. A. (2002). Meiotic arrest in the mouse follicle maintained by a Gs protein in the oocyte. *Science*, 297(5585), 1343-1345.
- Mehlmann, L. M., Terasaki, M., Jaffe, L. A., & Kline, D. (1995). Reorganization of the endoplasmic reticulum during meiotic maturation of the mouse oocyte. *Dev Biol*, 170(2), 607-615.
- Meijer, H. A., Radford, H. E., Wilson, L. S., Lissenden, S., & de Moor, C. H. (2007). Translational control of maskin mRNA by its 3' untranslated region. *Biol Cell*, 99(5), 239-250.
- Meinhardt, U., & Mullis, P. E. (2002). The essential role of the aromatase/p450arom. *Semin Reprod Med*, 20(3), 277-284.
- Mercer, J., & Helenius, A. (2008). Vaccinia virus uses macropinocytosis and apoptotic mimicry to enter host cells. *Science*, 320(5875), 531-535.
- Metkar, S. S., Wang, B., Aguilar-Santelises, M., Raja, S. M., Uhlin-Hansen, L., Podack, E., et al. (2002). Cytotoxic cell granule-mediated apoptosis: perforin delivers granzyme B-serglycin complexes into target cells without plasma membrane pore formation. *Immunity*, 16(3), 417-428.

- Minshall, N., Walker, J., Dale, M., & Standart, N. (1999). Dual roles of p82, the clam CPEB homolog, in cytoplasmic polyadenylation and translational masking. *RNA*, 5(1), 27-38.
- MMWR. (2000). Contribution of assisted reproductive technology and ovulation-inducing drugs to triplet and higher-order multiple births--United States, 1980-1997. *MMWR Morb Mortal Wkly Rep*, 49(24), 535-538.
- Mouillet, J. F., Yan, X., Ou, Q., Jin, L., Muglia, L. J., Crawford, P. A., et al. (2008). DEAD-box protein-103 (DP103, Ddx20) is essential for early embryonic development and modulates ovarian morphology and function. *Endocrinology*, 149(5), 2168-2175.
- Mtango, N. R., & Latham, K. E. (2007). Ubiquitin proteasome pathway gene expression varies in rhesus monkey oocytes and embryos of different developmental potential. *Physiol Genomics*, 31(1), 1-14.
- Mueller, P. L., Schreiber, J. R., Lucky, A. W., Schulman, J. D., Rodbard, D., & Ross, G. T. (1978). Follicle-stimulating hormone stimulates ovarian synthesis of proteoglycans in the estrogen-stimulated hypophysectomized immature female rat. *Endocrinology*, 102(3), 824-831.
- Mukhopadhyay, D., Houchen, C. W., Kennedy, S., Dieckgraefe, B. K., & Anant, S. (2003). Coupled mRNA stabilization and translational silencing of cyclooxygenase-2 by a novel RNA binding protein, CUGBP2. *Mol Cell*, 11(1), 113-126.
- Mulligan, M. K., Ponomarev, I., Hitzemann, R. J., Belknap, J. K., Tabakoff, B., Harris, R. A., et al. (2006). Toward understanding the genetics of alcohol drinking through transcriptome meta-analysis. *Proc Natl Acad Sci U S A*, 103(16), 6368-6373.
- Nakamura, Y., Hornsby, P. J., Casson, P., Morimoto, R., Satoh, F., Xing, Y., et al. (2009). Type 5 17beta-hydroxysteroid dehydrogenase (AKR1C3) contributes to testosterone production in the adrenal reticularis. *J Clin Endocrinol Metab*, 94(6), 2192-2198.
- Navot, D., Bergh, P. A., Williams, M. A., Garrisi, G. J., Guzman, I., Sandler, B., et al. (1991). Poor oocyte quality rather than implantation failure as a cause of age-related decline in female fertility. *Lancet*, 337(8754), 1375-1377.
- Ndiaye, K., Fayad, T., Silversides, D. W., Sirois, J., & Lussier, J. G. (2005). Identification of downregulated messenger RNAs in bovine granulosa cells of dominant follicles following stimulation with human chorionic gonadotropin. *Biol Reprod*, 73(2), 324-333.
- Neal, M. S., Reade, C. J., Younglai, E. V., Holloway, A. C., & Goodrow, G. J. (2008). Granulosa cell aromatase activity in women undergoing IVF: a comparison of good and poor responders. *J Obstet Gynaecol Can*, 30(2), 138-142.

- Norris, R. P., Ratzan, W. J., Freudzon, M., Mehlmann, L. M., Krall, J., Movsesian, M. A., et al. (2009). Cyclic GMP from the surrounding somatic cells regulates cyclic AMP and meiosis in the mouse oocyte. *Development*, 136(11), 1869-1878.
- Nyholt de Prada, J. K., Lee, Y. S., Latham, K. E., Chaffin, C. L., & VandeVoort, C. A. (2009). Role for cumulus cell-produced EGF-like ligands during primate oocyte maturation in vitro. *Am J Physiol Endocrinol Metab*, 296(5), E1049-1058.
- Obata, Y., Kaneko-Ishino, T., Koide, T., Takai, Y., Ueda, T., Domeki, I., et al. (1998). Disruption of primary imprinting during oocyte growth leads to the modified expression of imprinted genes during embryogenesis. *Development*, 125(8), 1553-1560.
- Oh, B., Hwang, S., McLaughlin, J., Solter, D., & Knowles, B. B. (2000). Timely translation during the mouse oocyte-to-embryo transition. *Development*, 127(17), 3795-3803.
- Oh, B., Hwang, S. Y., Solter, D., & Knowles, B. B. (1997). Spindlin, a major maternal transcript expressed in the mouse during the transition from oocyte to embryo. *Development*, 124(2), 493-503.
- Pangas, S. A., Jorgez, C. J., & Matzuk, M. M. (2004). Growth differentiation factor 9 regulates expression of the bone morphogenetic protein antagonist gremlin. *J Biol Chem*, 279(31), 32281-32286.
- Parakh, T. N., Hernandez, J. A., Grammer, J. C., Weck, J., Hunzicker-Dunn, M., Zeleznik, A. J., et al. (2006). Follicle-stimulating hormone/cAMP regulation of aromatase gene expression requires beta-catenin. *Proc Natl Acad Sci U S A*, 103(33), 12435-12440.
- Park-Sarge, O. K., & Mayo, K. E. (1994). Regulation of the progesterone receptor gene by gonadotropins and cyclic adenosine 3',5'-monophosphate in rat granulosa cells. *Endocrinology*, 134(2), 709-718.
- Park, J. Y., Su, Y. Q., Ariga, M., Law, E., Jin, S. L., & Conti, M. (2004). EGF-like growth factors as mediators of LH action in the ovulatory follicle. *Science*, 303(5658), 682-684.
- Park, O. K., & Mayo, K. E. (1991). Transient expression of progesterone receptor messenger RNA in ovarian granulosa cells after the preovulatory luteinizing hormone surge. *Mol Endocrinol*, 5(7), 967-978.
- Patterson, J. R., Wood, M. P., & Schisa, J. A. (2011). Assembly of RNP granules in stressed and aging oocytes requires nucleoporins and is coordinated with nuclear membrane blebbing. *Dev Biol*, 353(2), 173-185.
- Paynton, B. V., & Bachvarova, R. (1994). Polyadenylation and deadenylation of maternal mRNAs during oocyte growth and maturation in the mouse. *Mol Reprod Dev*, 37(2), 172-180.

- Peddinti, D., Memili, E., & Burgess, S. C. (2010). Proteomics-based systems biology modeling of bovine germinal vesicle stage oocyte and cumulus cell interaction. *PLoS One*, 5(6), e11240.
- Penning, T. M., Burczynski, M. E., Jez, J. M., Hung, C. F., Lin, H. K., Ma, H., et al. (2000). Human 3 α -hydroxysteroid dehydrogenase isoforms (AKR1C1-AKR1C4) of the aldo-keto reductase superfamily: functional plasticity and tissue distribution reveals roles in the inactivation and formation of male and female sex hormones. *Biochem J*, 351(Pt 1), 67-77.
- Pfaffl, M. W., Horgan, G. W., & Dempfle, L. (2002). Relative expression software tool (REST) for group-wise comparison and statistical analysis of relative expression results in real-time PCR. *Nucleic Acids Res*, 30(9), e36.
- Piko, L., & Clegg, K. B. (1982). Quantitative changes in total RNA, total poly(A), and ribosomes in early mouse embryos. *Dev Biol*, 89(2), 362-378.
- Pincus, G., & Enzmann, E. V. (1935). The Comparative Behavior of Mammalian Eggs in Vivo and in Vitro : I. The Activation of Ovarian Eggs. *J Exp Med*, 62(5), 665-675.
- Potireddy, S., Vassena, R., Patel, B. G., & Latham, K. E. (2006). Analysis of polysomal mRNA populations of mouse oocytes and zygotes: dynamic changes in maternal mRNA utilization and function. *Dev Biol*, 298(1), 155-166.
- Raja, S. M., Wang, B., Dantuluri, M., Desai, U. R., Demeler, B., Spiegel, K., et al. (2002). Cytotoxic cell granule-mediated apoptosis. Characterization of the macromolecular complex of granzyme B with serglycin. *J Biol Chem*, 277(51), 49523-49530.
- Raymond, V., Atwater, J. A., & Verma, I. M. (1989). Removal of an mRNA destabilizing element correlates with the increased oncogenicity of proto-oncogene fos. *Oncogene Res*, 5(1), 1-12.
- Reyland, M. E., Evans, R. M., & White, E. K. (2000). Lipoproteins regulate expression of the steroidogenic acute regulatory protein (StAR) in mouse adrenocortical cells. *J Biol Chem*, 275(47), 36637-36644.
- Reynolds, M. A., Schieve, L. A., Martin, J. A., Jeng, G., & Macaluso, M. (2003). Trends in multiple births conceived using assisted reproductive technology, United States, 1997-2000. *Pediatrics*, 111(5 Part 2), 1159-1162.
- Richter, J. D. (1991). Translational control during early development. *Bioessays*, 13(4), 179-183.
- Richter, J. D. (1999). Cytoplasmic polyadenylation in development and beyond. *Microbiol Mol Biol Rev*, 63(2), 446-456.
- Richter, J. D., & McGaughey, R. W. (1981). Patterns of polypeptide synthesis in mouse oocytes during germinal vesicle breakdown and during maintenance of the germinal vesicle stage by dibutyryl cAMP. *Dev Biol*, 83(1), 188-192.

- Rousseau, S., Morrice, N., Peggie, M., Campbell, D. G., Gaestel, M., & Cohen, P. (2002). Inhibition of SAPK2a/p38 prevents hnRNP A0 phosphorylation by MAPKAP-K2 and its interaction with cytokine mRNAs. *EMBO J*, 21(23), 6505-6514.
- Russell, D. L., Doyle, K. M., Gonzales-Robayna, I., Pipaon, C., & Richards, J. S. (2003). Egr-1 induction in rat granulosa cells by follicle-stimulating hormone and luteinizing hormone: combinatorial regulation by transcription factors cyclic adenosine 3',5'-monophosphate regulatory element binding protein, serum response factor, sp1, and early growth response factor-1. *Mol Endocrinol*, 17(4), 520-533.
- Saeed, A. I., Sharov, V., White, J., Li, J., Liang, W., Bhagabati, N., et al. (2003). TM4: a free, open-source system for microarray data management and analysis. *Biotechniques*, 34(2), 374-378.
- Salustri, A., Camaioni, A., Di Giacomo, M., Fulop, C., & Hascall, V. C. (1999). Hyaluronan and proteoglycans in ovarian follicles. *Hum Reprod Update*, 5(4), 293-301.
- Sapienza, C., Paquette, J., Tran, T. H., & Peterson, A. (1989). Epigenetic and genetic factors affect transgene methylation imprinting. *Development*, 107(1), 165-168.
- Sauer, M. V. (1998). The impact of age on reproductive potential: lessons learned from oocyte donation. *Maturitas*, 30(2), 221-225.
- Sawada, H., Yamahama, Y., Yamamoto, T., Mase, K., Ogawa, H., & Iino, T. (2006). A novel RNA helicase-like protein during early embryonic development in silkworm *Bombyx mori*: molecular characterization and intracellular localization. *Insect Biochem Mol Biol*, 36(12), 911-920.
- Schatten, G., & Schatten, H. (1987). Cytoskeletal alterations and nuclear architectural changes during mammalian fertilization. *Curr Top Dev Biol*, 23, 23-54.
- Schieve, L. A., Meikle, S. F., Ferre, C., Peterson, H. B., Jeng, G., & Wilcox, L. S. (2002). Low and very low birth weight in infants conceived with use of assisted reproductive technology. *N Engl J Med*, 346(10), 731-737.
- Schneider, W. J. (2009). Receptor-mediated mechanisms in ovarian follicle and oocyte development. *Gen Comp Endocrinol*, 163(1-2), 18-23.
- Schramm, R. D., & Bavister, B. D. (1996a). Development of in-vitro-fertilized primate embryos into blastocysts in a chemically defined, protein-free culture medium. *Hum Reprod*, 11(8), 1690-1697.
- Schramm, R. D., & Bavister, B. D. (1996b). Use of purified porcine follicle-stimulating hormone for ovarian stimulation of macaque monkeys. *Theriogenology*, 45(4), 727-732.
- Schramm, R. D., & Bavister, B. D. (1999a). A macaque model for studying mechanisms controlling oocyte development and maturation in human and non-human primates. *Hum Reprod*, 14(10), 2544-2555.

- Schramm, R. D., & Bavister, B. D. (1999b). Onset of nucleolar and extranucleolar transcription and expression of fibrillarin in macaque embryos developing in vitro. *Biol Reprod*, 60(3), 721-728.
- Schramm, R. D., Paprocki, A. M., & VandeVoort, C. A. (2003). Causes of developmental failure of in-vitro matured rhesus monkey oocytes: impairments in embryonic genome activation. *Hum Reprod*, 18(4), 826-833.
- Schramm, R. D., Tennier, M. T., Boatman, D. E., & Bavister, B. D. (1994). Effects of gonadotropins upon the incidence and kinetics of meiotic maturation of macaque oocytes in vitro. *Mol Reprod Dev*, 37(4), 467-472.
- Schultz, R. M. (1993). Regulation of zygotic gene activation in the mouse. *Bioessays*, 15(8), 531-538.
- Schultz, R. M. (2005). From egg to embryo: a peripatetic journey. *Reproduction*, 130(6), 825-828.
- Schultz, R. M., & Wassarman, P. M. (1977). Specific changes in the pattern of protein synthesis during meiotic maturation of mammalian oocytes in vitro. *Proc Natl Acad Sci U S A*, 74(2), 538-541.
- Sebbagh, M., Hamelin, J., Bertoglio, J., Solary, E., & Breard, J. (2005). Direct cleavage of ROCK II by granzyme B induces target cell membrane blebbing in a caspase-independent manner. *J Exp Med*, 201(3), 465-471.
- Segi, E., Haraguchi, K., Sugimoto, Y., Tsuji, M., Tsunekawa, H., Tamba, S., et al. (2003). Expression of messenger RNA for prostaglandin E receptor subtypes EP4/EP2 and cyclooxygenase isozymes in mouse periovulatory follicles and oviducts during superovulation. *Biol Reprod*, 68(3), 804-811.
- Sharma, S. C., & Richards, J. S. (2000). Regulation of AP1 (Jun/Fos) factor expression and activation in ovarian granulosa cells. Relation of JunD and Fra2 to terminal differentiation. *J Biol Chem*, 275(43), 33718-33728.
- Simon, A. M., Goodenough, D. A., Li, E., & Paul, D. L. (1997). Female infertility in mice lacking connexin 37. *Nature*, 385(6616), 525-529.
- Simon, R., Tassan, J. P., & Richter, J. D. (1992). Translational control by poly(A) elongation during *Xenopus* development: differential repression and enhancement by a novel cytoplasmic polyadenylation element. *Genes Dev*, 6(12B), 2580-2591.
- Simpson, E. R., Misso, M., Hewitt, K. N., Hill, R. A., Boon, W. C., Jones, M. E., et al. (2005). Estrogen--the good, the bad, and the unexpected. *Endocr Rev*, 26(3), 322-330.
- Solc, P., Schultz, R. M., & Motlik, J. (2010). Prophase I arrest and progression to metaphase I in mouse oocytes: comparison of resumption of meiosis and recovery from G2-arrest in somatic cells. *Mol Hum Reprod*, 16(9), 654-664.

- Sorensen, R. A., & Wassarman, P. M. (1976). Relationship between growth and meiotic maturation of the mouse oocyte. *Dev Biol*, 50(2), 531-536.
- Standart, N., & Minshall, N. (2008). Translational control in early development: CPEB, P-bodies and germinal granules. *Biochem Soc Trans*, 36(Pt 4), 671-676.
- Stebbins-Boaz, B., Cao, Q., de Moor, C. H., Mendez, R., & Richter, J. D. (1999). Maskin is a CPEB-associated factor that transiently interacts with eIF-4E. *Mol Cell*, 4(6), 1017-1027.
- Stebbins-Boaz, B., Hake, L. E., & Richter, J. D. (1996). CPEB controls the cytoplasmic polyadenylation of cyclin, Cdk2 and c-mos mRNAs and is necessary for oocyte maturation in *Xenopus*. *EMBO J*, 15(10), 2582-2592.
- Sternlicht, A. L., & Schultz, R. M. (1981). Biochemical studies of mammalian oogenesis: kinetics of accumulation of total and poly(A)-containing RNA during growth of the mouse oocyte. *J Exp Zool*, 215(2), 191-200.
- Stover, E. H., Borthwick, K. J., Bavalia, C., Eady, N., Fritz, D. M., Rungroj, N., et al. (2002). Novel ATP6V1B1 and ATP6V0A4 mutations in autosomal recessive distal renal tubular acidosis with new evidence for hearing loss. *J Med Genet*, 39(11), 796-803.
- Strauss, J. F., 3rd, Kallen, C. B., Christenson, L. K., Watari, H., Devoto, L., Arakane, F., et al. (1999). The steroidogenic acute regulatory protein (StAR): a window into the complexities of intracellular cholesterol trafficking. *Recent Prog Horm Res*, 54, 369-394; discussion 394-365.
- Su, Y. Q., Sugiura, K., & Eppig, J. J. (2009). Mouse oocyte control of granulosa cell development and function: paracrine regulation of cumulus cell metabolism. *Semin Reprod Med*, 27(1), 32-42.
- Sun, Q. Y., Wu, G. M., Lai, L., Park, K. W., Cabot, R., Cheong, H. T., et al. (2001). Translocation of active mitochondria during pig oocyte maturation, fertilization and early embryo development in vitro. *Reproduction*, 122(1), 155-163.
- Surani, M. A., Kothary, R., Allen, N. D., Singh, P. B., Fundele, R., Ferguson-Smith, A. C., et al. (1990). Genome imprinting and development in the mouse. *Dev Suppl*, 89-98.
- Sutcliffe, A. G., Peters, C. J., Bowdin, S., Temple, K., Reardon, W., Wilson, L., et al. (2006). Assisted reproductive therapies and imprinting disorders--a preliminary British survey. *Hum Reprod*, 21(4), 1009-1011.
- Szollosi, M. S., & Szollosi, D. (1988). 'Blebbing' of the nuclear envelope of mouse zygotes, early embryos and hybrid cells. *J Cell Sci*, 91 (Pt 2), 257-267.
- Tamba, S., Yodoi, R., Morimoto, K., Inazumi, T., Sukeno, M., Segi-Nishida, E., et al. (2010). Expression profiling of cumulus cells reveals functional changes during ovulation and central roles of prostaglandin EP2 receptor in cAMP signaling. *Biochimie*, 92(6), 665-675.

- Tay, J., Hodgman, R., & Richter, J. D. (2000). The control of cyclin B1 mRNA translation during mouse oocyte maturation. *Dev Biol*, 221(1), 1-9.
- Teilmann, S. C., Clement, C. A., Thorup, J., Byskov, A. G., & Christensen, S. T. (2006). Expression and localization of the progesterone receptor in mouse and human reproductive organs. *J Endocrinol*, 191(3), 525-535.
- Tesfaye, D., Ghanem, N., Carter, F., Fair, T., Sirard, M. A., Hoelker, M., et al. (2009). Gene expression profile of cumulus cells derived from cumulus-oocyte complexes matured either in vivo or in vitro. *Reprod Fertil Dev*, 21(3), 451-461.
- Toyama-Sorimachi, N., Sorimachi, H., Tobita, Y., Kitamura, F., Yagita, H., Suzuki, K., et al. (1995). A novel ligand for CD44 is serglycin, a hematopoietic cell lineage-specific proteoglycan. Possible involvement in lymphoid cell adherence and activation. *J Biol Chem*, 270(13), 7437-7444.
- Trounson, A., Wood, C., & Kausche, A. (1994). In vitro maturation and the fertilization and developmental competence of oocytes recovered from untreated polycystic ovarian patients. *Fertil Steril*, 62(2), 353-362.
- Tseng, L., & Mazella, J. (2002). Endometrial cell specific gene activation during implantation and early pregnancy. *Front Biosci*, 7, d1566-1574.
- Tsuchiya, N., Ochiai, M., Nakashima, K., Ubagai, T., Sugimura, T., & Nakagama, H. (2007). SND1, a component of RNA-induced silencing complex, is up-regulated in human colon cancers and implicated in early stage colon carcinogenesis. *Cancer Res*, 67(19), 9568-9576.
- Tusher, V. G., Tibshirani, R., & Chu, G. (2001). Significance analysis of microarrays applied to the ionizing radiation response. *Proc Natl Acad Sci U S A*, 98(9), 5116-5121.
- Vaccari, S., Weeks, J. L., 2nd, Hsieh, M., Menniti, F. S., & Conti, M. (2009). Cyclic GMP signaling is involved in the luteinizing hormone-dependent meiotic maturation of mouse oocytes. *Biol Reprod*, 81(3), 595-604.
- Valleley, E. M., Cordery, S. F., & Bonthron, D. T. (2007). Tissue-specific imprinting of the ZAC/PLAGL1 tumour suppressor gene results from variable utilization of monoallelic and biallelic promoters. *Hum Mol Genet*, 16(8), 972-981.
- Vanderhyden, B. C., Caron, P. J., Buccione, R., & Eppig, J. J. (1990). Developmental pattern of the secretion of cumulus expansion-enabling factor by mouse oocytes and the role of oocytes in promoting granulosa cell differentiation. *Dev Biol*, 140(2), 307-317.
- Vanderhyden, B. C., Telfer, E. E., & Eppig, J. J. (1992). Mouse oocytes promote proliferation of granulosa cells from preantral and antral follicles in vitro. *Biol Reprod*, 46(6), 1196-1204.

- VandeVoort, C. A., Leibo, S. P., & Tarantal, A. F. (2003). Improved collection and developmental competence of immature macaque oocytes. *Theriogenology*, *59*(3-4), 699-707.
- VandeVoort, C. A., & Tarantal, A. F. (1991). The macaque model for in vitro fertilization: superovulation techniques and ultrasound-guided follicular aspiration. *J Med Primatol*, *20*(3), 110-116.
- VandeVoort, C. A., & Tarantal, A. F. (2001). Recombinant human gonadotropins for macaque superovulation: repeated stimulations and post-treatment pregnancies. *J Med Primatol*, *30*(6), 304-307.
- Varrault, A., Gueydan, C., Delalbre, A., Bellmann, A., Houssami, S., Aknin, C., et al. (2006). Zac1 regulates an imprinted gene network critically involved in the control of embryonic growth. *Dev Cell*, *11*(5), 711-722.
- Vassalli, J. D., Huarte, J., Belin, D., Gubler, P., Vassalli, A., O'Connell, M. L., et al. (1989). Regulated polyadenylation controls mRNA translation during meiotic maturation of mouse oocytes. *Genes Dev*, *3*(12B), 2163-2171.
- Veeck, L. L., Wortham, J. W., Jr., Witmyer, J., Sandow, B. A., Acosta, A. A., Garcia, J. E., et al. (1983). Maturation and fertilization of morphologically immature human oocytes in a program of in vitro fertilization. *Fertil Steril*, *39*(5), 594-602.
- Verlhac, M. H., Terret, M. E., & Pintard, L. (2010). Control of the oocyte-to-embryo transition by the ubiquitin-proteolytic system in mouse and *C. elegans*. *Curr Opin Cell Biol*, *22*(6), 758-763.
- Viveiros, M. M., O'Brien, M., Wigglesworth, K., & Eppig, J. J. (2003). Characterization of protein kinase C-delta in mouse oocytes throughout meiotic maturation and following egg activation. *Biol Reprod*, *69*(5), 1494-1499.
- Volpe, A., Coukos, G., Uccelli, E., Droghini, F., Adamo, R., & Artini, P. G. (1991). Follicular fluid lipoproteins in preovulatory period and their relationship with follicular maturation and progesterone production by human granulosa-luteal cells in vivo and in vitro. *J Endocrinol Invest*, *14*(9), 737-742.
- Wang, H., Li, R., & Hu, Y. (2009). The alternative noncoding exons 1 of aromatase (Cyp19) gene modulate gene expression in a posttranscriptional manner. *Endocrinology*, *150*(7), 3301-3307.
- Wang, J., Saxe, J. P., Tanaka, T., Chuma, S., & Lin, H. (2009). Mili interacts with tudor domain-containing protein 1 in regulating spermatogenesis. *Curr Biol*, *19*(8), 640-644.
- Wang, S., Kou, Z., Jing, Z., Zhang, Y., Guo, X., Dong, M., et al. (2010). Proteome of mouse oocytes at different developmental stages. *Proc Natl Acad Sci U S A*, *107*(41), 17639-17644.
- Wen, X., Tozer, A. J., Li, D., Docherty, S. M., Al-Shawaf, T., & Iles, R. K. (2007). Human granulosa-lutein cell in vitro production of progesterone, inhibin A, inhibin B, and

activin A are dependent on follicular size and not the presence of the oocyte. *Fertil Steril*.

- Williams, K. J., & Fuki, I. V. (1997). Cell-surface heparan sulfate proteoglycans: dynamic molecules mediating ligand catabolism. *Curr Opin Lipidol*, 8(5), 253-262.
- Woodruff, T. K. (2010). The Oncofertility Consortium--addressing fertility in young people with cancer. *Nat Rev Clin Oncol*, 7(8), 466-475.
- Wright, V. C., Chang, J., Jeng, G., & Macaluso, M. (2006). Assisted reproductive technology surveillance--United States, 2003. *MMWR Surveill Summ*, 55(4), 1-22.
- Yeo, C. X., Gilchrist, R. B., & Lane, M. (2009). Disruption of bidirectional oocyte-cumulus paracrine signaling during in vitro maturation reduces subsequent mouse oocyte developmental competence. *Biol Reprod*, 80(5), 1072-1080.
- Yoshiko, Y., & Aubin, J. E. (2004). Stanniocalcin 1 as a pleiotropic factor in mammals. *Peptides*, 25(10), 1663-1669.
- Yu, J., Hecht, N. B., & Schultz, R. M. (2002). RNA-binding properties and translation repression in vitro by germ cell-specific MSY2 protein. *Biol Reprod*, 67(4), 1093-1098.
- Zhang, M., Su, Y. Q., Sugiura, K., Xia, G., & Eppig, J. J. (2010). Granulosa cell ligand NPPC and its receptor NPR2 maintain meiotic arrest in mouse oocytes. *Science*, 330(6002), 366-369.
- Zhang, X., Jafari, N., Barnes, R. B., Confino, E., Milad, M., & Kazer, R. R. (2005). Studies of gene expression in human cumulus cells indicate pentraxin 3 as a possible marker for oocyte quality. *Fertil Steril*, 83 Suppl 1, 1169-1179.
- Zheng, P., Patel, B., McMenamin, M., Moran, E., Paprocki, A. M., Kihara, M., et al. (2005a). Effects of follicle size and oocyte maturation conditions on maternal messenger RNA regulation and gene expression in rhesus monkey oocytes and embryos. *Biol Reprod*, 72(4), 890-897.
- Zheng, P., Patel, B., McMenamin, M., Reddy, S. E., Paprocki, A. M., Schramm, R. D., et al. (2004). The primate embryo gene expression resource: a novel resource to facilitate rapid analysis of gene expression patterns in non-human primate oocytes and preimplantation stage embryos. *Biol Reprod*, 70(5), 1411-1418.
- Zheng, P., Schramm, R. D., & Latham, K. E. (2005b). Developmental regulation and in vitro culture effects on expression of DNA repair and cell cycle checkpoint control genes in rhesus monkey oocytes and embryos. *Biol Reprod*, 72(6), 1359-1369.
- Zheng, P., Vassena, R., & Latham, K. (2006). Expression and downregulation of WNT signaling pathway genes in rhesus monkey oocytes and embryos. *Mol Reprod Dev*, 73(6), 667-677.